

# Adversarial Robustness of Discriminative Self-Supervised Learning in Vision

Ömer Veysel Çağatan

Ömer Faruk Tal

M. Emre Gürsoy

Department of Computer Engineering, Koç University

ocagatan19@ku.edu.tr, otal19@ku.edu.tr, emregursoy@ku.edu.tr

## Abstract

*Self-supervised learning (SSL) has advanced significantly in visual representation learning, yet comprehensive evaluations of its adversarial robustness remain limited. In this study, we evaluate the adversarial robustness of seven discriminative self-supervised models and one supervised model across diverse tasks, including ImageNet classification, transfer learning, segmentation, and detection. Our findings suggest that discriminative SSL models generally exhibit better robustness to adversarial attacks compared to their supervised counterpart on ImageNet, with this advantage extending to transfer learning when using linear evaluation. However, when fine-tuning is applied, the robustness gap between SSL and supervised models narrows considerably. Similarly, this robustness advantage diminishes in segmentation and detection tasks. We also investigate how various factors might influence adversarial robustness, including architectural choices, training duration, data augmentations, and batch sizes. Our analysis contributes to the ongoing exploration of adversarial robustness in visual self-supervised representation systems.*

## 1. Introduction

Self-supervised learning (SSL) [5], particularly discriminative approaches, has emerged as a foundational method for training models with remarkable capabilities in areas such as language [98], vision [80], and decision-making [60]. As these models become increasingly widespread and integrated into various applications, ensuring their reliability and safety has become a critical concern [8, 9].

One particular challenge is the surprising vulnerability of deep learning models to adversarial examples, where slight input alterations can significantly impact model performance [43, 96]. This phenomenon has sparked significant debate, seeking to understand and mitigate these vulnerabilities [4, 38, 91, 93, 97, 103–105]. One prominent theory [56] suggests that adversarial examples arise from the model’s sensitivity to non-robust features in the in-

put data. According to this view, both robust (stable) and non-robust (vulnerable) features contribute to classification, with adversarial attacks manipulating the latter to cause misclassification. However, this theory, developed primarily in the context of supervised learning, faces challenges when extended to other self-supervised paradigms. [66] indicates that non-robust features are less effective in SSL methods such as contrastive learning [20], masked image modeling [49], or diffusion models [52]. This discrepancy suggests that non-robust features may lack the transferability across learning paradigms that robust or natural features possess. Thus, it becomes essential to systematically evaluate and compare how different SSL approaches respond to adversarial attacks, particularly given the theoretical evidence suggesting their feature representations may differ fundamentally from supervised models.

These theoretical insights into how adversarial examples affect different learning paradigms highlight several critical gaps in our understanding of SSL’s adversarial robustness. Notwithstanding the progress made in understanding the adversarial robustness of SSL, particularly contrastive learning, which we extensively discuss in section 2, several key questions remain unresolved. First, with the wide variety of self-supervised representations available, employing different pretext tasks and data augmentations, which approaches demonstrate the greatest adversarial robustness? This remains unclear since most methods don’t provide any results on adversarial robustness unless it is a specific focus of the proposed approach. Secondly, robustness is typically assessed by the model’s accuracy on the pretraining dataset. Still, its adversarial impact on transfer learning or downstream tasks like detection and segmentation has not been thoroughly investigated [62].

The choice of model architecture also raises questions about robustness. Standard vision SSL pretraining typically utilizes a ResNet [47] as the backbone, but more recently, larger and more powerful models [15, 24, 80] have been developed using vision transformers [34]. This leads to the question: Which architecture demonstrates greater robustness under the same SSL objective and with comparable

parameter sizes?

Another factor to consider is the training duration. State-of-the-art SSL models are trained for longer durations compared to their supervised counterparts. Several studies indicate that this extended training consistently enhances performance, raising the question of whether this might compromise the models' adversarial robustness.

While previous work has examined aspects of adversarial robustness in SSL, our study provides the first comprehensive cross-model comparison across multiple tasks, architectures, and training regimes. We assess seven different SSL models (Barlow Twins [111], BYOL [44], DINO [15], MoCoV3 [24], SimCLR [20], SwAV [14], and VICReg [7]) alongside a supervised model against various adversarial attacks on ImageNet [90] and nine other image-recognition datasets. We also evaluate their robustness in segmentation and detection tasks. Our investigation addresses the following key questions:

**1. How does the adversarial robustness of various SSL models compare to that of supervised models on ImageNet?**

SSL models consistently demonstrate greater adversarial robustness than supervised models on ImageNet. Non-contrastive methods show particular resilience against IAA [16] attacks, while all SSL approaches exhibit strong resistance to UAP [17], with MoCoV3 demonstrating the strongest overall performance.

**2. Does SSL robustness transfer to downstream tasks like transfer learning, segmentation, and detection?**

The robustness advantages transfer effectively to classification tasks via linear probing and fine-tuning. However, in segmentation and detection, all models exhibit similar vulnerability regardless of pretraining methodology, suggesting task-specific architectural components may override backbone robustness properties.

**3. How does model architecture influence adversarial robustness under the same SSL objective?**

Architecture impact is highly objective-dependent. MoCoV3 shows reduced robustness with Vision Transformers, whereas DINO demonstrates improved performance with ViT compared to ResNet, challenging the notion that architectural effects are uniform across SSL paradigms.

**4. Does extending training duration compromise adversarial robustness in SSL models?**

Extended training either maintains or slightly enhances adversarial performance. For UAP attacks, performance improves meaningfully after more epochs in both SwAV and MoCoV3, indicating that longer training periods do not create a performance-robustness tradeoff.

## 2. Related Work

**Self Supervised Learning** Self-supervised learning(SSL) seeks to extract meaningful and general representations from unlabeled data by leveraging pretext tasks. These tasks can vary, such as predicting the next word [87] or neighboring words [31] in a text, reconstructing masked sections of an image [49], or ensuring that two different perspectives of the same image result in similar visual representations [20].

Avoiding collapse is a key challenge in SSL for computer vision, and various methods can be classified based on how they address this issue. Contrastive approaches like SimCLR [20] and MoCo [23, 24, 48] use an objective that pushes apart representations of different inputs (negative samples) while bringing together those of the same input (positive samples). The performance and scalability of these methods heavily depend on the number and selection of negative samples. In another category, distillation methods such as BYOL [44], SimSiam [22], and DINO [15], prevent collapse by introducing asymmetry between different encoder branches and employing algorithmic adjustments. Additional SSL techniques, including DeepCluster [13], SeLa [2], and SwAV [14], enforce a clustering structure in the feature space to avoid constant representations. Meanwhile, methods like Barlow Twins [111], Whitening MSE (W-MSE) [36], VICReg [7], CorInfoMax [82] prevent collapse by using feature decorrelation.

**Adversarial Self-Supervised Learning** While self-supervised learning (SSL) has outperformed supervised training [20], numerous studies highlight that contrastive learning remains susceptible to adversarial attacks when transferring the learned features to downstream classification tasks [51, 59]. To improve the robustness of contrastive learning, adversarial training has been adapted to self-supervised settings. In the absence of labels, adversarial examples are generated by maximizing the contrastive loss with respect to all input samples. Several prior works, such as ACL [57], RoCL [59], and CLAE [51], adopt this approach. Additionally, ACL incorporates the dual-BN technique [108] to further enhance performance. DeACL [112] introduces a two-stage approach, distilling a standard pre-trained encoder through adversarial training. Nguyen et al. [79] establishes an upper bound on the adversarial loss of a prediction model, which is based on the learned representations, for any downstream task. This upper bound is determined using the model's loss on clean data and a robustness regularization term, which helps make the prediction model more resistant to adversarial attacks. [45] demonstrates that adversarial sensitivity stems from the uniform distribution of data representations on a unit hypersphere in the representation space. The presence of false negative pairs during training contributes to this effect, increasing the model's vulnerability to input perturbations.

Although self-supervised adversarial training has made

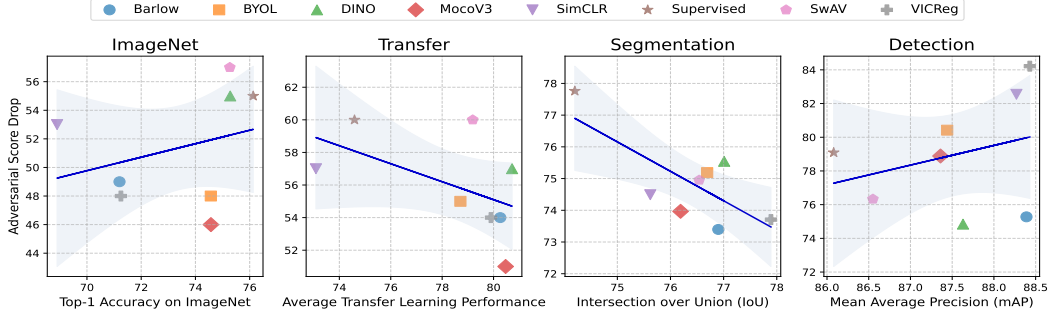


Figure 1. Performance scores for tasks such as ImageNet classification, transfer learning (with linear probing), segmentation, and detection (both with frozen backbones) are shown with the percentage drop in adversarial robustness. The shaded regions indicate the 95% confidence interval around the regression line. Note the consistent pattern of higher robustness (lower percentage drop) among SSL models compared to supervised approaches in classification tasks.

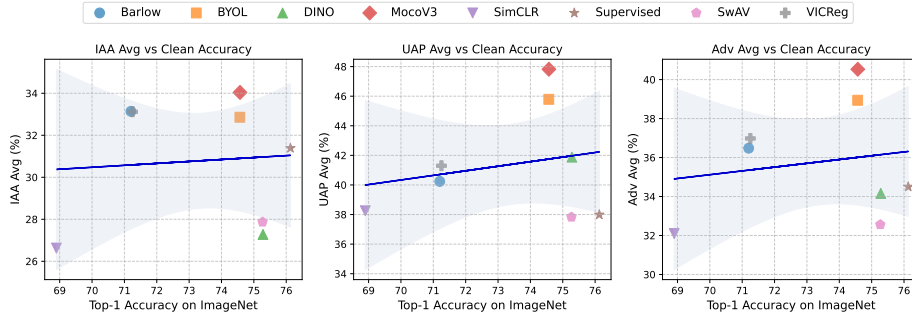


Figure 2. Averaged scores of SSL models on ImageNet across various attack types, including Instance Adversarial Attacks (IAA) and Universal Adversarial Perturbations (UAP). *Adv Avg* refers to the average score across all attacks combined. The shaded regions indicate the 95% confidence interval around the regression line.

progress, it still does not match the performance of supervised methods. Luo et al. [69] suggest that this shortfall is due to data augmentation and propose a dynamic data augmentation scheduler to achieve comparable results to supervised training. Xu et al. [109] efficiently apply ACL on the ImageNet [90] to obtain a robust representation using robustness-aware core set selection.

**Robustness of Self-Supervised Learning** [50] found that incorporating an extra self-supervised task in a multi-task framework can enhance the adversarial robustness of supervised models. In a similar vein, Carmon et al. [12] discovered that using additional unlabeled data also strengthens the model’s adversarial resilience. Furthermore, Chen et al. [21] created robust variants of pretext-based SSL tasks, showing that their integration with robust fine-tuning leads to a notable increase in robustness compared to standard adversarial training. Chhipa et al. [25] demonstrates a clear relationship between the performance of learned representations within SSL paradigms and the severity of distribution shifts and corruptions and highlights the critical impact of distribution shifts and image corruptions on the performance and resilience of SSL methods. Simi-

larly, Zhong et al. [113] conduct robustness tests to assess the behavioral differences between contrastive and supervised learning under changes in downstream or pre-training data distributions, while also exploring the effects of data augmentation and feature space characteristics. Kowalczyk et al. [62] conducts a comprehensive empirical evaluation of the adversarial robustness of self-supervised vision encoders across multiple downstream tasks, revealing the need for broader enhancements in encoder robustness. Goldblum et al. [42] benchmarks diverse pretrained models across multiple computer vision tasks, finding that supervised convolutional neural networks still outperform newer architectures on most metrics, while revealing self-supervised learning backbones show competitive potential when compared under equivalent conditions.

### 3. Experimental Setup

#### 3.1. SSL Models

While numerous SSL approaches have been proposed [81], we focus exclusively on the following well-known SSL models because of computational constraints: Barlow

Twins [111], BYOL [44], DINO [15], MoCoV3 [24], SimCLR [20], SwAV [14], and VICReg [7]. We primarily use ResNet50 [47] models since most SSL approaches only publicly release checkpoints in this format, with only DINO and MoCoV3 providing ViT [34] checkpoints. Our experiments utilize the best publicly available ImageNet checkpoints from official repositories. For BYOL, DINO, MoCoV3, SimCLR, and SwAV, complete model checkpoints were available. However, for Barlow Twins and VICReg, only backbone weights were provided, requiring us to perform linear evaluation using their official code, which resulted in a 2% decrease in performance. Furthermore, we assess a supervised baseline for comparison using a standard pre-trained ResNet50 model from the PyTorch library [83]. All models feature 23.5 million parameters in their backbones and were pre-trained on the ImageNet [90] training set (1.28 million images), with only the supervised baseline utilizing labels.

### 3.2. ImageNet and Transfer Learning

We use the benchmark suite introduced in the transfer learning study [54], which encompasses the target datasets like FGVC Aircraft [71], Caltech-101 [39], Stanford Cars [63], CIFAR 10 [64], CIFAR 100 [64], DTD [26], Oxford 102 Flowers [26], and Food-101 [10]. We follow Ericsson et al. [35] for both linear evaluation and fine-tuning of these datasets. We prioritized linear evaluation in our analysis as the backbone remains frozen during this process, allowing for a more equitable comparison of objectives within this setup. We apply the same adversarial techniques to ImageNet and transfer learning: Instance Adversarial Attacks (IAA) and Universal Adversarial Perturbations (UAP). In brief, instance-based methods generate unique perturbations for each image, while UAP creates a single perturbation that applies across the entire dataset. Details of all attack methods are provided in section 1 of the Supp. Mat. (Supplementary material).

### 3.3. Segmentation

For segmentation, we use the Pascal VOC 2012 dataset [37] and CityScapes [27] dataset, training a DeepLabV3+ model [18]. To conduct the attacks, we follow the setup from Rony et al. [89], utilizing Alma [89], Asma [89], DAG [106], DDN [89], FGSM [43], FMN [85], and PGD [70]. While our primary metric is the mean Intersection Over Union (mIOU), we also report the Attack Pixel Success Rate (APSR) introduced by [89]. Although our main focus is on using a frozen backbone, we also perform training following the standard procedure. Our CityScapes results include only the frozen backbone approach, while our Pascal VOC results include both frozen and unfrozen backbone configurations.

Table 1. Performance of various models on ImageNet, Transfer Learning, Segmentation (Pascal VOC), and Detection (INRIA Person) tasks with frozen backbones, showing original (Orig.) and adversarial (Adv.) scores with performance drops in red.

Model	ImageNet		Transfer Learning		Segmentation		Detection	
	Orig.	Adv.	Orig.	Adv.	Orig.	Adv.	Orig.	Adv.
Barlow Twins	71.2	36.5 <span style="color:red">↓49%</span>	80.3	37.8 <span style="color:red">↓54%</span>	76.9	20.5 <span style="color:red">↓73%</span>	88.4	21.9 <span style="color:red">↓75%</span>
BYOL	74.6	38.9 <span style="color:red">↓48%</span>	78.7	36.6 <span style="color:red">↓55%</span>	76.7	19.0 <span style="color:red">↓75%</span>	87.4	17.3 <span style="color:red">↓80%</span>
DINO	75.3	34.2 <span style="color:red">↓55%</span>	80.7	35.6 <span style="color:red">↓57%</span>	77.0	18.9 <span style="color:red">↓76%</span>	87.6	22.0 <span style="color:red">↓75%</span>
MoCoV3	74.6	40.5 <span style="color:red">↓46%</span>	80.5	40.3 <span style="color:red">↓51%</span>	76.2	19.9 <span style="color:red">↓74%</span>	87.3	18.5 <span style="color:red">↓79%</span>
SimCLR	68.9	32.1 <span style="color:red">↓53%</span>	73.1	33.0 <span style="color:red">↓57%</span>	75.6	19.3 <span style="color:red">↓74%</span>	87.7	13.1 <span style="color:red">↓85%</span>
Supervised	76.1	34.5 <span style="color:red">↓55%</span>	74.6	31.2 <span style="color:red">↓60%</span>	74.2	16.5 <span style="color:red">↓78%</span>	86.1	18.0 <span style="color:red">↓79%</span>
SwAV	75.3	32.6 <span style="color:red">↓57%</span>	79.2	32.4 <span style="color:red">↓60%</span>	76.5	19.2 <span style="color:red">↓75%</span>	86.6	20.5 <span style="color:red">↓76%</span>
VICReg	71.3	37.0 <span style="color:red">↓48%</span>	79.9	37.7 <span style="color:red">↓54%</span>	77.9	20.5 <span style="color:red">↓74%</span>	88.4	14.0 <span style="color:red">↓84%</span>

### 3.4. Detection

For object detection, we utilized the INRIA Person [28] and CoCo [67] datasets, and trained a Faster R-CNN [88]. To perform adversarial attacks, we followed the setup described by [53], employing the Transfer-based Self-Ensemble Attack (T-SEA). The T-SEA attack can be deployed using various methods and optimizers. In our experiments, we employed BIM [53], MIM [32], PGD [70], and Optim [53] methods. Additionally, we explored simpler methods that rely on common optimizers, such as Adam [61], SGD, and Nesterov [78]. Throughout our evaluation, we report the mean average precision (mAP) scores as the primary performance metric. While our primary focus was on employing a frozen backbone, we also conducted training experiments following the standard training procedures for comparative analysis. Our COCO results include only the frozen backbone approach.

## 4. Results and Discussion

In this section, we present our experimental findings on ImageNet, transfer learning, and detection and discuss each in turn. Figure 1 and table 1 summarize the performance of various SSL models compared to supervised learning across our main evaluation tasks in the frozen backbone setup. While we address the results individually, the full detailed results are provided in section 4 of the Supp. Mat..

### 4.1. ImageNet

**SSL vs Supervised.** Most robustness studies on contrastive learning [51, 57, 59, 79, 108, 112] focus on small datasets like CIFAR10 [64] and primarily evaluate robustness using adversarial attacks such as FGSM [43] and PGD [70]. While computational constraints explain the reluctance to scale to larger datasets like ImageNet [90], many evaluations inadequately incorporate Universal Adversarial Perturbations (UAP). Our findings, as shown in figure 2 contradict previous research by Gupta et al. [45]. Under IAA, MoCoV3 demonstrates the strongest robustness (54% drop), while SimCLR shows the weakest performance (61% drop).



For UAP attacks, MoCoV3 again leads (38% drop), while the supervised model and SwAV both show 50% drops. Notably, our results challenge the conclusion about contrastive vs. non-contrastive methods. MoCoV3, a contrastive model, consistently demonstrates the highest adversarial robustness with ResNet architecture, while DINO, which was claimed to perform better due to its non-contrastive nature, shows the weakest IAA robustness in our ResNet evaluation (64% drop). Our data reveals that Barlow, BYOL, MoCoV3, and VICReg all demonstrate comparable resilience against IAA (around 54% drop), contradicting the simple categorization of robustness based on contrastive versus non-contrastive approaches. Our comprehensive evaluation using diverse attack methods demonstrates that the relationship between self-supervised learning approaches and adversarial robustness is more complex than previously suggested. The full results are in section 4.1 of the Supp. Mat..

**What makes MoCoV3 robust?** Although MoCoV3 and SimCLR both utilize the InfoNCE [94, 101] objective, there is a stark contrast in their adversarial robustness. To understand this disparity, we evaluate MoCoV1 [48], MoCoV2 [23], and MoCoV3.

**A brief MoCo History.** *MoCoV1 introduced a dynamic dictionary with a queue and momentum-updated encoder to maintain consistent negative samples. MoCoV2 enhanced this with a multi-layer projection head and stronger data augmentation. MoCoV3 further evolved by eliminating the memory bank and incorporating a prediction head similar to BYOL and SimSiam [22].*

Our analysis reveals a clear progression in robustness across MoCo versions. While MoCoV1 demonstrates limited resilience with a 71% drop in overall adversarial accuracy, MoCoV2 shows significant improvement (52% drop), and MoCoV3 achieves the strongest performance (46% drop). The most dramatic enhancement occurs in UAP resistance, where MoCoV1’s performance drops by 77%, compared to MoCoV2’s 39% and MoCoV3’s 36%. The substantial improvement from MoCoV1 to MoCoV2 (7 % in clean accuracy, 27 percentage points in UAP robustness) primarily stems from the non-linear projector, with data augmentation providing marginal benefits. While [55] suggests non-linear projectors aren’t always essential, our results indicate they significantly enhance both performance and adversarial robustness. MoCoV3’s superior performance over MoCoV2 (an additional 7% in clean accuracy and 7 percentage points in UAP robustness) can be attributed to its prediction head and larger batch size. Unlike the transition from V1 to V2, MoCoV3 shows substantial improvements in both IAA (34% vs 25%) and UAP (48% vs 41%), highlighting the prediction head’s critical role in enhancing overall robustness. Our findings suggest that momentum, a common feature in robust models like MoCoV3 and BYOL, significantly contributes to adversar-

ial resilience, while MoCoV2’s performance more closely resembles that of SimCLR, which lacks this feature. The full results are in section 4.6 of the supplementary material.

#### Augmentations vs Algorithms.

Morningstar et al. [76] challenge the notion that SSL progress is primarily driven by algorithmic advancements, suggesting instead that augmentation diversity, along with data and model scale, play more critical roles. Their analysis argues that many algorithmic improvements, such as prediction networks or new loss functions, had minimal impact on downstream task performance compared to stronger augmentation techniques.

Our comprehensive analysis of the MoCo family evolution provides a more nuanced perspective on this debate. The substantial progression in adversarial robustness from MoCoV1 to MoCoV2 and further to MoCoV3 suggests that architectural innovations like non-linear projectors and prediction heads significantly impact robustness. MoCoV2’s dramatic improvement over MoCoV1, particularly in UAP performance, indicates that the multi-layer projection head provides substantial benefits beyond mere augmentation changes. Similarly, MoCoV3’s further enhancements in both IAA and UAP performance relative to MoCoV2 highlight the crucial role of the prediction head in overall robustness.

While our comparison lacks perfectly controlled baselines for augmentations across different objectives (with slight variations in augmentation between MoCoV2 and V3), this limitation stems from the unavailability of public checkpoints rather than our experimental design. Despite this constraint, the consistent improvements in adversarial performance strongly suggest that algorithmic innovations significantly contribute to adversarial robustness. Importantly, our findings demonstrate that higher clean accuracy doesn’t automatically translate to improved robustness on ImageNet.

Although the checkpoints from [76] are not publicly available, we conducted an ablation study on augmentation types and batch sizes using BYOL. BYOL is the only model in our SSL pool that includes configurations with varied augmentations and batch sizes. For this analysis, we consider four distinct models: BYOL-NC (without color distortions), BYOL-CC (with only color and crop augmentations), and the standard BYOL models with batch sizes of 128 (BYOL-128) and 512 (BYOL-512).

We observe that batch size and augmentation choices have varying effects on the adversarial robustness of BYOL variants. For IAA robustness, both BYOL-NC and BYOL-CC show similar performance (60% drop), while BYOL-128, BYOL-512, and standard BYOL demonstrate slightly better resilience (57%, 56%, and 56% drops, respectively). These modest differences suggest that batch size and augmentation have a limited impact on instance-level attack ro-

bustness.

For UAP attacks, we see more substantial variations: BYOL-128 (41% drop) and BYOL-512 (43% drop) perform comparably, while BYOL-NC and BYOL-CC show notably weaker performance (46% and 48% drops). Standard BYOL demonstrates a 39% drop, which is marginally better than the batch size variants but substantially better than the limited-augmentation models. The 7-9 percentage point difference between standard BYOL and the limited-augmentation variants suggests that comprehensive augmentation strategies may contribute to improved UAP robustness.

Interestingly, we note that BYOL-CC performs slightly worse than BYOL-NC despite having more augmentations, though this difference is too small to draw meaningful conclusions. Similarly, the differences between BYOL-128, BYOL-512, and standard BYOL in UAP robustness are relatively minor and should be interpreted cautiously. Our results indicate that the relationship between augmentation and adversarial robustness is complex and that meaningful improvements likely require more than just incremental changes to batch size or augmentation strategies. While our data hints at potential benefits from comprehensive augmentation for UAP robustness, the effects are modest and require further investigation with more controlled experiments. The full results are in section 4.7 of the supplementary material.

**ResNet vs ViT in Adversarial Robustness.** While ViTs are generally seen as more robust than CNNs [77], Bai et al. [3], Pinto et al. [84] demonstrate that with the right training methods, CNNs [65] can achieve comparable robustness. Despite ViT’s success [15, 24, 29, 34, 80], most SSL methods still use ResNet for validation. We examine MoCoV3 and DINO, as they are the only models that include ViT training, with our analysis covering both standard ViTs comparable to ResNet50 and larger ViT-B variants with approximately 4x more parameters.

Our results reveal notable architectural differences. DINO performs significantly better with ViT architectures than ResNet, with DINO-ViT-B achieving 45.19% adversarial average (42% drop from clean accuracy) compared to DINO-ResNet’s 55% drop. In contrast, MoCo struggles with transformer architectures, with MoCo-ViT showing poor performance at 61% drop, significantly worse than MoCoV3-ResNet at 46% drop. Even MoCoV3-ViT-B 51% drop underperforms its ResNet counterpart despite having 4x more parameters.

These differences are especially evident in UAP results, where DINO-ViT-B shows greater resilience (38% drop) than DINO-ResNet (44% drop), while MoCo-ViT performs poorly (26.31%, 64% drop) compared to MoCoV3-ResNet (36% drop). These findings suggest that the interaction between self-supervised approaches and model architectures

significantly impacts adversarial robustness, with DINO benefiting from ViT architecture while MoCo struggles with transformer models. The full results are in section 4.6 of the Supp. Mat..

**Impact of Training Duration.** SSL models tend to demonstrate better performance as training epochs increase [14, 20, 24]. However, due to computational constraints, many models are reported with different numbers of epochs. This prompts the question of whether longer training durations enhance or reduce adversarial robustness. As ViT models do not have checkpoints at various epochs, we focus on ResNet-based SSL models, specifically SwAV and MoCoV3, which offer multiple checkpoints throughout the training process. We find that both SwAV and MoCo show very marginal improvement of about 1% on IAA across various epochs, which is minimal compared to the rise in original accuracy. In contrast, both methods exhibit a modest increase in UAP performance after surpassing 100 epochs, with SwAV improving from 33% to 40% and MoCoV3 from 41% to 48%. Overall, our results suggest that despite differences in reported checkpoints, robustness generally remains largely stable during training for IAA, with slightly more noticeable but still modest gains for UAP. This indicates that training duration has a limited impact on adversarial robustness, even as clean accuracy continues to improve with extended training. The full results are in section 4.5 of the Supp. Mat.

## 4.2. Transfer Learning

In this section, we analyze how adversarial robustness transfers from ImageNet pre-training to downstream tasks. We examine whether vulnerability patterns established during pre-training persist when models are evaluated through linear probing or fine-tuning across various ResNet-based self-supervised and supervised learning approaches. This analysis quantifies robustness transfer relationships through both Spearman rank and Pearson correlations.

**LINEAR.** Our correlation analysis shows strong relationships between ImageNet and linear evaluation vulnerability. For performance drops, both Spearman and Pearson correlations are high across all attack types (Spearman—Adv: 0.93, UAP: 0.83, IAA: 0.79; Pearson—Adv: 0.94, UAP: 0.94, IAA: 0.88). These consistently high correlations suggest that robustness characteristics established during pre-training largely persist through linear probing. The performance drop analysis reveals method-specific robustness characteristics. MoCoV3 consistently exhibits smaller performance drops across both ImageNet (IAA: 54%, UAP: 36%) and linear evaluation (IAA: 56%, UAP: 43%), indicating its contrastive learning approach with momentum encoders develops features with inherently better transferable robustness properties. In contrast, supervised pre-training and clustering-based approaches like SwAV

Table 2. Component Contribution Analysis Across Datasets. Metrics include: Original Accuracy (Orig), Adversarial Accuracy (Adv) with relative performance drop percentage, Direction Ratio (D) and Magnitude Ratio (M). Ratio interpretation: Head dominant (<0.67), Balanced (0.67-1.5), Backbone dominant (>1.5).

Model	CIFAR-10					CIFAR-100					ImageNet				CIFAR-10 (FT)				CIFAR-100 (FT)						
	Orig	Adv ↓	D	M	Orig	Adv ↓	D	M	Orig	Adv ↓	D	M	Orig	Adv ↓	D	M	Orig	Adv ↓	D	M					
Barlow	92.3	33.0	↓64%	2.7	3.1	77.9	20.5	↓74%	1.4	5.0	71.2	42.4	↓40%	0.9	9.4	97.1	66.9	↓31%	1.5	2.4	84.6	45.0	↓57%	0.8	2.4
BYOL	93.0	31.0	↓67%	1.6	4.2	78.2	19.01	↓76%	1.07	6.0	74.6	39.4	↓47%	0.9	12.5	96.9	67.0	↓31%	1.2	1.4	83.9	61.2	↓27%	0.7	2.7
DINO	93.9	27.6	↓71%	3.2	3.3	79.7	16.0	↓80%	1.6	6.2	75.3	24.7	↓67%	1.2	14.1	96.9	77.8	↓20%	1.9	2.9	84.7	52.9	↓38%	1.79	4.6
MoCoV3	94.7	33.0	↓65%	2.5	1.7	80.2	19.3	↓76%	1.1	4.5	74.6	42.7	↓43%	0.7	10.9	96.9	72.0	↓26%	1.1	1.3	84.5	62.6	↓26%	0.7	2.6
SimCLR	91.0	37.9	↓58%	1.5	1.9	73.0	19.5	↓73%	1.3	3.5	68.9	24.3	↓65%	1.0	7.7	97.2	67.3	↓31%	1.0	1.9	84.4	43.0	↓50%	0.6	2.0
Supervised	91.4	42.8	↓53%	1.8	0.7	73.9	24.5	↓67%	1.3	1.5	76.1	38.8	↓49%	1.4	3.0	96.2	62.3	↓35%	2.0	0.5	82.6	59.3	↓28%	1.3	1.1
SwAV	93.9	19.4	↓79%	3.1	3.0	79.4	11.1	↓86%	1.8	6.4	75.3	24.7	↓67%	1.2	17.4	96.8	79.9	↓17%	1.7	2.7	84.4	54.6	↓35%	1.0	3.0
VICReg	92.8	33.0	↓64%	2.7	3.1	77.8	22.3	↓71%	1.3	4.3	71.3	42.4	↓40%	0.9	9.3	97.1	68.6	↓29%	1.4	2.4	84.3	43.4	↓48%	0.8	2.4

experience more severe drops in both settings, suggesting these methods may create more brittle representations.

The high correlation in adversarial vulnerability between ImageNet and linear evaluation indicates that linear probing provides a reliable assessment of a pre-trained model’s downstream robustness characteristics without requiring extensive adaptation. This finding has practical implications for model selection, suggesting that robustness evaluations on ImageNet can effectively predict linear transfer performance. The full results are in section 4.8 of the Supp. Mat..

**FINETUNE.** Fine-tuning reveals distinct transfer patterns by attack type. For IAA, the correlation between ImageNet and fine-tuned vulnerability nearly vanishes for performance drops (Spearman: 0.12, Pearson: 0.36), indicating that fine-tuning substantially reshapes defense against instance-specific attacks. Conversely, UAP vulnerability correlation remains high (Spearman: 0.88, Pearson: 0.93), suggesting that susceptibility to universal perturbations is more persistently encoded in the network regardless of parameter adaptation. This attack-dependent correlation disparity reveals that universal perturbation vulnerabilities, which exploit systematic weaknesses across the feature space, are deeply encoded in the network’s architecture and learning approach, while instance-specific vulnerabilities are more malleable through fine-tuning. The absolute magnitude of performance drops diminishes considerably after fine-tuning across all methods (IAA: 49% vs. 60% in linear, UAP: 43% vs. 49% in linear), highlighting fine-tuning’s effectiveness in mitigating vulnerability. MoCoV3 continues to demonstrate superior robustness with the smallest drops (IAA: 45%, UAP: 38%), while BYOL shows dramatic improvement from ImageNet to fine-tuning for IAA attacks (from 56% to 47%). These findings suggest different mechanisms for robustness transfer: UAP vulnerability appears tied to fundamental architectural and algorithmic properties that persist across transfer paradigms, while instance-specific attack vulnerability depends more on the fine-tuning process than initial representation properties. This distinction may be valuable for practical ap-

plications, suggesting that pre-training method selection strongly impacts universal attack robustness, while defense against instance-specific attacks can be substantially improved through appropriate fine-tuning strategies. The full results are in section 4.9 of the Supp. Mat..

**Attributing Adversarial Vulnerability.** Having established the correlations between ImageNet and transfer learning robustness patterns, we now seek to understand the underlying mechanisms causing these disparities across models and training paradigms. Specifically, we investigate whether adversarial vulnerability stems primarily from the backbone feature extractor or the classification head and how this attribution changes between linear probing and fine-tuning.

Our analysis investigates the relationship between adversarial robustness and component-specific vulnerability under FGSM<sub>1</sub> attack (detail in Supp. Mat.), focusing on two metrics: the Direction Ratio  $D = \frac{\text{mean}(1 - \cos(\mathbf{l}_{adv}))}{\text{mean}(1 - \cos(\mathbf{f}, \mathbf{f}_{adv}))}$ , which compares directional shifts in logits ( $\mathbf{l}$ ) versus backbone features ( $\mathbf{f}$ ), and the Magnitude Ratio  $M = \frac{\text{mean}(\|\mathbf{l} - \mathbf{l}_{adv}\|_2)}{\text{mean}(\|\mathbf{f} - \mathbf{f}_{adv}\|_2)}$ , quantifying relative sensitivity to perturbation magnitudes. We fit linear regression models using these ratios to predict adversarial accuracy drop across models.

For probed models, Direction Ratio strongly correlates with vulnerability ( $R^2 = 0.56\text{--}0.85$ ), suggesting that directional instability in the head dominates FGSM robustness. SwAV, with  $D = 3.1$  on CIFAR-10, suffers a 79% accuracy drop, while SimCLR ( $D = 1.5$ ) drops 58%. This may arise from the linear head’s limited capacity to compensate for adversarial noise, amplifying directional shifts in logit space.

After fine-tuning, this correlation weakens significantly ( $R^2 = 0.05\text{--}0.52$ ): SwAV achieves only a 17% drop despite retaining  $D = 1.7$ , implying that fine-tuning enables the head to stabilize predictions even under directional feature shifts. This pattern aligns with our transfer learning analysis, where fine-tuning disrupted the correlation between ImageNet and downstream instance-specific attack robustness. Regression figures are in section 2 of the Supp. Mat.

As in Table 2, self-supervised models exhibit higher pre-fine-tuning Magnitude Ratios (e.g., SwAV  $M = 17.4$  on ImageNet vs. supervised  $M = 3.0$ ), potentially due to their reliance on globally normalized feature spaces, where FGSM perturbations propagate more aggressively to logits. Fine-tuning reduces  $M$  across models (SwAV  $M = 2.7$  post-FT), aligning with improved robustness, possibly by suppressing logit magnitude distortions.

These patterns are specific to FGSM, as its single-step gradient reliance may emphasize head-layer instability, whereas iterative attacks could exploit backbone vulnerabilities differently. While our analysis tentatively links directional logit shifts ( $D$ ) and magnitude sensitivity ( $M$ ) to robustness, dataset-dependent variations—such as weaker correlations on CIFAR-100 FT—highlight the need for broader evaluation across threat models to generalize these insights.

We also measured inter-class and intra-class distances for both probed and fine-tuned CIFAR-10 representations; however, these metrics did not yield meaningful correlations that explain the observed differences in adversarial robustness. The detailed regression figures, inter/intra-class distance measurements, and t-SNE [102] visualizations of feature spaces are provided in section 3 of the Supp. Mat.

### 4.3. Segmentation

Unlike in classification, we observe no strong correlation between ImageNet robustness and segmentation performance across both PASCAL VOC and CityScapes datasets. Self-supervised approaches demonstrate competitive performance in clean conditions, with VICReg leading on PASCAL VOC (77.89 mIOU with frozen backbone) and SwAV on CityScapes (66.48 mIOU). All models suffer catastrophic performance degradation (74-84%) under adversarial attacks regardless of training methodology. This uniform degradation pattern suggests attacks primarily target segmentation modules rather than backbones.

Our experiments with frozen versus unfrozen backbones reveal that frozen backbones generally achieve both higher clean performance and slightly better adversarial robustness on PASCAL VOC. The supervised model’s exception to this pattern stems from using the standard MMSegmentation model for the unfrozen case due to reproduction challenges. These findings indicate that while SSL models produce competitive segmentation performance in clean conditions, they offer minimal advantage in terms of adversarial robustness for segmentation tasks—unlike their significant impact on object recognition. This highlights the need for robustness techniques specifically designed for segmentation architectures rather than focusing solely on backbone improvements. The full results are in section 4.2 of the Supp. Mat.

### 4.4. Detection

Detection results show distinct patterns from recognition and segmentation tasks. On INRIA Person with unfrozen backbones, SwAV demonstrates highest robustness (72% decrease), while the Supervised model shows poorest performance (89% decrease). With frozen backbones, Barlow Twins and DINO lead in robustness (both 75% decrease), while VICReg becomes unexpectedly vulnerable (84% decrease), contradicting its recognition performance.

COCO dataset results show improved robustness overall, with Barlow Twins maintaining the strongest performance (50% decrease) and the Supervised model remaining the least robust (67% decrease). This consistent weakness in the Supervised model suggests inherent robustness benefits from self-supervised pretraining.

These findings indicate that task-specific architectures significantly influence adversarial robustness, and robustness in ImageNet classification doesn’t necessarily transfer to detection tasks. This highlights the importance of task-specific evaluations and suggests that backbone architecture becomes less critical than overall model design for downstream applications. The full results are in section 4.3 of the Supp. Mat.

## 5. Conclusion

Our evaluation suggests that SSL models tend to exhibit better adversarial robustness than supervised approaches in image classification tasks, with MoCoV3 showing strong performance, possibly due to its momentum encoders and prediction head. This advantage appears less pronounced in segmentation and detection tasks, where task-specific architectures may have greater influence than backbone properties. We observe that architectural effects vary by objective: DINO performs well with ViT architectures, while MoCoV3 shows better results with CNNs. Our experiments indicate that extended training periods don’t seem to compromise robustness and may even slightly enhance it. We note that vulnerability to universal perturbations appears to transfer more consistently across learning paradigms, while susceptibility to instance-specific attacks can potentially be reduced through fine-tuning. These observations point to a complex relationship between SSL objectives, architectures, and downstream applications that merits further investigation. While our work provides insights into the adversarial robustness characteristics of various SSL approaches, many questions remain about the underlying mechanisms and optimal approaches for different vision tasks. We hope these findings contribute to the ongoing efforts toward developing more resilient visual representation learning methods.



## References

- [1] Maksym Andriushchenko, Francesco Croce, Nicolas Flammarion, and Matthias Hein. Square attack: a query-efficient black-box adversarial attack via random search. In *European conference on computer vision*, pages 484–501. Springer, 2020. 15
- [2] Yuki Markus Asano, Christian Rupprecht, and Andrea Vedaldi. Self-labelling via simultaneous clustering and representation learning, 2020. 2
- [3] Yutong Bai, Jieru Mei, Alan Yuille, and Cihang Xie. Are transformers more robust than cnns?, 2021. 6
- [4] Yang Bai, Yuyuan Zeng, Yong Jiang, Shu-Tao Xia, Xingjun Ma, and Yisen Wang. Improving adversarial robustness via channel-wise activation suppressing, 2022. 1
- [5] Randall Balestriero, Mark Ibrahim, Vlad Sobal, Ari S. Morcos, Shashank Shekhar, Tom Goldstein, Florian Bordes, Adrien Bardes, Grégoire Mialon, Yuandong Tian, Avi Schwarzschild, Andrew Gordon Wilson, Jonas Geiping, Quentin Garrido, Pierre Fernandez, Amir Bar, Hamed Pirsiavash, Yann LeCun, and Micah Goldblum. A cookbook of self-supervised learning. *ArXiv*, abs/2304.12210, 2023. 1
- [6] Yuanhao Ban and Yinpeng Dong. Pre-trained adversarial perturbations. *Advances in Neural Information Processing Systems*, 35:1196–1209, 2022. 16
- [7] Adrien Bardes, Jean Ponce, and Yann LeCun. Vircreg: Variance-invariance-covariance regularization for self-supervised learning, 2022. 2, 4
- [8] Yoshua Bengio, Geoffrey Hinton, Andrew Yao, Dawn Song, Pieter Abbeel, Trevor Darrell, Yuval Noah Harari, Ya-Qin Zhang, Lan Xue, Shai Shalev-Shwartz, Gillian Hadfield, Jeff Clune, Tegan Maharaj, Frank Hutter, Atılım Güneş Baydin, Sheila McIlraith, Qiqi Gao, Ashwin Acharya, David Krueger, Anca Dragan, Philip Torr, Stuart Russell, Daniel Kahneman, Jan Brauner, and Sören Mindermann. Managing extreme ai risks amid rapid progress. *Science*, 384(6698):842–845, 2024. 1
- [9] Rishi Bommasani, Drew A. Hudson, Ehsan Adeli, Russ Altman, Simran Arora, Sydney von Arx, Michael S. Bernstein, Jeannette Bohg, Antoine Bosselut, Emma Brunskill, Erik Brynjolfsson, Shyamal Buch, Dallas Card, Rodrigo Castellon, Niladri Chatterji, Annie Chen, Kathleen Creel, Jared Quincy Davis, Dora Demszky, Chris Donahue, Moussa Doumbouya, Esin Durmus, Stefano Ermon, John Etchemendy, Kawin Ethayarajh, Li Fei-Fei, Chelsea Finn, Trevor Gale, Lauren Gillespie, Karan Goel, Noah Goodman, Shelby Grossman, Neel Guha, Tatsunori Hashimoto, Peter Henderson, John Hewitt, Daniel E. Ho, Jenny Hong, Kyle Hsu, Jing Huang, Thomas Icard, Saahil Jain, Dan Jurafsky, Pratyusha Kalluri, Siddharth Karamcheti, Geoff Keeling, Fereshte Khani, Omar Khattab, Pang Wei Koh, Mark Krass, Ranjay Krishna, Rohith Kuditipudi, Ananya Kumar, Faisal Ladhak, Mina Lee, Tony Lee, Jure Leskovec, Isabelle Levent, Xiang Lisa Li, Xuechen Li, Tengyu Ma, Ali Malik, Christopher D. Manning, Suvir Mirchandani, Eric Mitchell, Zanele Munyikwa, Suraj Nair, Avanika Narayan, Deepak Narayanan, Ben Newman, Allen Nie, Juan Carlos Niebles, Hamed Nilforoshan, Julian Nyarko, Giray Ogut, Laurel Orr, Isabel Papadimitriou, Joon Sung Park, Chris Piech, Eva Portelance, Christopher Potts, Aditi Raghunathan, Rob Reich, Hongyu Ren, Frieda Rong, Yusuf Roohani, Camilo Ruiz, Jack Ryan, Christopher Ré, Dorsa Sadigh, Shiori Sagawa, Keshav Santhanam, Andy Shih, Krishnan Srinivasan, Alex Tamkin, Rohan Taori, Armin W. Thomas, Florian Tramèr, Rose E. Wang, William Wang, Bohan Wu, Jiajun Wu, Yuhuai Wu, Sang Michael Xie, Michihiro Yasunaga, Jiaxuan You, Matei Zaharia, Michael Zhang, Tianyi Zhang, Xikun Zhang, Yuhui Zhang, Lucia Zheng, Kaitlyn Zhou, and Percy Liang. On the opportunities and risks of foundation models, 2022. 1
- [10] Lukas Bossard, Matthieu Guillaumin, and Luc Van Gool. Food-101 – mining discriminative components with random forests. In *Computer Vision – ECCV 2014*, pages 446–461, Cham, 2014. Springer International Publishing. 4
- [11] Nicholas Carlini and David Wagner. Towards evaluating the robustness of neural networks. In *2017 IEEE Symposium on Security and Privacy (SP)*, pages 39–57. IEEE, 2017. 14
- [12] Yair Carmon, Aditi Raghunathan, Ludwig Schmidt, Percy Liang, and John C. Duchi. Unlabeled data improves adversarial robustness, 2022. 3
- [13] Mathilde Caron, Piotr Bojanowski, Armand Joulin, and Matthijs Douze. Deep clustering for unsupervised learning of visual features, 2019. 2
- [14] Mathilde Caron, Ishan Misra, Julien Mairal, Priya Goyal, Piotr Bojanowski, and Armand Joulin. Unsupervised learning of visual features by contrasting cluster assignments. 2020. 2, 4, 6
- [15] Mathilde Caron, Hugo Touvron, Ishan Misra, Hervé Jégou, Julien Mairal, Piotr Bojanowski, and Armand Joulin. Emerging properties in self-supervised vision transformers. *2021 IEEE/CVF International Conference on Computer Vision (ICCV)*, pages 9630–9640, 2021. 1, 2, 4, 6
- [16] Anirban Chakraborty, Manar Alam, Vishal Dey, Anupam Chattopadhyay, and Debdeep Mukhopadhyay. Adversarial attacks and defences: A survey, 2018. 2
- [17] Ashutosh Chabey, Nikhil Agrawal, Kavya Barnwal, Keerat K Guliani, and Pramod Mehta. Universal adversarial perturbations: A survey. *arXiv preprint arXiv:2005.08087*, 2020. 2, 15
- [18] Liang-Chieh Chen, Yukun Zhu, George Papandreou, Florian Schroff, and Hartwig Adam. Encoder-decoder with atrous separable convolution for semantic image segmentation, 2018. 4
- [19] Pin-Yu Chen, Yash Sharma, Huan Zhang, Jinfeng Yi, and Cho-Jui Hsieh. Ead: elastic-net attacks to deep neural networks via adversarial examples. In *Proceedings of the AAAI conference on artificial intelligence*, 2018. 15
- [20] Ting Chen, Simon Kornblith, Mohammad Norouzi, and Geoffrey E. Hinton. A simple framework for contrastive learning of visual representations. *ArXiv*, abs/2002.05709, 2020. 1, 2, 4, 6
- [21] Tianlong Chen, Sijia Liu, Shiyu Chang, Yu Cheng, Lisa Amini, and Zhangyang Wang. Adversarial robustness: From self-supervised pre-training to fine-tuning, 2020. 3

- [22] Xinlei Chen and Kaiming He. Exploring simple siamese representation learning. *2021 IEEE/CVF Conference on Computer Vision and Pattern Recognition (CVPR)*, pages 15745–15753, 2020. 2, 5
- [23] Xinlei Chen, Haoqi Fan, Ross Girshick, and Kaiming He. Improved baselines with momentum contrastive learning. *arXiv preprint arXiv:2003.04297*, 2020. 2, 5
- [24] Xinlei Chen\*, Saining Xie\*, and Kaiming He. An empirical study of training self-supervised vision transformers. *arXiv preprint arXiv:2104.02057*, 2021. 1, 2, 4, 6
- [25] Prakash Chandra Chhipa, Johan Rodahl Holmgren, Kanjar De, Rajkumar Saini, and Marcus Liwicki. Can self-supervised representation learning methods withstand distribution shifts and corruptions?, 2023. 3
- [26] Mircea Cimpoi, Subhransu Maji, Iasonas Kokkinos, Sammy Mohamed, and Andrea Vedaldi. Describing textures in the wild, 2013. 4
- [27] Marius Cordts, Mohamed Omran, Sebastian Ramos, Timo Rehfeld, Markus Enzweiler, Rodrigo Benenson, Uwe Franke, Stefan Roth, and Bernt Schiele. The cityscapes dataset for semantic urban scene understanding, 2016. 4
- [28] N. Dalal and B. Triggs. Histograms of oriented gradients for human detection. In *2005 IEEE Computer Society Conference on Computer Vision and Pattern Recognition (CVPR'05)*, pages 886–893 vol. 1, 2005. 4
- [29] Mostafa Dehghani, Josip Djolonga, Basil Mustafa, Piotr Padlewski, Jonathan Heek, Justin Gilmer, Andreas Steiner, Mathilde Caron, Robert Geirhos, Ibrahim Alabdulmohsin, Rodolphe Jenatton, Lucas Beyer, Michael Tschannen, Anurag Arnab, Xiao Wang, Carlos Riquelme, Matthias Minderer, Joan Puigcerver, Utku Evci, Manoj Kumar, Sjoerd van Steenkiste, Gamaleldin F. Elsayed, Aravindh Mahendran, Fisher Yu, Avital Oliver, Fantine Huot, Jasmijn Bastings, Mark Patrick Collier, Alexey Gritsenko, Vighnesh Birodkar, Cristina Vasconcelos, Yi Tay, Thomas Mensink, Alexander Kolesnikov, Filip Pavetić, Dustin Tran, Thomas Kipf, Mario Lučić, Xiaohua Zhai, Daniel Keysers, Jeremiah Harmsen, and Neil Houlsby. Scaling vision transformers to 22 billion parameters, 2023. 6
- [30] Yingpeng Deng and Lina J Karam. Universal adversarial attack via enhanced projected gradient descent. In *2020 IEEE International Conference on Image Processing (ICIP)*, pages 1241–1245. IEEE, 2020. 15
- [31] Jacob Devlin, Ming-Wei Chang, Kenton Lee, and Kristina Toutanova. Bert: Pre-training of deep bidirectional transformers for language understanding, 2019. 2
- [32] Yinpeng Dong, Fangzhou Liao, Tianyu Pang, Hang Su, Jun Zhu, Xiaolin Hu, and Jianguo Li. Boosting adversarial attacks with momentum, 2018. 4
- [33] Yinpeng Dong, Tianyu Pang, Hang Su, and Jun Zhu. Evading defenses to transferable adversarial examples by translation-invariant attacks. In *Proceedings of the IEEE/CVF Conference on Computer Vision and Pattern Recognition*, pages 4312–4321, 2019. 14
- [34] Alexey Dosovitskiy, Lucas Beyer, Alexander Kolesnikov, Dirk Weissenborn, Xiaohua Zhai, Thomas Unterthiner, Mostafa Dehghani, Matthias Minderer, Georg Heigold, Sylvain Gelly, Jakob Uszkoreit, and Neil Houlsby. An image is worth 16x16 words: Transformers for image recognition at scale, 2021. 1, 4, 6
- [35] Linus Ericsson, Henry Gouk, and Timothy M. Hospedales. How well do self-supervised models transfer?, 2021. 4
- [36] Aleksandr Ermolov, Aliaksandr Siarohin, Enver Sangineto, and Nicu Sebe. Whitening for self-supervised representation learning, 2021. 2
- [37] M. Everingham, L. Van Gool, C. K. I. Williams, J. Winn, and A. Zisserman. The PASCAL Visual Object Classes Challenge 2012 (VOC2012) Results. <http://www.pascal-network.org/challenges/VOC/voc2012/workshop/index.html>. 4
- [38] Alhussein Fawzi, Seyed-Mohsen Moosavi-Dezfooli, and Pascal Frossard. Robustness of classifiers: from adversarial to random noise, 2016. 1
- [39] Li Fei-Fei, R. Fergus, and P. Perona. Learning generative visual models from few training examples: An incremental bayesian approach tested on 101 object categories. In *2004 Conference on Computer Vision and Pattern Recognition Workshop*, pages 178–178, 2004. 4
- [40] Lianli Gao, Qilong Zhang, Jingkuan Song, Xianglong Liu, and Heng Tao Shen. Patch-wise attack for fooling deep neural network. In *Computer Vision—ECCV 2020: 16th European Conference, Glasgow, UK, August 23–28, 2020, Proceedings, Part XXVIII 16*, pages 307–322. Springer, 2020. 14
- [41] Lianli Gao, Qilong Zhang, Jingkuan Song, and Heng Tao Shen. Patch-wise++ perturbation for adversarial targeted attacks. *arXiv preprint arXiv:2012.15503*, 2020. 14
- [42] Micah Goldblum, Hossein Souri, Renkun Ni, Manli Shu, Viraj Prabhu, Gowthami Somepalli, Prithvijit Chattopadhyay, Mark Ibrahim, Adrien Bardes, Judy Hoffman, Rama Chellappa, Andrew Gordon Wilson, and Tom Goldstein. Battle of the backbones: A large-scale comparison of pre-trained models across computer vision tasks, 2023. 3
- [43] Ian J Goodfellow, Jonathon Shlens, and Christian Szegedy. Explaining and harnessing adversarial examples. *arXiv preprint arXiv:1412.6572*, 2014. 1, 4, 14
- [44] Jean-Bastien Grill, Florian Strub, Florent Altch’e, Corentin Tallec, Pierre H. Richemond, Elena Buchatskaya, Carl Doersch, Bernardo Ávila Pires, Zhaohan Daniel Guo, Mohammad Gheshlaghi Azar, Bilal Piot, Koray Kavukcuoglu, Rémi Munos, and Michal Valko. Bootstrap your own latent: A new approach to self-supervised learning. *ArXiv*, abs/2006.07733, 2020. 2, 4
- [45] Rohit Gupta, Naveed Akhtar, Ajmal Mian, and Mubarak Shah. Contrastive self-supervised learning leads to higher adversarial susceptibility, 2022. 2, 4
- [46] Jamie Hayes and George Danezis. Learning universal adversarial perturbations with generative models. In *2018 IEEE Security and Privacy Workshops (SPW)*, pages 43–49. IEEE, 2018. 15
- [47] Kaiming He, Xiangyu Zhang, Shaoqing Ren, and Jian Sun. Deep residual learning for image recognition, 2015. 1, 4
- [48] Kaiming He, Haoqi Fan, Yuxin Wu, Saining Xie, and Ross Girshick. Momentum contrast for unsupervised visual rep-

- resentation learning. *arXiv preprint arXiv:1911.05722*, 2019. 2, 5
- [49] Kaiming He, Xinlei Chen, Saining Xie, Yanghao Li, Piotr Dollár, and Ross B. Girshick. Masked autoencoders are scalable vision learners. *2022 IEEE/CVF Conference on Computer Vision and Pattern Recognition (CVPR)*, pages 15979–15988, 2021. 1, 2
- [50] Dan Hendrycks, Mantas Mazeika, Saurav Kadavath, and Dawn Song. Using self-supervised learning can improve model robustness and uncertainty, 2019. 3
- [51] Chih-Hui Ho and Nuno Vasconcelos. Contrastive learning with adversarial examples, 2020. 2, 4
- [52] Jonathan Ho, Ajay Jain, and Pieter Abbeel. Denoising diffusion probabilistic models, 2020. 1
- [53] Hao Huang, Ziyang Chen, Huanran Chen, Yongtao Wang, and Kevin Zhang. T-sea: Transfer-based self-ensemble attack on object detection. In *Proceedings of the IEEE/CVF conference on computer vision and pattern recognition*, pages 20514–20523, 2023. 4
- [54] Minyoung Huh, Pulkit Agrawal, and Alexei A. Efros. What makes imagenet good for transfer learning?, 2016. 4
- [55] Mark Ibrahim, David Klindt, and Randall Balestriero. Occam’s razor for self supervised learning: What is sufficient to learn good representations?, 2024. 5
- [56] Andrew Ilyas, Shibani Santurkar, Dimitris Tsipras, Logan Engstrom, Brandon Tran, and Aleksander Madry. Adversarial examples are not bugs, they are features, 2019. 1
- [57] Ziyu Jiang, Tianlong Chen, Ting Chen, and Zhangyang Wang. Robust pre-training by adversarial contrastive learning, 2020. 2, 4
- [58] Valentin Khrulkov and Ivan Oseledets. Art of singular vectors and universal adversarial perturbations. In *Proceedings of the IEEE Conference on Computer Vision and Pattern Recognition*, pages 8562–8570, 2018. 15
- [59] Minseon Kim, Jihoon Tack, and Sung Ju Hwang. Adversarial self-supervised contrastive learning, 2020. 2, 4
- [60] Moo Jin Kim, Karl Pertsch, Siddharth Karamcheti, Ted Xiao, Ashwin Balakrishna, Suraj Nair, Rafael Rafailov, Ethan Foster, Grace Lam, Pannag Sanketi, Quan Vuong, Thomas Kollar, Benjamin Burchfiel, Russ Tedrake, Dorsa Sadigh, Sergey Levine, Percy Liang, and Chelsea Finn. Openvla: An open-source vision-language-action model, 2024. 1
- [61] Diederik P. Kingma and Jimmy Ba. Adam: A method for stochastic optimization, 2017. 4
- [62] Antoni Kowalczyk, Jan Dubiński, Atiyeh Ashari Ghomi, Yi Sui, George Stein, Jiapeng Wu, Jesse C. Cresswell, Franziska Boenisch, and Adam Dziedzic. Benchmarking robust self-supervised learning across diverse downstream tasks, 2024. 1, 3
- [63] Jonathan Krause, Michael Stark, Jia Deng, and Li Fei-Fei. 3d object representations for fine-grained categorization. In *2013 IEEE International Conference on Computer Vision Workshops*, pages 554–561, 2013. 4
- [64] Alex Krizhevsky. Learning multiple layers of features from tiny images. 2009. 4
- [65] Y. Lecun, L. Bottou, Y. Bengio, and P. Haffner. Gradient-based learning applied to document recognition. *Proceedings of the IEEE*, 86(11):2278–2324, 1998. 6
- [66] Ang Li, Yifei Wang, Yiwen Guo, and Yisen Wang. Adversarial examples are not real features, 2024. 1
- [67] Tsung-Yi Lin, Michael Maire, Serge Belongie, Lubomir Bourdev, Ross Girshick, James Hays, Pietro Perona, Deva Ramanan, C. Lawrence Zitnick, and Piotr Dollár. Microsoft coco: Common objects in context, 2015. 4
- [68] Yantao Lu, Yunhan Jia, Jianyu Wang, Bai Li, Weiheng Chai, Lawrence Carin, and Senem Velipasalar. Enhancing cross-task black-box transferability of adversarial examples with dispersion reduction. In *Proceedings of the IEEE/CVF conference on Computer Vision and Pattern Recognition*, pages 940–949, 2020. 15
- [69] Rundong Luo, Yifei Wang, and Yisen Wang. Rethinking the effect of data augmentation in adversarial contrastive learning, 2023. 3
- [70] Aleksander Madry, Aleksandar Makelov, Ludwig Schmidt, Dimitris Tsipras, and Adrian Vladu. Towards deep learning models resistant to adversarial attacks. *arXiv preprint arXiv:1706.06083*, 2017. 4, 14
- [71] Subhansu Maji, Esa Rahtu, Juho Kannala, Matthew Blaschko, and Andrea Vedaldi. Fine-grained visual classification of aircraft, 2013. 4
- [72] Seyed-Mohsen Moosavi-Dezfooli, Alhussein Fawzi, Omar Fawzi, and Pascal Frossard. Universal adversarial perturbations. In *Proceedings of the IEEE conference on computer vision and pattern recognition*, pages 1765–1773, 2017. 15
- [73] Konda Reddy Mopuri, Utsav Garg, and R Venkatesh Babu. Fast feature fool: A data independent approach to universal adversarial perturbations. *arXiv preprint arXiv:1707.05572*, 2017. 16
- [74] Konda Reddy Mopuri, Aditya Ganeshan, and R Venkatesh Babu. Generalizable data-free objective for crafting universal adversarial perturbations. *IEEE transactions on pattern analysis and machine intelligence*, 41(10):2452–2465, 2018. 16
- [75] Konda Reddy Mopuri, Utkarsh Ojha, Utsav Garg, and R Venkatesh Babu. Nag: Network for adversary generation. In *Proceedings of the IEEE conference on computer vision and pattern recognition*, pages 742–751, 2018. 15
- [76] Warren Morningstar, Alex Bijamov, Chris Duvarney, Luke Friedman, Neha Kalibhat, Luyang Liu, Philip Mansfield, Renan Rojas-Gomez, Karan Singhal, Bradley Green, and Sushant Prakash. Augmentations vs algorithms: What works in self-supervised learning, 2024. 5
- [77] Muzammal Naseer, Salman Khan, Munawar Hayat, Fahad Shahbaz Khan, and Fatih Porikli. A self-supervised approach for adversarial robustness. In *Proceedings of the IEEE/CVF Conference on Computer Vision and Pattern Recognition*, pages 262–271, 2020. 6, 15
- [78] Yurii Nesterov. A method for solving the convex programming problem with convergence rate  $o(1/k^2)$ . *Proceedings of the USSR Academy of Sciences*, 269:543–547, 1983. 4
- [79] A. Tuan Nguyen, Ser Nam Lim, and Philip Torr. Task-agnostic robust representation learning, 2022. 2, 4

- [80] Maxime Oquab, Timothée Darcet, Théo Moutakanni, Huy Vo, Marc Szafraniec, Vasil Khalidov, Pierre Fernandez, Daniel Haziza, Francisco Massa, Alaaeldin El-Nouby, Mahmoud Assran, Nicolas Ballas, Wojciech Galuba, Russell Howes, Po-Yao Huang, Shang-Wen Li, Ishan Misra, Michael Rabbat, Vasu Sharma, Gabriel Synnaeve, Hu Xu, Hervé Jegou, Julien Mairal, Patrick Labatut, Armand Joulin, and Piotr Bojanowski. Dinov2: Learning robust visual features without supervision, 2024. 1, 6
- [81] Utku Ozbulak, Hyun Jung Lee, Beril Boga, Esra Timothy Anzaku, Homin Park, Arnout Van Messem, Wesley De Neve, and Joris Vankerschaver. Know your self-supervised learning: A survey on image-based generative and discriminative training, 2023. 3
- [82] Serdar Ozsoy, Shadi Hamdan, Serkan Ö. Arik, Deniz Yuret, and Alper T. Erdogan. Self-supervised learning with an information maximization criterion, 2022. 2
- [83] Adam Paszke, Sam Gross, Francisco Massa, Adam Lerer, James Bradbury, Gregory Chanan, Trevor Killeen, Zeming Lin, Natalia Gimelshein, Luca Antiga, Alban Desmaison, Andreas Köpf, Edward Yang, Zach DeVito, Martin Raison, Alykhan Tejani, Sasank Chilamkurthy, Benoit Steiner, Lu Fang, Junjie Bai, and Soumith Chintala. Pytorch: An imperative style, high-performance deep learning library, 2019. 4
- [84] Francesco Pinto, Philip H. S. Torr, and Puneet K. Dokania. An impartial take to the cnn vs transformer robustness contest, 2022. 6
- [85] Maura Pintor, Fabio Roli, Wieland Brendel, and Battista Biggio. Fast minimum-norm adversarial attacks through adaptive norm constraints, 2021. 4
- [86] Jary Pomponi, Simone Scardapane, and Aurelio Uncini. Pixle: a fast and effective black-box attack based on rearranging pixels. In *2022 International Joint Conference on Neural Networks (IJCNN)*, pages 1–7. IEEE, 2022. 15
- [87] Alec Radford and Karthik Narasimhan. Improving language understanding by generative pre-training. 2018. 2
- [88] Shaoqing Ren, Kaiming He, Ross Girshick, and Jian Sun. Faster r-cnn: Towards real-time object detection with region proposal networks, 2016. 4
- [89] Jérôme Rony, Jean-Christophe Pesquet, and Ismail Ben Ayed. Proximal splitting adversarial attacks for semantic segmentation. In *IEEE Conference on Computer Vision and Pattern Recognition (CVPR)*, 2023. 4
- [90] Olga Russakovsky, Jia Deng, Hao Su, Jonathan Krause, Sanjeev Satheesh, Sean Ma, Zhiheng Huang, Andrej Karpathy, Aditya Khosla, Michael Bernstein, Alexander C. Berg, and Li Fei-Fei. Imagenet large scale visual recognition challenge, 2015. 2, 3, 4
- [91] Ludwig Schmidt, Shibani Santurkar, Dimitris Tsipras, Kunal Talwar, and Aleksander Mądry. Adversarially robust generalization requires more data, 2018. 1
- [92] Leo Schwinn, René Raab, An Nguyen, Dario Zanca, and Bjoern Eskofier. Exploring misclassifications of robust neural networks to enhance adversarial attacks. *Applied Intelligence*, 53(17):19843–19859, 2023. 14
- [93] Ali Shafahi, W. Ronny Huang, Christoph Studer, Soheil Feizi, and Tom Goldstein. Are adversarial examples inevitable?, 2020. 1
- [94] Kihyuk Sohn. Improved deep metric learning with multi-class n-pair loss objective. In *Neural Information Processing Systems*, 2016. 5
- [95] Jiawei Su, Danilo Vasconcellos Vargas, and Kouichi Sakurai. One pixel attack for fooling deep neural networks. *IEEE Transactions on Evolutionary Computation*, 23(5): 828–841, 2019. 15
- [96] Christian Szegedy, Wojciech Zaremba, Ilya Sutskever, Joan Bruna, Dumitru Erhan, Ian Goodfellow, and Rob Fergus. Intriguing properties of neural networks. *arXiv preprint arXiv:1312.6199*, 2013. 1
- [97] Thomas Tanay and Lewis Griffin. A boundary tilting perspective on the phenomenon of adversarial examples, 2016. 1
- [98] Hugo Touvron, Thibaut Lavril, Gautier Izacard, Xavier Martinet, Marie-Anne Lachaux, Timothée Lacroix, Baptiste Rozière, Naman Goyal, Eric Hambro, Faisal Azhar, Aurelien Rodriguez, Armand Joulin, Edouard Grave, and Guillaume Lample. Llama: Open and efficient foundation language models, 2023. 1
- [99] Florian Tramèr, Alexey Kurakin, Nicolas Papernot, Ian Goodfellow, Dan Boneh, and Patrick McDaniel. Ensemble adversarial training: Attacks and defenses. *arXiv preprint arXiv:1705.07204*, 2017. 14
- [100] Jonathan Uesato, Brendan O’donoghue, Pushmeet Kohli, and Aaron Oord. Adversarial risk and the dangers of evaluating against weak attacks. In *International conference on machine learning*, pages 5025–5034. PMLR, 2018. 15
- [101] Aaron van den Oord, Yazhe Li, and Oriol Vinyals. Representation learning with contrastive predictive coding, 2019. 5
- [102] Laurens van der Maaten and Geoffrey Hinton. Visualizing data using t-sne. *Journal of Machine Learning Research*, 9 (86):2579–2605, 2008. 8
- [103] Yisen Wang, Difan Zou, Jinfeng Yi, James Bailey, Xingjun Ma, and Quanquan Gu. Improving adversarial robustness requires revisiting misclassified examples. In *ICLR*, 2020. 1
- [104] Yisen Wang, Xingjun Ma, James Bailey, Jinfeng Yi, Bowen Zhou, and Quanquan Gu. On the convergence and robustness of adversarial training, 2022.
- [105] Dongxian Wu, Shu tao Xia, and Yisen Wang. Adversarial weight perturbation helps robust generalization, 2020. 1
- [106] Cihang Xie, Jianyu Wang, Zhishuai Zhang, Yuyin Zhou, Lingxi Xie, and Alan Yuille. Adversarial examples for semantic segmentation and object detection, 2017. 4
- [107] Cihang Xie, Zhishuai Zhang, Yuyin Zhou, Song Bai, Jianyu Wang, Zhou Ren, and Alan L Yuille. Improving transferability of adversarial examples with input diversity. In *Proceedings of the IEEE/CVF conference on computer vision and pattern recognition*, pages 2730–2739, 2019. 14
- [108] Cihang Xie, Mingxing Tan, Boqing Gong, Jiang Wang, Alan Yuille, and Quoc V. Le. Adversarial examples improve image recognition, 2020. 2, 4



- [109] Xilie Xu, Jingfeng Zhang, Feng Liu, Masashi Sugiyama, and Mohan Kankanhalli. Efficient adversarial contrastive learning via robustness-aware coreset selection, 2023. [3](#)
- [110] Zhixing Ye, Xinwen Cheng, and Xiaolin Huang. Fg-uap: Feature-gathering universal adversarial perturbation. In *2023 International Joint Conference on Neural Networks (IJCNN)*, pages 1–8. IEEE, 2023. [15](#), [16](#)
- [111] Jure Zbontar, Li Jing, Ishan Misra, Yann LeCun, and Stéphane Deny. Barlow twins: Self-supervised learning via redundancy reduction, 2021. [2](#), [4](#)
- [112] Chaoning Zhang, Kang Zhang, Chenshuang Zhang, Axi Niu, Jiu Feng, Chang D. Yoo, and In So Kweon. Decoupled adversarial contrastive learning for self-supervised adversarial robustness, 2022. [2](#), [4](#)
- [113] Yuanyi Zhong, Haoran Tang, Junkun Chen, Jian Peng, and Yu-Xiong Wang. Is self-supervised learning more robust than supervised learning?, 2022. [3](#)
- [114] Wen Zhou, Xin Hou, Yongjun Chen, Mengyun Tang, Xiangqi Huang, Xiang Gan, and Yong Yang. Transferable adversarial perturbations. In *Proceedings of the European Conference on Computer Vision (ECCV)*, pages 452–467, 2018. [14](#)

## Supplementary Materials

### 1. Adversarial Attacks

#### 1.1. Instance Adversarial Attacks

Instance adversarial methods, or per-instance generation, involve crafting distinct perturbations for each individual image within the dataset on which the model has been trained or fine-tuned. The generation of these perturbations relies on various techniques, which are determined by the specific goals of the attack, the level of access granted to the model—such as full access to model weights, predictions alone, or prediction scores (logits)—and the distance metrics employed. While multiple classification schemes for adversarial attacks exist, we adopt the widely accepted taxonomy for clarity and consistency.

White-box attacks, in this context, presume complete access to the model, including its architecture and parameters. The primary approach utilizes the gradients derived from the loss function to generate adversarial perturbations. These perturbations are then applied to the image within the constraints of specific distance metrics, such as  $l_0$ ,  $l_1$ ,  $l_2$ , or  $l_\infty$ . Specifically,  $l_0$  measures the number of altered pixels,  $l_1$  quantifies the total absolute difference between images,  $l_2$  computes the Euclidean distance, and  $l_\infty$  captures the magnitude of the largest perturbation applied to any pixel.

Gradient-based methods exploit the gradient of the neural network’s loss function with respect to the input data, strategically altering the input to increase the loss and induce misclassification. The foundational work in this domain is attributed to the Fast Gradient Sign Method (FGSM) [43], which represents the first successful application of gradient-based adversarial perturbations. The Fast Gradient Sign Method (FGSM) computes the gradient of the cross-entropy loss with respect to the input image to determine the perturbation direction that maximizes the loss. The adversarial example is then generated by applying this perturbation in a single step. Due to this one-step update, FGSM is classified as a single-step adversarial attack.

Other FGSM methods apply gradient update more than one time (iteratively) using much smaller step sizes to remain in predetermined  $l_p$  ball. PI-FGSM modify the gradient update rule by focusing on patch-based rather than pixel-wise perturbations [40, 41]. DI-FGSM employs random padding and resizing operations to enhance data input for auxiliary models [107]. TAP also tries to increase cross-model transferability by introducing distance maximization between intermediate feature maps of the adversarial and benign datapoints. It also regularize the images to reduce high frequency perturbations as they claim Convolution may act as a smoother, and it will increase the black-box transferability performance of perturbation [114]. TI-FGSM is also another iterative FGSM method, which uses translated version of benign input to enhance black-box transferability of adversarial attacks to models which are defended with various methods. TIFGSM suggest that these defended models uses different discriminative regions than the model on which adversarial examples are generated, which makes these adversarial examples less effective. TIFGSM uses diversified (shifted and padded) inputs which are obtained by approximating the gradients with convolution kernels [33].

On the other hand, Projected Gradient Descent (PGD) employs an iterative approach, projecting updates back onto the  $l_\infty$  ball of the original data point to generate adversarial perturbations [70]. The key distinction between PGD and FGSM variants, lies in the fact that PGD treats each iteration as a solution to the same optimization problem. PGD ensures that each iterative step remains within the neighborhood of the original data point, while iterative FGSM methods use the newly generated steps to continue further processing.

As with FGSM-based adversarial attacks, several improvements have been made to PGD to address specific needs [70]. For example, PGD- $l_2$  incorporates the  $l_2$  norm instead of the  $l_\infty$  norm to better fool target models [70].

The Jitter attack introduces a novel objective function for adversarial perturbation generation, departing from the conventional Cross-Entropy objective. The study suggests that many adversarial attacks predominantly fool a limited set of classes rather than broadly deceiving the entire model. The proposed objective seeks to enhance the fooling rate across a wider range of classes, aiming for more generalized misclassification [92].

Improving the transferability of per-instance attacks can, however, lead to reduced effectiveness against auxiliary models, and vice-versa [40, 99]. Therefore, various strategies have been proposed to optimize attack performance based on the level of access to the target model.

In contrast, optimization-based attacks approach the generation of adversarial examples as an optimization problem, where a specific objective is minimized subject to given constraints. While gradient-based methods update images directly using gradient information and typically rely on the  $l_\infty$  norm as a boundary, optimization-based methods employ a more formal problem definition that allows for the use of advanced optimization techniques. Consequently, different  $l_p$  norm is utilized in these methods alongside with  $l_\infty$  norms.

[11] constructs a minimization problem—focusing on minimizing the distance between adversarial examples and the original data points across several  $l$  norms—to develop the CW attack, one of the most prominent adversarial attack methods.

The EADEN attacks adopt a similar approach to the CW attack but introduce a modification to the loss function by incorporating an additional  $l_1$  distance term in the minimization problem. The  $l_1$  distance, which measures the total variation of the perturbation, promotes sparsity in the adversarial perturbation. While sparsity is not widely employed in adversarial example generation, it is commonly used in image denoising and restoration techniques. These methods utilize the Iterative Shrinkage-Thresholding Algorithm (ISTA) to solve the corresponding optimization problem [19].

While white-box attacks exploit full access to the model, this is often not a realistic scenario. In many cases, model weights are not shared, or gradient information is unavailable. Although efforts have been made to enhance cross-model transferability, as discussed previously, there are also specific attack schemes designed to target models in black-box settings. For example, the Square Attack leverages random search combined with model scores—probability distributions over class predictions—to generate perturbations. In essence, the algorithm makes random modifications to the input data and retains changes that yield progress toward the objective function [1].

These black-box attacks leverages gradient-free approaches remain relatively underexplored. For instance, the Simultaneous Perturbation Stochastic Approximation (SPSA) method estimates gradients by perturbing the input in random directions, enabling the approximation of gradients for objectives that cannot be differentiated analytically. This approach offers deeper insights into the model’s behavior, with the paper also claiming that the stochastic perturbations introduced by sampling allow algorithms to converge toward a global minimum [100].

Among black-box attacks, some methods focus on  $l_0$  norm-based perturbations. Pixle, for instance, is a black-box attack that utilizes random search and the  $l_0$  norm, altering a small number of pixels to generate adversarial examples [86]. On a more constrained scale, the OnePixel attack modifies only a single pixel, maintaining an  $l_0$  norm of 1, and despite its simplicity, it is capable of fooling models to some extent. However, it is less effective than other methods due to its significant restrictions. This raises important questions about our understanding of Deep Neural Networks and their vulnerability to minimal perturbations [95].

## 1.2. Universal Adversarial Perturbations

The Universal Adversary (UAP) represents a singular perturbation crafted for an entire image dataset. The rationale behind UAP is to identify a perturbation, subject to specified constraints, capable of deceiving the model across a majority of images in the dataset, as initially demonstrated by [72], which utilizes DeepFool to create an average perturbation for the entire dataset. It has been empirically observed that universal adversaries exhibit heightened transferability across diverse models and datasets compared to instance methods. UAP’s are important as they are independent from the input - to some extent - they reveal intrinsic characteristics of models of interest [17, 110].

Two primary techniques are employed for crafting UAPs: (1) generation with generative models, as evidenced by works such as [46, 75], and (2) learning a perturbation designed to disrupt the representations acquired by the models.

UAPs can be further categorized into two classes: data-dependent attacks, which require a comprehensive and general dataset that the attacker seeks to compromise (e.g., ImageNet), and data-independent attacks, which do not rely on any specific dataset.

The first example of UAP, referred to here as UAP-DeepFool (to avoid confusion with the broader class of UAP attacks), utilizes the DeepFool per-instance adversarial attack method which computes perturbations by manipulating the geometry of decision boundaries. UAP-DeepFool iteratively determines the worst-case direction for each data point, and aggregating the results into a universal perturbation - if it is successful -, which is then projected onto an  $l_\infty$  ball [72]. Following this work, UAPEPGD replaces the DeepFool approach with Projected Gradient Descent (PGD), an optimization-based adversarial attack method, to craft stronger adversarial examples [30].

ASV - to our best knowledge - is the first UAP that does not require label information, relying solely on images to generate UAPs. Adversarial Semantic Vectors (ASVs) represent one of the first UAP methods that do not require label information, relying solely on images to generate UAPs. The study suggests that since adversarial perturbations typically exhibit small magnitudes, perturbations in the non-linear maps computed by deep neural networks (DNNs) can be approximated using the Jacobian matrix [58]. Similarly, the STD (Dispersion Reduction) attack seeks to reduce the "contrast" of the internal feature map by targeting the lower layers of Convolutional Neural Networks (CNNs). These lower layers typically detect simple image features such as edges and textures, which are common across datasets and CNN models. By reducing the contrast (measured as the standard deviation of feature maps), the resulting images become indistinguishable to the model [68].

Self-Supervised Perturbation (SSP) takes a different approach, arguing that adversarial examples generated through gradients using labels fail to capture intrinsic properties of models. SSP aims to maximize "feature distortion," the changes in the network’s internal representation caused by adversarial examples compared to the original image, in order to fool subsequent layers in the model [77].

FG-UAP builds upon this by exploiting a phenomenon referred to as "Neural Collapse," where, as noted, different class activations converge to class means, allowing a single common perturbation to fool the model across a wide range of images. This collapse happens primarily in the final layers of the model, and FG-UAP targets these regions to generate effective UAPs [110].

Another label-independent UAP method, L4A, focuses on the success of adversarial perturbations during cross-finetuning. L4A targets the lower layers of models, which remain more stable during finetuning (as they detect simple features), and utilizes the Frobenius norm for optimization, with variants such as L4A-base, L4A-fuse, and L4A-ugs. L4A-base attacks the lowest layer, L4A-fuse attacks lowest 2 layers and L4A-ugs uses samples from a Gaussian distribution where mean and standard deviation is in close range of downstream task [6].

Data-independent UAP methods do not utilize any dataset for adversarial perturbation generation, instead focusing on the intrinsic characteristics of models. Fast Feature Fool (FFF) was the first adversarial attack method that did not use a dataset. It aims to disrupt the features learned at individual CNN layers, proposing that non-discriminative activations can lead to eventual misclassification. FFF over-saturates the learned features at multiple layers, misleading subsequent layers in the network [73]. Following that work GD-UAP, changes the objective a little bit and add other variations such as "mean-std" and "sampled" versions to improve perturbation performance. The "mean-std" variant uses the mean and standard deviation of the test dataset to better align perturbations with dataset characteristics to prevent perturbation dataset mismatch, while the "sampled" version employs a small sample from the dataset to capture its statistics and semantics [74]. In our work, we have also integrated "mean-std" and "one-sample" versions of GD-UAP to FFF, since they are highly similar as GD-UAP is a follow-up work FFF. PD-UAP, another data-independent method, focuses on predictive uncertainty rather than any specific image data, aligning perturbations with task-specific objectives [73].

To accommodate both Vision Transformers (ViTs) and ResNets, we have adapted some of these attacks, originally designed for CNNs, to work with ViTs. For low-level layer attacks, we applied them to the first few blocks of the ViT model, following methods like SSP and L4A. For FFF, which typically uses mean of ReLU activations and a logarithmic operation, we modified the procedure to suit ViTs, which employ GeLU activations (capable of taking values below zero), by applying an absolute value operator between the mean and logarithmic functions. In conducting these experiments, we strove to maintain fair comparisons and minimized the introduction of tweaks to the original methodologies.



### 1.3. FGSM and PGD versions

Attack Version	Attack Type	$\epsilon$	Step Count	Norm
$FGSM_1$	FGSM	0.25	-	$\infty$
$FGSM_2$	FGSM	1	-	$\infty$
$PGD_1$	PGD	0.25	20	$\infty$
$PGD_2$	PGD	1	20	$\infty$
$PGD_3$	PGD	0.25	40	$\infty$
$PGD_4$	PGD	1	40	$\infty$
$PGD_5$	PGD	0.5	40	$\ \cdot\ _2$

Table 3. Hyperparameters of the different FGSM and PGD attacks that we use in ImageNet and transfer learning.

### 1.4. Categories

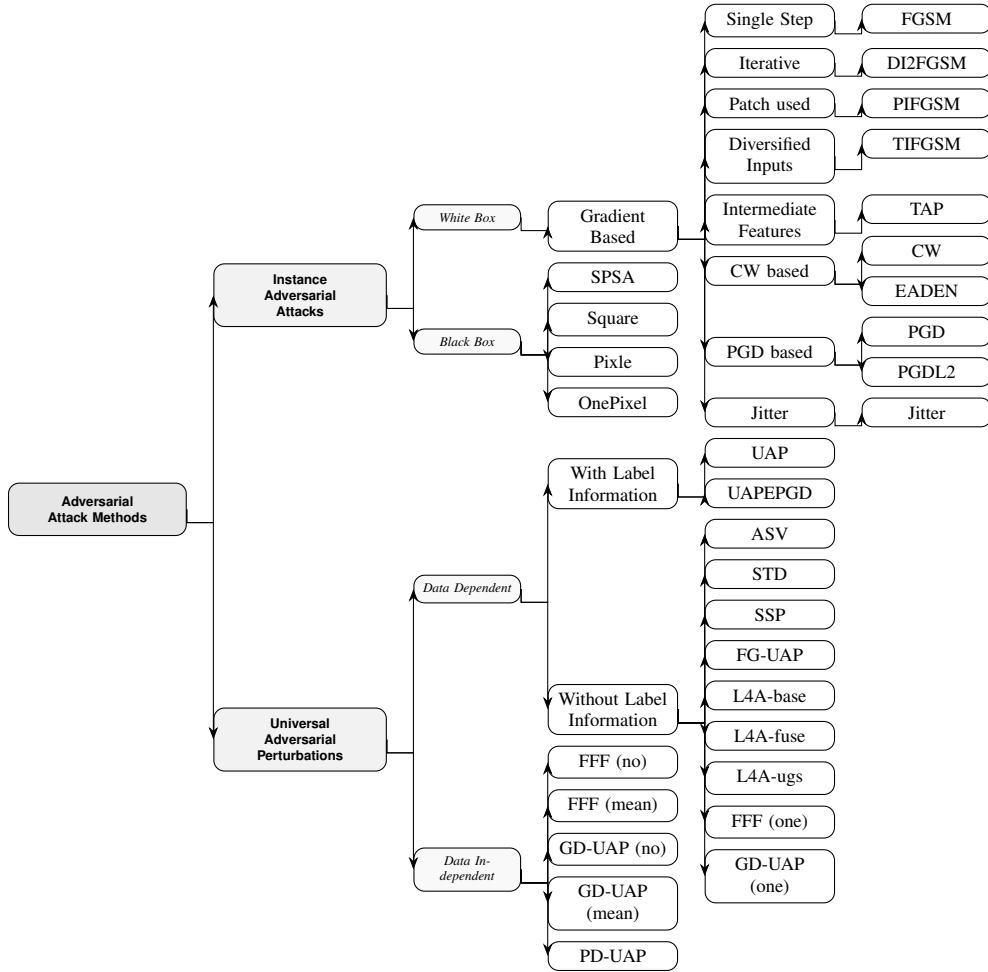


Figure 3. Classification of Selected Adversarial Attack Methods

## 2. Regression Visualization

Regression Analysis of Adversarial Drop% vs. Direction (D) and Magnitude (M) Ratios

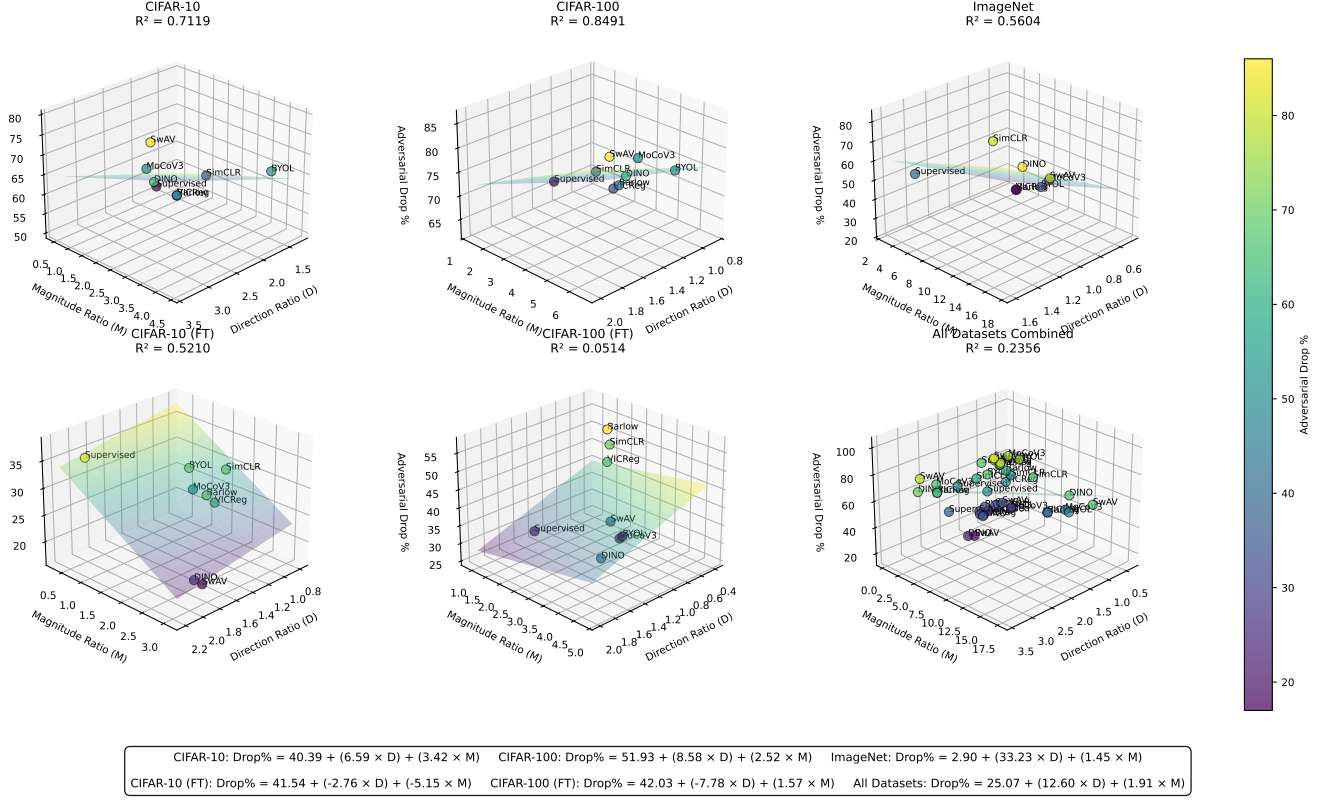


Figure 4. Regression analysis of adversarial performance drop percentage as a function of Direction Ratio (D) and Magnitude Ratio (M) across different datasets. The 3D plots show the fitted regression planes for CIFAR-10, CIFAR-100, and ImageNet datasets (top row), their fine-tuned counterparts (bottom left and center), and the combined analysis (bottom right). Each data point represents a different self-supervised learning method, color-coded by drop percentage. The  $R^2$  values highlight the strong explanatory power for non-fine-tuned datasets (0.56-0.85) compared to fine-tuned ones (0.05-0.52). Note the positive coefficients for D and M in non-fine-tuned scenarios versus negative coefficients in fine-tuned contexts, suggesting fundamentally different robustness mechanisms. Regression equations are displayed below each corresponding plot.

### 3. t-SNE and Inter/Intra Class Distance Visualization

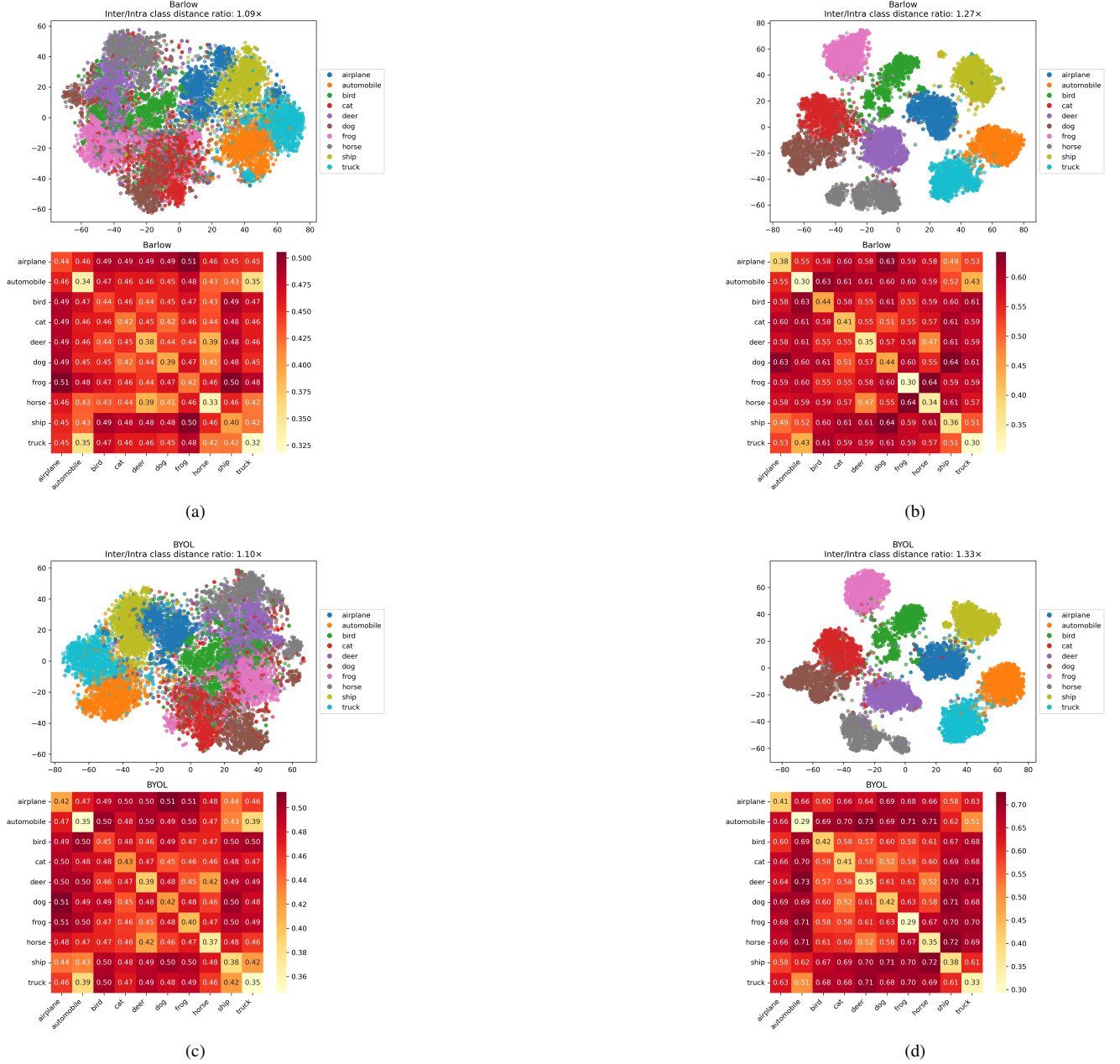
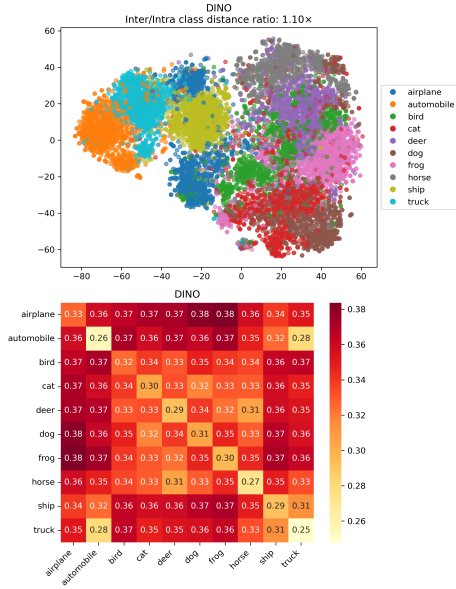
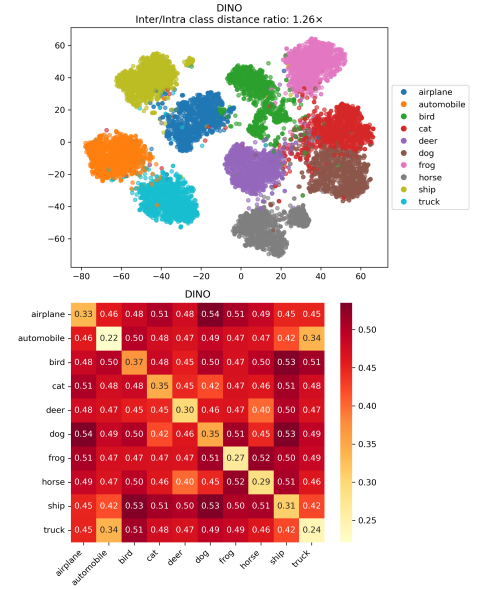


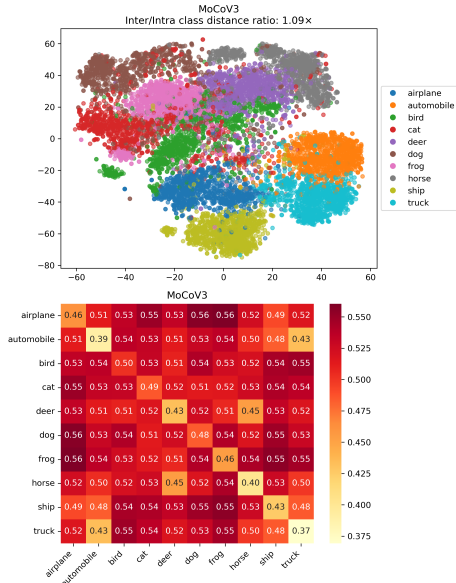
Figure 5. Comparison of feature representations for CIFAR-10 images using ResNet50 with different self-supervised learning (SSL) methods. **Top row:** Results from Barlow. **Bottom row:** Results from BYOL. For each SSL method, **left** panels show results from **probed** models and **right** panels show results from **fine-tuned** models. Within each panel, the **upper** plots display t-SNE visualizations of the 2048-dimensional feature vectors using Euclidean distance, with points colored by class and Inter/Intra class distance ratios indicated. The **lower** plots show the corresponding class-wise distance matrices computed using cosine similarity, with the average distances between samples from each pair of classes. Higher Inter/Intra class distance ratios indicate better class separation in the feature space.



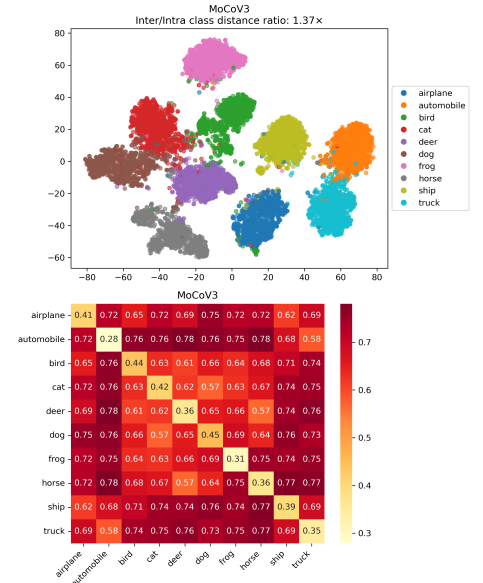
(a)



(b)



(c)



(d)

Figure 6. Comparison of feature representations for CIFAR-10 images using ResNet50 with different self-supervised learning (SSL) methods. **Top row:** Results from DINO. **Bottom row:** Results from MoCoV3. For each SSL method, **left** panels show results from **probed** models and **right** panels show results from **fine-tuned** models. Within each panel, the **upper** plots display t-SNE visualizations of the 2048-dimensional feature vectors using Euclidean distance, with points colored by class and Inter/Intra class distance ratios indicated. The **lower** plots show the corresponding class-wise distance matrices computed using cosine similarity, with the average distances between samples from each pair of classes. Higher Inter/Intra class distance ratios indicate better class separation in the feature space.



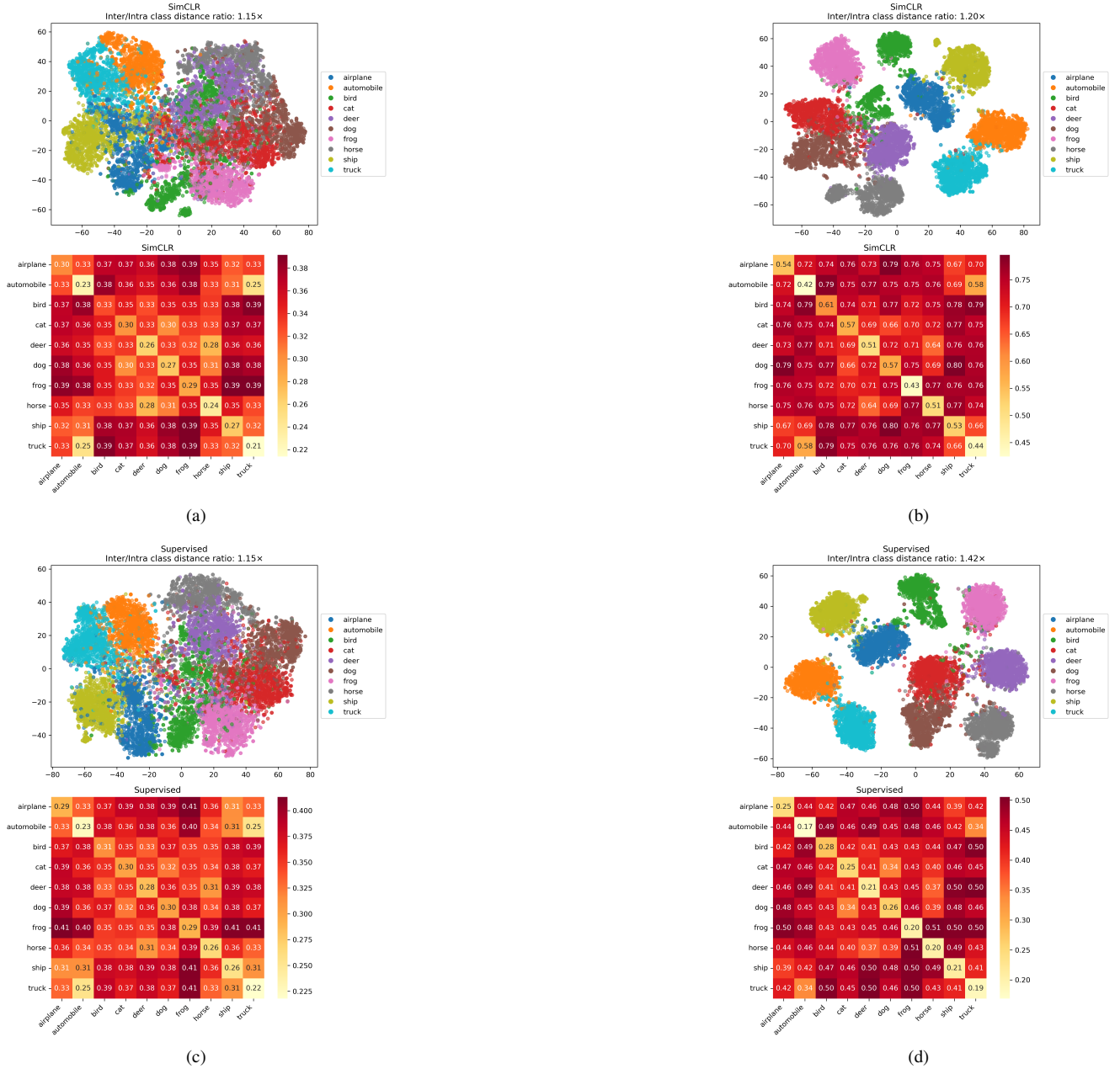


Figure 7. Comparison of feature representations for CIFAR-10 images using ResNet50 with different self-supervised learning (SSL) methods. **Top row:** Results from SimCLR. **Bottom row:** Results from Supervised. For each SSL method, **left** panels show results from **probed** models and **right** panels show results from **fine-tuned** models. Within each panel, the **upper** plots display t-SNE visualizations of the 2048-dimensional feature vectors using Euclidean distance, with points colored by class and Inter/Intra class distance ratios indicated. The **lower** plots show the corresponding class-wise distance matrices computed using cosine similarity, with the average distances between samples from each pair of classes. Higher Inter/Intra class distance ratios indicate better class separation in the feature space.

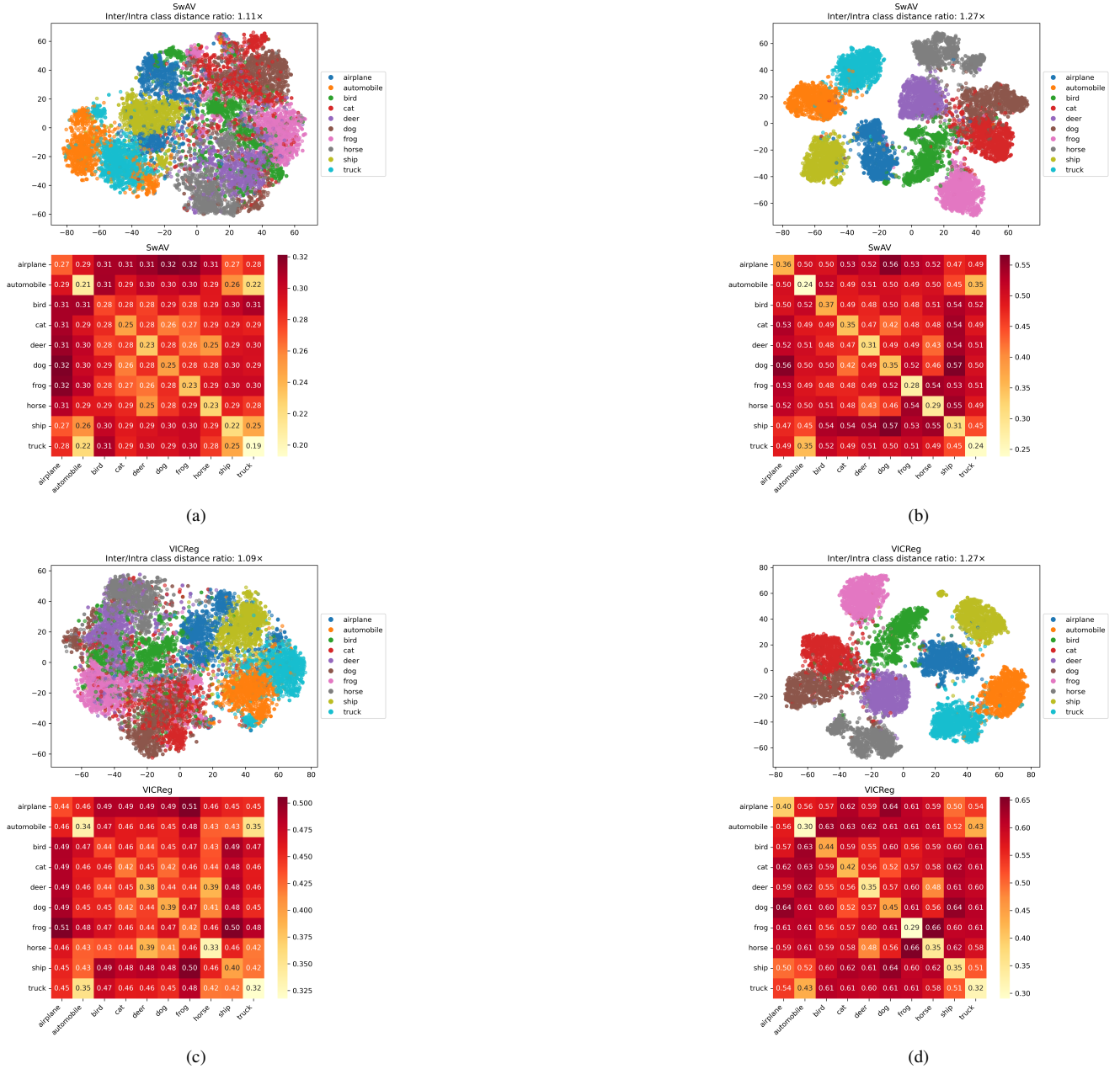


Figure 8. Comparison of feature representations for CIFAR-10 images using ResNet50 with different self-supervised learning (SSL) methods. **Top row:** Results from SwAV. **Bottom row:** Results from VICReg. For each SSL method, **left** panels show results from **probed** models and **right** panels show results from **fine-tuned** models. Within each panel, the **upper** plots display t-SNE visualizations of the 2048-dimensional feature vectors using Euclidean distance, with points colored by class and Inter/Intra class distance ratios indicated. The **lower** plots show the corresponding class-wise distance matrices computed using cosine similarity, with the average distances between samples from each pair of classes. Higher Inter/Intra class distance ratios indicate better class separation in the feature space.

## 4. Full Results

### 4.1. ImageNet

Table 4. This table presents the results of various instance and universal adversarial perturbation (UAP) attacks on the Imagenet-1k dataset, with all UAP attack names in *italics*. Different configurations of FGSM and PGD are denoted, such as  $FGSM_1$  and  $PGD_1$ . Average results for universal adversarial perturbations (UAP Avg.), instance adversarial attacks (IAA Avg.), and overall adversarial performance (Adv Avg.) are reported at the bottom, including percentage drops relative to clean accuracy.

	Barlow	BYOL	DINO	MoCoV3	SimCLR	Supervised	SwAV	VICReg
$FGSM_1$	42.41	39.41	24.68	42.67	24.29	38.83	24.71	42.42
$FGSM_2$	18.11	13.47	5.66	15.53	8.84	12.18	6.35	18.11
$PGD_1$	42.38	39.63	25.65	42.39	26.6	35.26	26.48	42.41
$PGD_2$	1.48	0.65	0.18	1.06	0.25	0.37	0.18	1.5
$PGD_3$	42.6	39.82	25.85	42.56	26.79	35.39	26.73	42.6
$PGD_4$	1.19	0.5	0.14	0.82	0.2	0.28	0.14	1.2
$PGD_5$	5.18	3.44	0.67	4.79	0.9	1.9	0.69	5.15
DIFGSM	52	52.71	41.12	54.09	42.57	51.43	45.65	52.49
CW	0.18	0.02	0	0.02	0.02	0.02	0	0.19
Jitter	59.83	61.92	60.26	62.47	56.4	62.75	61.16	59.84
TIFGSM	61.04	62.27	56.98	61.47	55.63	62.16	60.07	59.91
PIFGSM	34.38	29.83	14.54	34.1	13.34	28.64	14.12	34.43
EADEN	0	0	0	0	0	0	0	0
OnePixel	69.34	72.5	72.83	72.64	66.47	73.27	72.73	69.38
Pixel	25.22	28.67	19.41	31.45	21.75	23.21	16.95	25.23
SPSA	66.59	69.59	68.11	69.93	63.01	69.48	68.61	66.63
Square	4.44	2.62	1.3	3.15	4.22	0.87	1.99	4.49
TAP	70.31	74.36	73.78	73.72	68.1	68.98	75.05	70.33
ASV	62.17	68.46	68.69	67.59	61.84	64.28	67.66	62.51
FFF (mean-std)	53.72	62.38	59.45	46.78	56.79	53.45	61.14	54.76
FFF (no-data)	39.64	31.94	40.73	57.39	53.52	42.49	32.15	38.68
FFF (one-sample)	30.53	54.41	16.15	57.18	28.63	40.57	29.96	30.14
FG-UAP	4.34	1.83	2.3	3.08	1.03	1.89	2.17	1.95
GD-UAP (mean-std)	56.92	61.1	49.85	53.59	55.51	59.6	57.38	58.07
GD-UAP (no-data)	33.41	37.96	26.59	43.66	37.05	36.01	36.07	31.29
GD-UAP (one-sample)	42.17	37.54	25.9	35.1	14.11	25.27	36.37	40.08
LAA-base	42.17	36.35	51.13	41.09	7.83	26.73	10.9	28.36
LAA-fuse	28.33	36.01	50.69	40.39	8.34	26.01	10.94	28.55
LAA-ugs	27.56	60.03	56.83	65.27	53.08	34.27	49.91	58.23
PD-UAP	65.06	54.06	45.06	56.248	60.96	46.79	51.75	65.07
SSP	27.7	41.05	38.55	48.56	35.06	9.43	23.27	33.26
STD	49.19	58.08	52.44	53.44	50.3	56.16	56.08	48.88
UAP (DeepFool)	13.23	20.25	15.18	24.25	23.72	13.67	8.59	13.22
UAPEPGD	67.74	67.21	70.6	71.57	64.36	71.26	70.98	67.88
Clean Accuracy	71.20	74.57	75.28	74.57	68.90	76.13	75.27	71.26
IAA Avg.	33.14 ↓54%	32.86 ↓56%	27.28 ↓64%	34.04 ↓54%	26.63 ↓61%	31.39 ↓59%	27.87 ↓63%	33.12 ↓54%
UAP Avg.	40.24 ↓43%	45.79 ↓39%	41.88 ↓44%	47.82 ↓36%	38.25 ↓44%	37.99 ↓50%	37.83 ↓50%	41.30 ↓42%
Adv Avg.	36.48 ↓49%	38.94 ↓48%	34.16 ↓55%	40.53 ↓46%	32.10 ↓53%	34.50 ↓55%	32.56 ↓57%	36.98 ↓48%

## 4.2. Segmentation

### 4.2.1. Pascal VOC 2012

Metric	Barlow	BYOL	DINO	MocoV3	SimCLR	Supervised	SwAV	VICReg
<b>Alma</b>								
mIOU ( $\uparrow$ )	0.35	0.33	0.34	0.4	0.31	0.26	0.38	0.39
APSR ( $\downarrow$ )	99.02	99.01	99.02	98.91	99	99.01	99.01	98.99
<b>Asma</b>								
mIOU ( $\uparrow$ )	49.4	63.39	61.36	61.57	32.06	77.3	62.12	50.38
APSR ( $\downarrow$ )	15.39	10.95	11.38	12.18	22.78	5.29	11.56	14.48
<b>DAG</b>								
mIOU ( $\uparrow$ )	0.02	0.02	0.02	0.02	0.03	0.05	0.02	0.02
APSR ( $\downarrow$ )	99.87	99.91	99.89	99.88	99.83	99.74	99.89	99.89
<b>DDN</b>								
mIOU ( $\uparrow$ )	5.62	4.64	5.11	7.16	1.67	1.52	6.91	4.94
APSR ( $\downarrow$ )	89.66	92.6	92.75	88.01	97.24	88.56	90.77	87.23
<b>FGSM</b>								
mIOU ( $\uparrow$ )	30.35	29.28	30.41	29.43	32.15	38.31	29.4	29.84
APSR ( $\downarrow$ )	35.91	45.62	39.66	41.71	33.55	21.36	42.94	39.31
<b>FMN</b>								
mIOU ( $\uparrow$ )	5.4	5.29	4.86	5.19	5.07	2.74	4.9	6.2
APSR ( $\downarrow$ )	91.18	92.25	91.02	91.42	89.88	93.53	91.94	89.99
<b>PGD</b>								
mIOU ( $\uparrow$ )	12.67	13.16	12.75	13.06	12.88	10.92	12.98	13.04
APSR ( $\downarrow$ )	70.07	82	77	79.27	71.15	67.4	77.31	72.43
<b>Clean mIOU (<math>\uparrow</math>)</b>	72.63	70.37	71.65	71.25	71.96	77.35	70.8	70.33
<b>Clean APSR (<math>\downarrow</math>)</b>	7.18	8.29	7.64	7.83	7.2	5.27	8.21	8.01
<b>Adversarial mIOU (<math>\uparrow</math>)</b>	14.83 $\downarrow 80\%$	16.59 $\downarrow 78\%$	16.41 $\downarrow 77\%$	16.69 $\downarrow 77\%$	12.02 $\downarrow 83\%$	18.73 $\downarrow 76\%$	16.67 $\downarrow 77\%$	14.97 $\downarrow 79\%$
<b>Adversarial APSR (<math>\downarrow</math>)</b>	71.59 $\uparrow 64\%$	74.62 $\uparrow 66\%$	72.96 $\uparrow 65\%$	73.05 $\uparrow 65\%$	73.35 $\uparrow 66\%$	67.84 $\uparrow 64\%$	73.35 $\uparrow 65\%$	71.76 $\uparrow 64\%$

Table 5. Performance metrics (mIOU and APSR) for various self-supervised and supervised models under different adversarial attacks, using unfrozen backbones. Clean and adversarial scores are reported, with percentage changes in adversarial performance noted. Higher mIOU and lower APSR indicate better results



Metric	Barlow	BYOL	DINO	MocoV3	SimCLR	Supervised	SwAV	VICReg
<b>Alma</b>								
mIOU ( $\uparrow$ )	0.39	0.31	0.37	0.37	0.55	0.28	0.35	0.41
APSR ( $\downarrow$ )	99.02	99.02	99.02	99.02	98.45	99.01	99.02	99.02
<b>Asma</b>								
mIOU ( $\uparrow$ )	76.06	72.84	75.32	72.84	70.42	69.84	74.09	76.74
APSR ( $\downarrow$ )	6.01	7.23	6.14	7.58	5.98	8.18	6.75	5.98
<b>DAG</b>								
mIOU ( $\uparrow$ )	0.03	0.04	0.02	0.04	0.04	0.02	0.03	0.03
APSR ( $\downarrow$ )	99.90	99.87	99.89	99.87	99.82	99.87	99.88	99.89
<b>DDN</b>								
mIOU ( $\uparrow$ )	10.81	9.76	6.91	10.74	6.62	2.95	8.57	11.12
APSR ( $\downarrow$ )	79.62	75.93	82.58	78.71	75.20	87.30	83.48	80.41
<b>FGSM</b>								
mIOU ( $\uparrow$ )	35.16	31.90	30.88	35.18	36.25	27.70	32.37	34.99
APSR ( $\downarrow$ )	33.29	33.63	36.12	33.63	27.35	36.99	36.10	33.69
<b>FMN</b>								
mIOU ( $\uparrow$ )	6.63	6.23	6.22	6.42	8.92	4.23	6.48	6.56
APSR ( $\downarrow$ )	87.73	87.10	87.12	87.70	81.28	91.30	87.23	87.23
<b>PGD</b>								
mIOU ( $\uparrow$ )	14.13	12.12	12.12	13.25	12.23	10.49	12.31	13.51
APSR ( $\downarrow$ )	76.16	75.49	75.49	76.60	73.38	78.37	80.82	77.62
<b>Clean mIOU (<math>\uparrow</math>)</b>	76.90	76.69	77.01	76.19	75.62	74.20	76.54	77.89
<b>Clean APSR (<math>\downarrow</math>)</b>	5.75	5.74	5.38	6.01	5.98	6.35	5.79	5.48
<b>Adversarial mIOU (<math>\uparrow</math>)</b>	20.46 $\downarrow 73\%$	19.03 $\downarrow 75\%$	18.83 $\downarrow 76\%$	19.83 $\downarrow 74\%$	19.29 $\downarrow 74\%$	16.50 $\downarrow 78\%$	19.17 $\downarrow 75\%$	20.48 $\downarrow 74\%$
<b>Adversarial APSR (<math>\downarrow</math>)</b>	68.82 $\uparrow 63\%$	68.32 $\uparrow 63\%$	69.48 $\uparrow 64\%$	69.02 $\uparrow 63\%$	65.92 $\uparrow 60\%$	71.57 $\uparrow 65\%$	70.47 $\uparrow 65\%$	69.12 $\uparrow 64\%$

Table 6. Performance metrics (mIOU and APSR) for various self-supervised and supervised models under different adversarial attacks, using frozen backbones. Clean and adversarial scores are reported, with percentage changes in adversarial performance noted. Higher mIOU and lower APSR indicate better results.

#### 4.2.2. CityScapes

Metric	Barlow	BYOL	DINO	MocoV3	SimCLR	Supervised	SwAV	VICReg
<b>IOU (Higher Better)</b>	65.48	62.05	65.87	63.88	58.82	62.57	66.48	65.64
<b>APSR (Lower Better)</b>	6.4	7.05	6.08	6.68	7.35	7.38	6.27	6.29
<b>Alma</b>								
IOU	3.82	3.45	3.72	2.99	8.43	4.58	5.51	4.08
APSR	91.4	91.89	91.09	93.99	77.65	89.24	86.44	90.41
<b>Asma</b>								
IOU	50.9	18.62	64.88	51.93	33.41	58.43	63.07	65.38
APSR	17.3	44.51	7.49	13.76	21.71	8.87	8.75	6.73
<b>DAG</b>								
IOU	0.19	0.27	0.21	0.33	0.27	0.21	0.15	0.24
APSR	99.8	99.74	99.75	99.72	99.57	99.6	99.76	99.79
<b>DDN</b>								
IOU	1.49	1.99	1.66	1.18	1.12	1.59	0.51	1.36
APSR	84.79	82.15	84.35	82.85	94.06	81	97.32	83.05
<b>FGSM</b>								
IOU	30.31	26.22	28.75	30.92	30.64	28.19	28.68	20.33
APSR	31.97	39.57	30.72	26.8	24.97	31.38	33.62	31.99
<b>FMN</b>								
IOU	8.03	9.19	6.04	8.2	16.77	7.81	8.48	8.2
APSR	77.75	72.11	81.38	77.35	58.44	74.76	77.34	75.44
<b>PGD</b>								
IOU	10	10.71	7.76	12.23	9.94	11.59	11.43	9.62
APSR	71.92	66.84	75.79	72.8	70.34	68.75	71.46	70.16
<b>Average IOU</b>	14.96 <sub>↓77%</sub>	10.06 <sub>↓84%</sub>	16.15 <sub>↓75%</sub>	15.40 <sub>↓76%</sub>	14.37 <sub>↓76%</sub>	16.06 <sub>↓74%</sub>	16.83 <sub>↓75%</sub>	15.60 <sub>↓76%</sub>
<b>Average APSR</b>	67.85 <sub>↑61%</sub>	70.97 <sub>↑64%</sub>	67.22 <sub>↑61%</sub>	66.75 <sub>↑56%</sub>	63.82 <sub>↑57%</sub>	64.80 <sub>↑62%</sub>	67.81 <sub>↑61%</sub>	65.37 <sub>↑60%</sub>

Table 7. Updated performance metrics (mIOU and APSR) for various self-supervised and supervised models under different adversarial attacks, using frozen backbones. Clean and adversarial scores are reported, with percentage changes in adversarial performance noted. Higher mIOU and lower APSR indicate better results.

### 4.3. Detection

#### 4.3.1. INRIA Person

Table 8. Adversarial Attack Results on Detection using unfrozen SSL and Supervised Models as backbones. The table presents performance metrics under clean and adversarial conditions for various attack types (Optim, BIM, MIM, SGD, PGD, Optim-Adam, Optim-Nesterov). The last two rows display clean mean Average Precision (mAP) and the average performance under adversarial attacks, with the percentage decrease in performance highlighted in red

	Barlow	BYOL	DINO	MocoV3	SimCLR	Supervised	SwAV	VICReg
Optim	6.18	1.68	1.77	4.87	1.06	1.54	4.27	2.12
BIM	32.78	26.93	31.82	21.63	12.6	1.75	40.84	23.22
MIM	11.89	26.24	5.2	10.7	3.1	1.94	10.69	7.85
SGD	6.13	2.89	7.59	20.15	2.45	2.4	13.71	2.99
PGD	84.58	78.44	80.97	81.96	80.45	57.76	80.54	77.52
Optim-Adam	6.43	1.49	2.07	7.49	1.31	1.32	4.47	1.99
Optim-Nesterov	2.34	1.58	1.31	5.24	1.43	2.55	4.34	1.42
Clean mAP	89.14	88.98	89.74	89.74	88.16	86.45	88.60	89.45
Adv mAP.	21.48↓76%	19.89↓78%	18.68↓79%	21.72↓76%	14.63↓83%	9.89↓89%	22.69↓72%	16.73↓81%

Table 9. Adversarial Attack Results on Detection using frozen SSL and Supervised Models as backbones. The table presents performance metrics under clean and adversarial conditions for various attack types (Optim, BIM, MIM, SGD, PGD, Optim-Adam, Optim-Nesterov). The last two rows display clean mean Average Precision (mAP) and the average performance under adversarial attacks, with the percentage decrease in performance highlighted in red

	Barlow	BYOL	DINO	MocoV3	SimCLR	Supervised	SwAV	VICReg
Optim	3.98	1.05	2	2.6	0.78	0.56	1.51	0.39
BIM	44.87	32.24	54.93	26.72	6.79	42.8	44.47	10.32
MIM	11.37	3.04	10.32	5.72	6.0	4.73	10.87	2.68
SGD	3.21	1.28	2.95	9.44	1.42	1.02	2.85	1.72
PGD	83.08	80.83	79.65	79.83	74.68	75.29	79.14	81.27
Optim-Adam	4.71	0.76	3.5	2.03	0.75	0.87	3.46	0.67
Optim-Nesterov	1.75	0.64	0.97	2.77	0.94	0.72	1.1	0.64
Clean mAP	88.39	87.44	87.63	87.36	87.67	87.67	86.55	88.43
Adv mAP	21.85↓75%	17.12↓80%	22.05↓75%	18.44↓79%	13.05↓85%	18.00↓79%	20.49↓76%	13.96↓84%

### 4.3.2. COCO

Table 10. Adversarial Attack Results on Detection using frozen SSL and Supervised Models as backbones. The table presents performance metrics under clean and adversarial conditions for various attack types (Optim, BIM, MIM, SGD, PGD, Optim-Adam, Optim-Nesterov). The last two rows display clean mean Average Precision (mAP) and the average performance under adversarial attacks, with the percentage decrease in performance highlighted in red

	Barlow	BYOL	DINO	MocoV3	SimCLR	Supervised	SwAV	VICReg
Optim	18.6	16.47	11.05	15.43	11.71	9.12	13.8	13.97
BIM	18.6	18.58	21.02	18.23	13.06	16.74	20.03	18.47
MIM	21.07	18.37	16.38	16.47	14.05	13.01	17.55	17.67
SGD	17.62	18.38	19.19	21.7	12.96	9.22	17.41	16.69
PGD	21.05	20.5	21.68	22.22	14.2	19.61	21.44	20.96
Optim-Adam	19.15	16.36	11.12	15.83	12	9.06	13.92	14.09
Optim-Nesterov	15.76	16.62	13.37	15.31	11.67	9.08	13.91	13.44
Clean mAP	37.93	39.49	38.57	40.49	32.17	37.01	38.45	38.55
Adv Avg.	18.84↓50%	17.90↓55%	16.26↓58%	17.88↓56%	12.80↓60%	12.26↓67%	16.87↓56%	16.47↓57%



#### 4.4. ResNet vs ViT

Table 11. This table presents the results of various instance and universal adversarial perturbation (UAP) attacks on the Imagenet-1k dataset, with all UAP attack names in *italics*. Different configurations of FGSM and PGD are denoted, such as  $FGSM_1$  and  $PGD_1$ . Average results for universal adversarial perturbations (UAP Avg.), instance adversarial attacks (IAA Avg.), and overall adversarial performance (Adv Avg.) are reported at the bottom, including percentage drops relative to clean accuracy

	MoCoV3-ViT-B	DINO-ViT-B	MoCo-ViT	DINO-ViT	DINO-ResNet	MoCoV3-ResNet
$FGSM_1$	46.69	58.36	34.63	51.42	24.68	42.67
$FGSM_2$	13.21	22.17	0.32	0.97	5.66	15.53
$PGD_1$	45.06	57.88	33.35	50.98	25.65	42.39
$PGD_2$	1.14	8.58	0.00	0.00	0.18	1.06
$PGD_3$	45.1	57.89	33.46	50.95	25.85	42.56
$PGD_4$	1.05	8.36	0.17	3.84	0.14	0.82
$PGD_5$	6.86	22.58	2.12	13.57	0.67	4.79
DIFGSM	45.13	57.89	51.91	59.81	41.12	54.09
CW	0	0	0	0	0.02	
Jitter	63.52	68.96	58.25	66.30	60.26	62.47
TIFGSM	66.17	68.58	61.84	65.23	56.98	61.47
PIFGSM	38.14	55.06	25.78	47.64	14.54	34.10
EADEN	0	0	0	0	0	0
OnePixel	74.93	76.67	71.28	75.47	72.83	72.64
Pixel	42.85	49.51	34.69	44.08	19.41	31.45
SPSA	71.18	74.35	66.20	72.47	68.11	69.93
Square	1.87	2.78	1.22	1.67	1.30	3.15
TAP	75.66	76.78	72.34	75.60	73.78	73.72
ASV	0.10	0.10	0.10	0.10	68.69	67.59
FFF (mean-std)	76.38	77.45	72.55	76.71	59.45	46.78
FFF (no-data)	76.34	77.45	72.66	76.71	40.73	57.39
FFF (one-sample)	76.34	77.45	72.55	76.71	16.15	57.18
FG-UAP	1.37	6.79	0.72	3.51	2.30	3.08
GD-UAP (no-data)	53.08	43.49	1.16	7.30	26.59	43.66
GD-UAP (mean-std)	56.97	68.29	28.80	64.17	49.85	53.59
GD-UAP (one-sample)	16.00	64.12	2.04	52.85	25.90	35.10
L4A-base	23.14	19.58	0.69	46.28	51.13	41.09
L4A-fuse	24.13	19.06	0.73	46.30	50.69	40.39
L4A-ugs	6.01	21.65	2.35	0.27	56.83	65.27
PD-UAP	74.72	76.81	70.61	74.91	45.06	56.25
SSP	29.27	60.91	2.52	56.53	38.55	48.56
STD	54.52	72.43	23.01	71.66	52.44	53.44
UAP (DeepFool)	2.19	8.50	1.15	8.56	15.18	24.25
UAPEPGD	73.86	76.26	69.34	74.51	70.60	71.57
Clean Accuracy	76.66	77.99	73.21	76.95	75.28	74.57
IAA Avg.	35.47 ↓54%	42.58 ↓45%	30.42 ↓58%	37.78 ↓51%	27.29 ↓64%	34.05 ↓54%
UAP Avg.	40.28 ↓47%	48.15 ↓38%	26.31 ↓64%	46.07 ↓40%	41.88 ↓44%	47.82 ↓36%
Adv Avg.	37.73 ↓51%	45.19 ↓42%	28.49 ↓61%	41.67 ↓46%	34.15 ↓55%	40.53 ↓46%

#### 4.5. ImageNet Across Training Epochs

Table 12. This table presents the results of various instance and universal adversarial perturbation (UAP) attacks on the Imagenet-1k dataset, with all UAP attack names in *italics*. Different configurations of FGSM and PGD are denoted, such as  $FGSM_1$  and  $PGD_1$ . Average results for universal adversarial perturbations (UAP Avg.), instance adversarial attacks (IAA Avg.), and overall adversarial performance (Adv Avg.) are reported at the bottom, including percentage drops relative to clean accuracy.

	MoCoV3-100	MoCoV3-300	MoCoV3-1000
$FGSM_1$	38.87	42.6	42.67
$FGSM_2$	7.94	8.38	15.53
$PGD_1$	37.89	41.99	42.39
$PGD_2$	0.49	0.09	1.06
$PGD_3$	38.06	42.14	42.56
$PGD_4$	1.75	1.22	0.82
$PGD_5$	5.4	5.49	4.79
DIFGSM	49.21	52.65	54.09
CW	0.02	0.02	0.02
Jitter	56.45	60.53	62.47
TIFGSM	57.39	61.86	61.47
PIFGSM	31.24	34.41	34.1
EADEN	0	0	0
OnePixel	66.79	70.76	72.64
Pixel	26.27	29.41	31.45
SPSA	64.05	68.02	69.93
Square	2.05	2.01	3.15
TAP	67.85	71.9	73.72
ASV	62.59	66.11	67.59
FFF (mean-std)	50.05	59.76	46.78
FFF (no-data)	32.96	36.39	57.39
FFF (one-sample)	40.81	58.32	57.18
FG-UAP	2.72	5.07	3.08
GD-UAP (mean-std)	49.56	53.45	43.66
GD-UAP (no-data)	37.00	46.68	53.59
GD-UAP (one-sample)	32.04	37.17	35.10
L4A-base	40.09	33.66	41.09
L4A-fuse	40.07	33.70	40.39
L4A-ugs	51.79	64.64	65.27
PD-UAP	40.96	55.29	56.25
SSP	42.24	26.80	48.56
STD	49.03	51.07	53.44
UAP (DeepFool)	24.71	26.99	24.25
UAPEPGD	65.51	69.75	71.57
Clean Accuracy	68.91	72.82	74.57
IAA Avg.	30.65 ↓56%	32.97 ↓55%	34.05 ↓54%
UAP Avg.	41.39 ↓40%	45.30 ↓38%	47.82 ↓36%
Adv Avg.	35.70 ↓48%	38.77 ↓47%	40.53 ↓47%

Table 13. This table presents the results of various instance and universal adversarial perturbation (UAP) attacks on the Imagenet-1k dataset, with all UAP attack names in *italics*. Different configurations of FGSM and PGD are denoted, such as  $FGSM_1$  and  $PGD_1$ . Average results for universal adversarial perturbations (UAP Avg.), instance adversarial attacks (IAA Avg.), and overall adversarial performance (Adv Avg.) are reported at the bottom, including percentage drops relative to clean accuracy

	SwAV-100	SwAV-200	SwAV-400	SwAV-800
$FGSM_1$	18.08	19.99	21.9	24.71
$FGSM_2$	4.01	4.34	5.2	6.35
$PGD_1$	18.94	21.3	23.7	26.48
$PGD_2$	0.31	0.17	0.17	0.18
$PGD_3$	19.08	21.44	23.88	26.73
$PGD_4$	0.3	0.15	0.14	0.14
$PGD_5$	0.73	0.59	0.52	0.69
DIFGSM	39.31	42.01	42.31	45.65
CW	0.0	0.0	0.0	0.0
Jitter	56.67	59.15	60.43	61.16
TIFGSM	53.11	55.14	56.44	60.07
PIFGSM	10	10.87	11.76	14.12
EADEN	0	0	0	0
OnePixel	68.73	70.83	71.64	72.73
Pixel	13.21	16.03	18.08	16.95
SPSA	63.94	66.25	67.38	68.61
Square	0.35	0.36	0.5	1.99
TAP	71.79	73.56	74.37	75.05
ASV	64.00	63.90	67.06	67.66
<i>FFF (mean-std)</i>	55.81	58.52	62.60	61.14
<i>FFF (no-data)</i>	35.02	24.83	35.81	32.15
<i>FFF (one-sample)</i>	24.75	24.22	34.59	29.96
<i>FG-UAP</i>	1.86	3.56	2.29	2.17
<i>GD-UAP (mean-std)</i>	54.07	58.14	58.08	57.38
<i>GD-UAP (no-data)</i>	22.09	29.45	26.57	36.07
<i>GD-UAP (one-sample)</i>	21.33	35.80	37.18	36.37
<i>L4A-base</i>	18.63	17.66	33.43	10.90
<i>L4A-fuse</i>	18.58	17.908	34.73	10.94
<i>L4A-ugs</i>	34.02	37.03	50.20	49.91
<i>PD-UAP</i>	41.58	54.83	51.53	51.75
<i>SSP</i>	12.12	25.74	16.642	23.27
<i>STD</i>	45.74	53.71	45.88	56.08
<i>UAP (DeepFool)</i>	10.17	10.09	10.79	8.59
<i>UAPEPGD</i>	67.13	69.01	70.07	70.98
Clean Accuracy	72.02	73.82	74.57	75.27
IAA Avg.	24.36 ↓66%	25.68 ↓65%	26.58 ↓64%	27.87 ↓63%
UAP Avg.	32.93 ↓54%	36.52 ↓51%	39.84 ↓47%	37.83 ↓50%
Adv Avg.	28.40 ↓60%	30.78 ↓58%	32.82 ↓56%	32.55 ↓57%

#### 4.6. Imagenet With Different MoCo Versions

Table 14. This table presents the results of various instance and universal adversarial perturbation (UAP) attacks on the Imagenet-1k dataset, with all UAP attack names in *italics*. Different configurations of FGSM and PGD are denoted, such as  $FGSM_1$  and  $PGD_1$ . Average results for universal adversarial perturbations (UAP Avg.), instance adversarial attacks (IAA Avg.), and overall adversarial performance (Adv Avg.) are reported at the bottom, including percentage drops relative to clean accuracy

	MoCoV1	MoCoV2	MoCoV3
$FGSM_1$	15.91	22.01	42.67
$FGSM_2$	6.25	5.17	15.53
$PGD_1$	17.89	24.00	42.39
$PGD_2$	0.09	0.54	1.06
$PGD_3$	17.96	24.14	42.56
$PGD_4$	0.06	0.52	0.82
$PGD_5$	0.21	1.33	4.79
DIFGSM	34.85	40.39	54.09
CW	0	0	0.02
Jitter	50.04	53.09	62.47
TIFGSM	48.70	49.50	61.47
PIFGSM	8.53	13.20	34.10
EADEN	0	0	0
OnePixel	56.67	64.63	72.64
Pixel	3.10	17.85	31.45
SPSA	50.62	60.57	69.93
Square	0.80	0.42	3.15
TAP	58.55	65.24	73.72
ASV	18.756	60.99	67.59
<i>FFF (mean-std)</i>	30.34	46.83	46.78
<i>FFF (no-data)</i>	19.47	33.01	57.39
<i>FFF (one-sample)</i>	5.40	42.08	57.18
<i>FG-UAP</i>	0.838	3.78	3.08
<i>GD-UAP (mean-std)</i>	5.88	51.28	53.39
<i>GD-UAP (no-data)</i>	18.34	44.34	43.66
<i>GD-UAP (one-sample)</i>	3.50	39.28	35.10
<i>L4A-base</i>	2.15	37.09	41.09
<i>L4A-fuse</i>	2.19	36.79	40.39
<i>L4A-ugs</i>	2.25	30.16	65.27
<i>PD-UAP</i>	33.96	50.06	56.25
<i>SSP</i>	4.59	42.66	48.56
<i>STD</i>	23.09	46.31	53.44
<i>UAP (DeepFool)</i>	4.34	30.64	24.25
<i>UAPEPGD</i>	47.67	63.44	71.57
Clean Accuracy	60.64	67.72	74.57
IAA Avg.	20.56 ↓66%	24.59 ↓64%	34.05 ↓54%
UAP Avg.	13.92 ↓77%	41.17 ↓39%	47.82 ↓36%
Adv Avg.	17.44 ↓71%	32.40 ↓52%	40.53 ↓46%



#### 4.7. BYOL Ablations

Table 15. This table presents the results of various instance and universal adversarial perturbation (UAP) attacks on the Imagenet-1k dataset, with all UAP attack names in *italics*. Different configurations of FGSM and PGD are denoted, such as  $FGSM_1$  and  $PGD_1$ . Average results for universal adversarial perturbations (UAP Avg.), instance adversarial attacks (IAA Avg.), and overall adversarial performance (Adv Avg.) are reported at the bottom, including percentage drops relative to clean accuracy.

	BYOL-NC	BYOL-CC	BYOL-128	BYOL-512	BYOL
$FGSM_1$	23.45	31.23	35.33	37.51	39.41
$FGSM_2$	10.6	11.36	13.62	13.92	13.47
$PGD_1$	25.57	30.86	35.32	37.69	39.63
$PGD_2$	0.68	0.79	1.3	1	0.65
$PGD_3$	25.83	30.89	35.52	37.69	39.82
$PGD_4$	0.59	0.66	1.1	0.83	0.5
$PGD_5$	1.22	1.89	3.51	3.69	3.44
DIFGSM	35.73	45.67	47.83	49.61	52.71
CW	0.02	0.01	0.1	0.02	0.02
Jitter	53	56.81	57.7	60.02	61.92
TIFGSM	40.89	58.33	56.77	60.11	62.27
PIFGSM	12.27	22.2	25.86	28.48	29.83
EADEN	0	0	0	0	0
OnePixel	61.18	66.27	67.31	68.89	72.5
Pixel	27.1	9.84	25	26.13	28.67
SPSA	55.76	63.8	64.24	66.94	69.59
Square	0.28	2.13	2.11	2.04	2.62
TAP	39.38	68.58	69.31	71.71	74.36
ASV	51.27	51.41	62.74	66.16	68.46
FFF (mean-std)	43.19	51.74	51.84	60.94	62.38
FFF (no-data)	42.24	30.11	39.31	43.11	31.94
FFF (one-sample)	16.55	23.80	36.39	37.32	54.41
FG-UAP	1.15	1.85	3.20	3.53	1.83
GD-UAP (no-data)	39.36	54.65	53.00	56.74	61.10
GD-UAP (mean-std)	32.64	38.54	41.85	42.88	37.96
GD-UAP (one-sample)	33.28	25.60	37.95	35.48	37.54
L4A-base	40.59	32.82	32.86	22.65	36.35
L4A-fuse	39.98	32.97	32.77	22.58	36.01
L4A-ugs	39.77	35.36	54.70	53.27	60.03
PD-UAP	39.90	41.47	50.45	50.02	54.06
SSP	21.82	35.16	26.31	22.75	41.05
STD	36.97	47.11	53.42	53.72	58.08
UAP (DeepFool)	18.58	10.96	19.48	22.53	20.25
UAPEPGD	56.11	65.48	66.16	68.83	71.21
Clean Accuracy	63.77	69.15	69.67	72.09	74.57
IAA Avg.	22.98 ↓60%	27.85 ↓60%	30.11 ↓57%	31.46 ↓56%	32.86 ↓56%
UAP Avg.	34.59 ↓46%	36.19 ↓48%	41.40 ↓41%	41.41 ↓43%	45.79 ↓39%
Adv Avg.	28.44 ↓55%	31.78 ↓54%	35.42 ↓49%	36.14 ↓50%	38.94 ↓48%

## 4.8. Transfer Learning (Linear)

Table 16. Combined results from transfer learning datasets showing Clean accuracy, UAP Avg., IAA Avg., and Adv Avg. with percentage drops relative to Clean accuracy.

		Barlow	BYOL	DINO	MocoV3	SimCLR	Supervised	SwAV	VICReg
Aircraft	Clean	56.88	56.34	60.25	58.75	46.77	44.89	54.01	56.43
	IAA	16.29 $\downarrow 71\%$	14.87 $\downarrow 73\%$	15.27 $\downarrow 75\%$	17.41 $\downarrow 70\%$	11.93 $\downarrow 74\%$	9.82 $\downarrow 78\%$	13.82 $\downarrow 74\%$	16.38 $\downarrow 71\%$
	UAP	20.22 $\downarrow 64\%$	19.64 $\downarrow 65\%$	19.25 $\downarrow 68\%$	25.57 $\downarrow 56\%$	16.30 $\downarrow 65\%$	15.54 $\downarrow 65\%$	16.01 $\downarrow 70\%$	19.82 $\downarrow 64\%$
	Adv	18.14 $\downarrow 68\%$	17.11 $\downarrow 70\%$	17.14 $\downarrow 72\%$	21.25 $\downarrow 64\%$	13.99 $\downarrow 70\%$	12.51 $\downarrow 72\%$	14.85 $\downarrow 73\%$	18.00 $\downarrow 68\%$
Caltech	Clean	90.54	90.99	90.31	92.89	89.10	90.25	90.36	90.57
	IAA	53.60 $\downarrow 41\%$	54.06 $\downarrow 41\%$	47.42 $\downarrow 47\%$	58.23 $\downarrow 37\%$	49.79 $\downarrow 44\%$	44.10 $\downarrow 51\%$	45.55 $\downarrow 50\%$	53.64 $\downarrow 41\%$
	UAP	66.48 $\downarrow 27\%$	69.06 $\downarrow 16\%$	65.18 $\downarrow 28\%$	74.95 $\downarrow 7\%$	66.50 $\downarrow 23\%$	65.08 $\downarrow 27\%$	59.24 $\downarrow 20\%$	65.95 $\downarrow 26\%$
	Adv	59.66 $\downarrow 34\%$	61.12 $\downarrow 33\%$	55.78 $\downarrow 38\%$	66.10 $\downarrow 29\%$	57.66 $\downarrow 35\%$	53.97 $\downarrow 40\%$	51.99 $\downarrow 42\%$	59.44 $\downarrow 34\%$
Cars	Clean	64.20	57.62	65.62	63.61	43.81	47.10	59.78	64.12
	IAA	19.90 $\downarrow 69\%$	15.84 $\downarrow 73\%$	17.54 $\downarrow 73\%$	20.12 $\downarrow 68\%$	11.14 $\downarrow 75\%$	9.56 $\downarrow 80\%$	14.95 $\downarrow 75\%$	19.66 $\downarrow 69\%$
	UAP	30.44 $\downarrow 53\%$	26.86 $\downarrow 54\%$	25.52 $\downarrow 61\%$	34.77 $\downarrow 45\%$	15.93 $\downarrow 64\%$	17.44 $\downarrow 63\%$	19.95 $\downarrow 67\%$	28.17 $\downarrow 56\%$
	Adv	24.86 $\downarrow 61\%$	21.02 $\downarrow 64\%$	22.13 $\downarrow 66\%$	27.01 $\downarrow 57\%$	13.90 $\downarrow 68\%$	13.27 $\downarrow 72\%$	17.93 $\downarrow 70\%$	24.58 $\downarrow 62\%$
CIFAR 10	Clean	92.78	93.05	93.85	94.67	90.98	91.40	93.90	92.79
	IAA	32.34 $\downarrow 65\%$	31.19 $\downarrow 66\%$	28.07 $\downarrow 70\%$	32.85 $\downarrow 65\%$	30.00 $\downarrow 67\%$	31.74 $\downarrow 65\%$	27.37 $\downarrow 71\%$	32.45 $\downarrow 65\%$
	UAP	23.40 $\downarrow 75\%$	22.13 $\downarrow 76\%$	25.83 $\downarrow 72\%$	25.63 $\downarrow 73\%$	27.29 $\downarrow 70\%$	18.81 $\downarrow 79\%$	21.49 $\downarrow 77\%$	22.63 $\downarrow 76\%$
	Adv	28.14 $\downarrow 70\%$	26.93 $\downarrow 71\%$	27.02 $\downarrow 71\%$	29.46 $\downarrow 69\%$	28.73 $\downarrow 68\%$	25.66 $\downarrow 72\%$	24.61 $\downarrow 74\%$	27.83 $\downarrow 70\%$
CIFAR 100	Clean	77.86	78.18	76.67	80.19	72.97	73.86	79.41	77.79
	IAA	23.34 $\downarrow 70\%$	22.65 $\downarrow 71\%$	20.45 $\downarrow 74\%$	22.77 $\downarrow 72\%$	18.36 $\downarrow 75\%$	21.72 $\downarrow 71\%$	19.59 $\downarrow 75\%$	24.05 $\downarrow 69\%$
	UAP	10.93 $\downarrow 86\%$	11.78 $\downarrow 85\%$	12.55 $\downarrow 84\%$	12.49 $\downarrow 84\%$	10.60 $\downarrow 85\%$	8.27 $\downarrow 89\%$	9.55 $\downarrow 88\%$	11.19 $\downarrow 86\%$
	Adv	17.50 $\downarrow 77\%$	17.54 $\downarrow 77\%$	16.68 $\downarrow 79\%$	17.94 $\downarrow 78\%$	14.71 $\downarrow 80\%$	15.39 $\downarrow 76\%$	14.87 $\downarrow 75\%$	18.00 $\downarrow 77\%$
DTD	Clean	79.97	76.76	77.02	75.43	73.19	72.13	77.45	77.61
	IAA	40.02 $\downarrow 50\%$	37.65 $\downarrow 51\%$	38.88 $\downarrow 50\%$	40.14 $\downarrow 50\%$	33.50 $\downarrow 54\%$	33.86 $\downarrow 53\%$	38.96 $\downarrow 50\%$	41.30 $\downarrow 47\%$
	UAP	63.57 $\downarrow 17\%$	61.54 $\downarrow 20\%$	61.52 $\downarrow 20\%$	62.51 $\downarrow 17\%$	59.00 $\downarrow 19\%$	53.20 $\downarrow 26\%$	59.85 $\downarrow 23\%$	64.98 $\downarrow 16\%$
	Adv	51.11 $\downarrow 34\%$	48.90 $\downarrow 36\%$	49.53 $\downarrow 36\%$	50.67 $\downarrow 33\%$	45.51 $\downarrow 38\%$	42.96 $\downarrow 40\%$	48.79 $\downarrow 37\%$	52.45 $\downarrow 32\%$
Flowers	Clean	94.92	93.36	95.23	94.07	90.57	90.59	93.84	94.92
	IAA	47.71 $\downarrow 50\%$	43.94 $\downarrow 53\%$	43.76 $\downarrow 54\%$	47.25 $\downarrow 50\%$	40.25 $\downarrow 56\%$	34.86 $\downarrow 62\%$	39.92 $\downarrow 58\%$	47.94 $\downarrow 50\%$
	UAP	57.51 $\downarrow 39\%$	59.58 $\downarrow 36\%$	58.50 $\downarrow 39\%$	66.71 $\downarrow 29\%$	55.73 $\downarrow 38\%$	46.55 $\downarrow 49\%$	46.21 $\downarrow 51\%$	57.29 $\downarrow 40\%$
	Adv	52.32 $\downarrow 45\%$	51.30 $\downarrow 45\%$	50.70 $\downarrow 47\%$	56.41 $\downarrow 40\%$	47.54 $\downarrow 48\%$	40.36 $\downarrow 55\%$	42.88 $\downarrow 54\%$	52.34 $\downarrow 45\%$
Food	Clean	76.09	73.07	78.42	73.83	67.24	69.05	76.51	75.81
	IAA	27.50 $\downarrow 64\%$	24.15 $\downarrow 67\%$	24.09 $\downarrow 69\%$	27.69 $\downarrow 62\%$	21.03 $\downarrow 69\%$	19.81 $\downarrow 71\%$	23.39 $\downarrow 69\%$	26.37 $\downarrow 65\%$
	UAP	40.06 $\downarrow 47\%$	37.88 $\downarrow 48\%$	39.60 $\downarrow 50\%$	42.42 $\downarrow 43\%$	30.05 $\downarrow 55\%$	25.37 $\downarrow 63\%$	30.51 $\downarrow 60\%$	38.54 $\downarrow 49\%$
	Adv	33.41 $\downarrow 56\%$	30.61 $\downarrow 58\%$	31.39 $\downarrow 60\%$	34.62 $\downarrow 53\%$	25.28 $\downarrow 62\%$	22.43 $\downarrow 68\%$	26.74 $\downarrow 65\%$	32.10 $\downarrow 58\%$
Pets	Clean	89.13	89.08	89.15	90.77	83.23	92.06	87.47	89.13
	IAA	45.87 $\downarrow 49\%$	44.48 $\downarrow 50\%$	39.48 $\downarrow 56\%$	50.74 $\downarrow 44\%$	37.75 $\downarrow 55\%$	41.79 $\downarrow 55\%$	36.73 $\downarrow 58\%$	45.95 $\downarrow 48\%$
	UAP	69.99 $\downarrow 21\%$	72.36 $\downarrow 19\%$	67.33 $\downarrow 24\%$	76.55 $\downarrow 16\%$	66.09 $\downarrow 21\%$	71.36 $\downarrow 22\%$	64.99 $\downarrow 26\%$	70.52 $\downarrow 21\%$
	Adv	57.22 $\downarrow 36\%$	57.60 $\downarrow 35\%$	52.58 $\downarrow 41\%$	62.88 $\downarrow 31\%$	51.09 $\downarrow 39\%$	55.71 $\downarrow 39\%$	50.03 $\downarrow 43\%$	57.52 $\downarrow 35\%$
All	Clean	80.26	78.71	80.72	80.47	73.09	74.59	79.19	79.90
	IAA	34.06 $\downarrow 58\%$	32.09 $\downarrow 59\%$	30.55 $\downarrow 62\%$	35.24 $\downarrow 56\%$	28.19 $\downarrow 62\%$	27.47 $\downarrow 63\%$	28.92 $\downarrow 63\%$	34.19 $\downarrow 57\%$
	UAP	41.89 $\downarrow 49\%$	41.67 $\downarrow 49\%$	41.32 $\downarrow 50\%$	45.98 $\downarrow 44\%$	38.39 $\downarrow 50\%$	35.27 $\downarrow 55\%$	36.20 $\downarrow 55\%$	41.72 $\downarrow 49\%$
	Adv	37.75 $\downarrow 54\%$	36.60 $\downarrow 55\%$	35.62 $\downarrow 57\%$	40.31 $\downarrow 51\%$	33.00 $\downarrow 57\%$	31.15 $\downarrow 60\%$	32.35 $\downarrow 60\%$	37.74 $\downarrow 54\%$

#### 4.8.1. AirCraft

Table 17. This table presents the results of various instance and universal adversarial perturbation (UAP) attacks on the AirCraft dataset, with all UAP attack names in *italics*. Different configurations of FGSM and PGD are denoted, such as  $FGSM_1$  and  $PGD_1$ . Average results for universal adversarial perturbations (UAP Avg.), instance adversarial attacks (IAA Avg.), and overall adversarial performance (Adv Avg.) are reported at the bottom, including percentage drops relative to clean accuracy.

	Barlow	BYOL	DINO	MoCoV3	SimCLR	Supervised	SwAV	VICReg
$FGSM_1$	8.92	5.94	4.84	11.41	2.7	2.58	3.64	8.86
$FGSM_2$	1.52	0.69	0.45	1.95	0.78	0.81	2.57	1.8
$PGD_1$	10.03	5.72	4.54	10.96	3.44	1.61	4	10.18
$PGD_2$	0.06	0	0	0.12	0.24	0.18	0.64	0.06
$PGD_3$	10.27	6.02	4.63	11.09	3.27	1.61	3.83	10.06
$PGD_4$	0.06	0	0	0.12	0.18	0.12	0.61	0.06
$PGD_5$	0.12	0.03	0	0.24	0.18	0.24	0.79	0.12
DIFGSM	24.56	24.16	20.83	28.01	19.39	19.43	16.74	27.41
CW	0	0	0	0	0	0	0	0
Jitter	45.87	44.28	48.39	45.42	37.43	31.98	43.75	44.73
TIFGSM	32.78	31.08	29.68	35.76	28.31	18.99	29.83	33.04
PIFGSM	3.62	2.1	1.62	4.46	0.9	0.6	1.71	3.44
EADEN	0	0	0	0	0	0	0	0
OnePixel	51.75	49.39	54.93	53.41	41.4	36.01	47.55	51.54
Pixel	3.67	1.9	2.17	6.16	2.8	1.48	2.26	3.8
SPSA	44.36	42.91	44.2	46.6	30.76	28.51	38.42	44.31
Square	0.03	0	0	0.03	0.03	0	0	0.03
TAP	55.53	53.4	58.55	57.72	42.93	32.54	52.48	55.35
ASV	21.31	25.20	28.18	39.65	22.87	20.31	23.38	21.18
FFF (mean-std)	17.59	25.94	23.81	28.10	17.91	13.76	20.00	17.40
FFF (no-data)	14.86	17.93	10.41	25.14	10.69	7.07	6.54	15.05
FFF (one-sample)	13.21	13.21	3.21	13.12	11.94	7.67	6.81	10.69
FG-UAP	2.36	1.52	2.14	1.99	1.55	1.27	3.32	2.05
GD-UAP (mean-std)	18.95	18.03	15.16	21.30	15.17	22.07	15.71	16.51
GD-UAP (no-data)	16.79	11.39	7.79	23.47	18.70	11.18	7.32	15.83
GD-UAP (one-sample)	3.41	1.90	3.24	5.61	1.56	4.48	6.11	3.48
LAA-base	31.12	24.98	32.35	37.42	27.29	15.81	15.24	31.54
LAA-fuse	31.47	25.71	32.00	38.29	27.28	15.84	16.27	31.11
LAA-ugs	41.55	36.54	42.27	40.98	25.42	26.53	32.97	41.93
PD-UAP	26.27	13.53	8.70	18.34	17.58	11.92	10.62	26.54
SSP	22.28	23.89	27.06	31.55	22.69	12.69	20.22	23.39
STD	20.66	26.74	26.68	33.18	12.77	25.20	23.94	19.70
UAP (DeepFool)	7.05	10.30	8.59	13.81	8.29	24.45	15.34	6.45
UAPEPGD	34.64	37.38	36.34	37.23	19.05	28.45	32.37	34.22
Clean Accuracy	56.88	56.34	60.25	58.75	46.77	44.89	54.01	56.43
IAA Avg.	16.29 ↓71%	14.87 ↓73%	15.27 ↓75%	17.41 ↓70%	11.93 ↓74%	9.82 ↓78%	13.82 ↓74%	16.38 ↓71%
UAP Avg.	20.22 ↓64%	19.64 ↓65%	19.25 ↓68%	25.57 ↓56%	16.30 ↓65%	15.54 ↓65%	16.01 ↓70%	19.82 ↓64%
Adv Avg.	18.14 ↓68%	17.11 ↓70%	17.14 ↓72%	21.25 ↓64%	13.99 ↓70%	12.51 ↓72%	14.85 ↓73%	18.00 ↓68%

#### 4.8.2. Caltech 101

Table 18. This table presents the results of various instance and universal adversarial perturbation (UAP) attacks on the Caltech 101 dataset, with all UAP attack names in *italics*. Different configurations of FGSM and PGD are denoted, such as  $FGSM_1$  and  $PGD_1$ . Average results for universal adversarial perturbations (UAP Avg.), instance adversarial attacks (IAA Avg.), and overall adversarial performance (Adv Avg.) are reported at the bottom, including percentage drops relative to clean accuracy.

	Barlow	BYOL	DINO	MoCoV3	SimCLR	Supervised	SwAV	VICReg
$FGSM_1$	75.31	75.58	66.93	79.84	66.06	62.11	63.12	75.3
$FGSM_2$	53.82	52.44	37.84	59.58	47.67	27.38	36.13	53.82
$PGD_1$	74.27	75.19	65.57	79.35	64.94	58.96	61.96	74.34
$PGD_2$	9.61	10.47	2.24	17.17	11.14	1.64	2.05	9.34
$PGD_3$	74.43	75.39	65.7	79.81	65	59.24	62.28	74.68
$PGD_4$	7.62	9	1.81	14.79	10.22	1.19	1.69	7.53
$PGD_5$	17.17	18.64	5.48	25.45	13.11	4.35	3.91	16.86
DIFGSM	80.24	81.09	76.38	83.66	76.16	71.28	75.23	79.97
CW	0.68	0.94	0.3	0.79	0.49	0.22	0.31	0.68
Jitter	83.43	83.41	81.7	86.82	80.89	77.36	79.34	83.85
TIFGSM	85.73	86.72	83.63	88.69	82.73	79.58	81.98	85.98
PIFGSM	68.03	68.03	53.66	74.14	50.54	49	45.82	67.98
EADEN	0	0	0	0	0	0	0	0
OnePixel	89.85	90.57	89.43	92.25	87.67	88.7	89.52	89.88
Pixel	53.89	57.26	40.6	67.39	49.57	39.02	32.73	54.58
SPSA	88.89	88.82	87.45	91.08	86.51	85.73	87.2	89.04
Square	11.43	8.71	4.7	14.98	15.14	1.03	6.53	11.37
TAP	90.48	90.91	90.16	92.36	88.52	87.13	90.12	90.48
ASV	87.36	88.54	87.05	91.07	86.34	84.57	86.72	87.61
<i>FFF (mean-std)</i>	83.37	79.83	83.83	88.14	81.32	72.29	80.73	83.66
<i>FFF (no-data)</i>	73.92	51.35	58.54	77.23	75.82	55.89	55.47	71.03
<i>FFF (one-sample)</i>	42.23	51.33	65.30	79.74	44.95	65.27	65.96	37.53
<i>FG-UAP</i>	8.78	6.05	10.58	15.68	17.41	5.23	8.04	9.26
<i>GD-UAP (mean-std)</i>	83.06	81.74	65.43	78.92	80.73	78.18	72.84	81.71
<i>GD-UAP (no-data)</i>	58.14	62.99	51.64	73.74	73.92	58.89	62.15	59.71
<i>GD-UAP (one-sample)</i>	33.34	68.44	18.83	37.63	27.16	71.42	43.55	38.20
<i>L4A-base</i>	70.40	79.34	84.44	86.36	63.87	66.12	27.52	70.06
<i>L4A-fuse</i>	69.97	78.93	84.56	85.72	63.84	64.96	27.34	69.21
<i>L4A-ugs</i>	88.72	88.78	86.75	92.23	83.99	82.42	85.82	88.82
<i>PD-UAP</i>	88.58	75.06	73.89	86.96	84.04	71.07	75.22	88.18
<i>SSP</i>	73.96	82.74	78.66	85.34	80.62	57.39	64.53	71.47
<i>STD</i>	88.03	89.12	84.49	90.76	84.99	86.23	85.52	88.12
<i>UAP (DeepFool)</i>	24.67	30.67	21.12	37.96	29.01	33.89	18.49	21.36
<i>UAPEPGD</i>	89.13	90.02	87.70	91.76	86.07	87.37	87.94	89.29
Clean Accuracy	90.54	90.99	90.31	92.89	89.1	90.25	90.36	90.57
IAA Avg.	53.60 $\downarrow 41\%$	54.06 $\downarrow 41\%$	47.42 $\downarrow 47\%$	58.23 $\downarrow 37\%$	49.79 $\downarrow 44\%$	44.10 $\downarrow 51\%$	45.55 $\downarrow 50\%$	53.64 $\downarrow 41\%$
UAP Avg.	66.48 $\downarrow 26.58\%$	69.06 $\downarrow 15.8\%$	65.18 $\downarrow 27.9\%$	74.95 $\downarrow 7.4\%$	66.50 $\downarrow 23.2\%$	65.08 $\downarrow 26.8\%$	59.24 $\downarrow 20.3\%$	65.95 $\downarrow 24.2\%$
Adv Avg.	59.66 $\downarrow 34.1\%$	61.12 $\downarrow 32.8\%$	55.78 $\downarrow 38.2\%$	66.10 $\downarrow 28.8\%$	57.66 $\downarrow 35.3\%$	53.97 $\downarrow 40.2\%$	51.99 $\downarrow 42.5\%$	59.44 $\downarrow 34.4\%$

### 4.8.3. Cars

Table 19. This table presents the results of various instance and universal adversarial perturbation (UAP) attacks on the Cars dataset, with all UAP attack names in *italics*. Different configurations of FGSM and PGD are denoted, such as  $FGSM_1$  and  $PGD_1$ . Average results for universal adversarial perturbations (UAP Avg.), instance adversarial attacks (IAA Avg.), and overall adversarial performance (Adv Avg.) are reported at the bottom, including percentage drops relative to clean accuracy.

	Barlow	BYOL	DINO	MoCoV3	SimCLR	Supervised	SwAV	VICReg
$FGSM_1$	14.55	8.27	6.34	16.32	3.18	2.1	3.48	14.48
$FGSM_2$	1.41	0.6	0.51	1.39	0.9	0.16	0.5	1.42
$PGD_1$	14.15	7.76	5.83	15.3	3.42	1.6	3.03	13.94
$PGD_2$	0.02	0	0	0	0.19	0.09	0	0.02
$PGD_3$	14.3	8.05	5.83	15.5	3.52	1.67	3.11	14.33
$PGD_4$	0.01	0	0	0	0.17	0.07	0	0.01
$PGD_5$	0	0.01	0	0	0.19	0	0.02	0
DIFGSM	33.68	24.49	28.83	32.76	17.55	14.05	22.04	30.92
CW	0	0	0	0	0	0	0	0
Jitter	44.21	36.41	45.44	42.21	26.4	23.85	40.67	43.86
TIFGSM	44.26	35.39	39.8	43.84	27.62	22.01	34.77	44
PIFGSM	6.32	3.3	1.54	8.54	0.75	0.6	0.65	6.39
EADEN	0	0	0	0	0	0	0	0
OnePixel	60.73	53.74	61.77	59.99	39.56	39.56	55.33	60.63
Pixel	6.63	5.1	5.02	8.17	4.14	1.92	2.3	6.33
SPSA	54.22	45.44	51.11	54.88	30.33	31.59	44.47	54.05
Square	0.06	0.01	0	0.04	0	0	0.01	0.05
TAP	63.71	56.62	63.75	63.26	42.74	32.92	58.79	63.51
ASV	43.05	35.78	42.81	51.73	28.26	27.47	33.37	41.80
FFF (mean-std)	35.13	34.85	34.66	38.75	22.62	19.05	26.25	34.98
FFF (no-data)	23.84	15.97	12.54	29.39	18.54	15.92	10.19	17.47
FFF (one-sample)	17.76	22.51	19.75	38.42	12.64	16.70	29.70	19.15
FG-UAP	2.69	0.82	1.78	1.04	2.18	0.92	1.27	2.90
GD-UAP (mean-std)	41.11	29.44	26.35	39.20	23.24	24.42	27.16	40.33
GD-UAP (no-data)	17.31	20.43	15.52	27.40	15.31	13.08	19.67	18.77
GD-UAP (one-sample)	5.92	17.22	4.99	12.35	3.51	5.88	16.04	6.47
LAA-base	33.94	28.37	34.16	37.86	9.80	8.62	6.39	33.17
LAA-fuse	33.29	28.72	33.13	38.13	8.72	8.68	6.72	33.03
LAA-ugs	56.10	38.76	47.90	55.12	29.59	21.00	34.34	55.49
PD-UAP	48.19	26.53	22.61	34.37	23.79	17.17	12.26	47.34
SSP	21.66	33.84	31.08	38.27	17.26	8.03	19.59	24.26
STD	37.64	31.02	34.57	39.36	16.42	24.72	28.23	36.97
UAP (DeepFool)	16.91	20.25	25.59	20.54	14.21	32.35	28.93	17.85
UAPEPGD	52.56	45.27	49.12	54.36	26.15	34.96	40.44	51.96
Clean Accuracy	64.20	57.62	65.62	63.61	43.81	47.10	59.78	64.12
IAA Avg.	19.90 ↓69%	15.84 ↓73%	17.54 ↓73%	20.12 ↓68%	11.14 ↓75%	9.56 ↓80%	14.95 ↓75%	19.66 ↓69%
UAP	30.44 ↓53%	26.86 ↓54%	25.52 ↓61%	34.77 ↓45%	15.93 ↓64%	17.44 ↓63%	19.95 ↓67%	28.17 ↓56%
Adv Avg.	24.86 ↓61%	21.02 ↓64%	22.13 ↓66%	27.01 ↓57%	13.90 ↓68%	13.27 ↓72%	17.93 ↓70%	24.58 ↓62%

#### 4.8.4. CIFAR 10

Table 20. This table presents the results of various instance and universal adversarial perturbation (UAP) attacks on the CIFAR 10 dataset, with all UAP attack names in *italics*. Different configurations of FGSM and PGD are denoted, such as  $FGSM_1$  and  $PGD_1$ . Average results for universal adversarial perturbations (UAP Avg.), instance adversarial attacks (IAA Avg.), and overall adversarial performance (Adv Avg.) are reported at the bottom, including percentage drops relative to clean accuracy.

	Barlow	BYOL	DINO	MoCoV3	SimCLR	Supervised	SwAV	VICReg
$FGSM_1$	32.95	31.04	27.57	33.04	37.86	42.84	19.38	33.04
$FGSM_2$	53.83	50.24	52.58	52.51	59.88	29.71	47.54	53.94
$PGD_1$	34.76	29.2	22.25	35.16	23.51	36.92	21.04	34.64
$PGD_2$	0.02	0	0	0	0.03	0	0	0.01
$PGD_3$	34.02	28.38	20.85	34.44	22.48	36.51	20.71	34.23
$PGD_4$	0.02	0.02	0	0	0.03	0	0	0
$PGD_5$	0	0	0	0	0.01	0	0	0
DIFGSM	56.24	52.78	42.53	55.48	52.39	55.9	39.2	54.64
CW	0	0	0	0	0.06	0	0	0
Jitter	66.67	62.37	59.8	66.97	55.15	70.7	58.5	67.63
TIFGSM	52.32	48.88	41.23	50.64	56.11	56.88	42.38	54.51
PIFGSM	0.39	0.22	0.04	0.28	0.45	5.18	0	0.41
EADEN	0	0	0	0	0	0	0	0
OnePixel	87.36	86.09	88.42	87.78	82.28	85.59	81.11	87.21
Pixle	5.55	2.15	4.44	3.02	1.82	2.22	1.93	5.41
SPSA	69.6	79.09	55.69	80.73	60.51	71.34	68.81	69.9
Square	0	0	0.05	0	0	0	0	0
TAP	88.51	91.06	89.82	91.4	87.56	77.66	92.14	88.59
ASV	50.49	71.15	66.54	67.20	51.96	36.61	70.25	50.81
FFF (mean-std)	22.27	23.90	30.37	30.11	30.74	13.79	26.08	22.83
FFF (no-data)	14.30	10.41	12.37	19.61	31.12	13.33	10.83	12.70
FFF (one-sample)	10.00	10.00	9.99	10.00	10.00	11.15	10.03	10.05
FG-UAP	10.16	6.68	11.38	9.99	8.25	10.01	10.00	10.06
GD-UAP (mean-std)	33.92	18.14	22.02	17.21	28.83	19.01	17.66	26.04
GD-UAP (no-data)	13.37	10.56	12.09	10.58	10.51	12.33	10.28	11.49
GD-UAP (one-sample)	10.00	11.94	10.00	10.00	10.00	9.79	10.22	10.00
LAA-base	10.12	10.62	26.26	12.13	10.08	13.28	10.97	10.16
LAA-fuse	10.12	10.51	28.99	12.59	10.01	13.29	11.16	10.09
LAA-ugs	12.89	16.29	50.54	41.20	50.43	14.48	10.19	12.90
PD-UAP	67.51	16.31	14.67	12.94	49.02	14.89	40.65	66.96
SSP	12.66	10.13	10.01	41.45	15.03	10.42	9.92	11.01
STD	23.12	41.06	27.91	30.18	52.46	27.27	20.45	24.00
UAP (DeepFool)	8.93	13.05	16.73	9.92	12.51	18.11	11.23	9.14
UAPEPGD	64.61	73.37	63.41	74.96	55.63	63.25	63.91	63.76
Clean Accuracy	92.78	93.05	93.85	94.67	90.98	91.4	93.9	92.79
IAA Avg.	32.34 $\downarrow 65\%$	31.19 $\downarrow 66\%$	28.07 $\downarrow 70\%$	32.85 $\downarrow 65\%$	30.00 $\downarrow 67\%$	31.74 $\downarrow 65\%$	27.37 $\downarrow 71\%$	32.45 $\downarrow 65\%$
UAP Avg.	23.40 $\downarrow 74.77$	22.13 $\downarrow 76.21$	25.83 $\downarrow 72.48$	25.63 $\downarrow 72.93$	27.29 $\downarrow 70.01$	18.81 $\downarrow 79.42$	21.49 $\downarrow 77.11$	22.63 $\downarrow 75.62$
Adv Avg.	28.14 $\downarrow 70\%$	26.93 $\downarrow 71\%$	27.02 $\downarrow 71\%$	29.46 $\downarrow 69\%$	28.73 $\downarrow 68\%$	25.66 $\downarrow 72\%$	24.61 $\downarrow 74\%$	27.83 $\downarrow 70\%$



#### 4.8.5. CIFAR 100

Table 21. This table presents the results of various instance and universal adversarial perturbation (UAP) attacks on the CIFAR 100 dataset, with all UAP attack names in *italics*. Different configurations of FGSM and PGD are denoted, such as  $FGSM_1$  and  $PGD_1$ . Average results for universal adversarial perturbations (UAP Avg.), instance adversarial attacks (IAA Avg.), and overall adversarial performance (Adv Avg.) are reported at the bottom, including percentage drops relative to clean accuracy.

	Barlow	BYOL	DINO	MoCoV3	SimCLR	Supervised	SwAV	VICReg
$FGSM_1$	20.52	19.01	16.03	19.29	19.49	24.51	11.07	22.34
$FGSM_2$	34.07	31.02	34.08	28.84	30.06	18.20	29.16	35.71
$PGD_1$	19.74	14.42	11.47	18.38	8.92	19.09	10.29	20.98
$PGD_2$	0.04	0	0	0.02	0.12	0	0.01	0.06
$PGD_3$	19.33	14.18	11.09	17.69	8.24	18.85	9.92	20.67
$PGD_4$	0.06	0.01	0	0.01	0.08	0	0	0.02
$PGD_5$	0	0	0	0	0.18	0.01	0	0
DIFGSM	38.20	35.26	27.54	32.23	32.56	34.97	26.31	39.47
CW	0.01	0	0	0.06	0.02	0	0	0.04
Jitter	66.85	62.15	59.33	65.89	42.01	67.10	53.82	66.73
TIFGSM	34.84	36.35	27.80	30.79	35.15	36.82	29.15	37.30
PIFGSM	0.78	0.34	0.17	0.58	0.36	3.29	0.09	1.10
EADEN	0	0	0	0	0	0	0	0
OnePixel	67.73	66.25	69.87	67.64	58.73	64.76	61.41	68.19
Pixle	0.48	0.96	0.56	0.90	0.96	1.40	0.43	0.55
SPSA	47.25	54.96	38.62	53.70	28.82	48.30	44.86	49.46
Square	0.06	0.01	0.04	0	0	0	0.01	0.05
TAP	70.29	72.88	69.76	73.97	65.1	53.57	76.14	70.29
ASV	34.24	49.85	45.83	39.93	26.05	29.08	42.43	36.42
<i>FFF (mean-std)</i>	10.69	15.61	9.80	9.78	14.54	3.56	15.74	11.36
<i>FFF (no-data)</i>	2.50	1.02	3.68	3.11	2.47	3.00	1.60	1.61
<i>FFF (one-sample)</i>	1.03	1.02	1.02	0.90	1.30	1.21	1.11	1.00
<i>FG-UAP</i>	1.00	1.06	0.76	0.96	1.01	1.05	1.00	1.00
<i>GD-UAP (mean-std)</i>	9.68	13.00	6.89	5.14	11.58	8.36	7.28	9.36
<i>GD-UAP (no-data)</i>	1.05	2.15	1.11	1.40	4.18	2.51	1.11	1.06
<i>GD-UAP (one-sample)</i>	1.97	1.18	1.00	1.29	1.28	1.03	1.94	1.41
<i>L4A-base</i>	1.79	3.18	17.08	5.35	1.09	4.42	0.75	1.68
<i>L4A-fuse</i>	1.64	3.00	17.30	5.23	1.20	4.16	0.81	1.66
<i>L4A-ugs</i>	4.31	11.44	27.63	23.33	28.02	11.62	2.36	4.77
<i>PD-UAP</i>	47.61	6.95	6.56	10.54	22.54	2.65	20.47	48.33
<i>SSP</i>	1.13	1.69	4.49	29.29	6.20	1.75	1.08	1.16
<i>STD</i>	10.57	24.42	11.34	14.05	19.14	13.12	8.17	10.82
<i>UAP (DeepFool)</i>	1.72	2.44	3.88	4.03	2.57	2.65	4.80	1.69
<i>UAPEPGD</i>	43.92	50.47	42.35	45.49	26.42	42.15	42.14	45.77
Clean Accuracy	77.86	78.18	76.67	80.19	72.97	73.86	79.41	77.79
IAA Avg.	23.34 ↓70%	22.65 ↓71%	20.45 ↓74%	22.77 ↓72%	18.36 ↓75%	21.72 ↓71%	19.59 ↓75%	24.05 ↓69%
UAP Avg.	10.93 ↓86%	11.78 ↓85%	12.55 ↓84%	12.49 ↓84%	10.60 ↓85%	8.27 ↓89%	9.55 ↓88%	11.19 ↓86%
Adv Avg.	17.50 ↓77%	17.54 ↓77%	16.68 ↓79%	17.94 ↓78%	14.71 ↓80%	15.39 ↓76%	14.87 ↓75%	18.00 ↓77%

#### 4.8.6. DTD

Table 22. This table presents the results of various instance and universal adversarial perturbation (UAP) attacks on the DTD dataset, with all UAP attack names in *italics*. Different configurations of FGSM and PGD are denoted, such as  $FGSM_1$  and  $PGD_1$ . Average results for universal adversarial perturbations (UAP Avg.), instance adversarial attacks (IAA Avg.), and overall adversarial performance (Adv Avg.) are reported at the bottom, including percentage drops relative to clean accuracy.

	Barlow	BYOL	DINO	MoCoV3	SimCLR	Supervised	SwAV	VICReg
$FGSM_1$	50.43	46.76	48.88	51.65	38.4	42.02	48.99	52.71
$FGSM_2$	23.24	21.28	23.94	24.63	17.87	17.66	25.80	26.54
$PGD_1$	50.05	46.01	47.93	51.17	39.31	40.05	48.99	51.65
$PGD_2$	6.91	4.57	3.46	6.38	2.13	3.19	3.35	6.91
$PGD_3$	50.11	46.54	48.14	51.17	39.04	40.27	48.62	51.65
$PGD_4$	6.54	3.94	2.82	5.96	1.7	2.93	3.03	6.60
$PGD_5$	14.89	12.23	11.81	16.76	3.99	10.37	10.53	16.22
DIFGSM	59.84	52.87	60.05	59.79	52.02	54.47	60.27	64.20
CW	0.32	0.32	0.74	0.69	0.43	0.64	0.90	0.90
Jitter	67.39	65.90	66.91	66.17	62.02	60.48	68.51	68.30
TIFGSM	67.77	65.32	67.93	66.06	62.07	62.34	67.39	68.88
PIFGSM	42.77	38.83	40.16	45.53	26.76	35.43	38.40	43.94
EADEN	0	0	0	0	0	0	0	0
OnePixel	75.32	75.43	76.17	74.41	71.12	70.69	75.96	76.28
Pixel	49.89	46.28	46.97	49.57	40.48	37.62	41.38	50.90
SPSA	72.87	71.81	73.51	72.39	67.98	66.91	73.78	74.15
Square	8.09	5.96	6.7	7.77	5.74	1.49	8.46	8.67
TAP	74.10	73.78	73.72	72.50	72.07	62.98	76.97	75.05
ASV	71.01	70.59	72.18	68.83	67.39	62.98	70.69	72.07
FFF (mean-std)	62.93	59.15	65.27	61.70	61.65	50.85	65.90	64.20
FFF (no-data)	58.62	54.15	55.32	56.33	62.61	43.99	49.73	60.59
FFF (one-sample)	55.32	53.88	49.36	57.23	40.69	37.02	38.62	57.02
FG-UAP	21.70	20.90	19.26	26.86	23.14	19.95	19.15	23.83
GD-UAP (mean-std)	62.13	58.46	59.41	57.39	61.97	54.89	61.38	63.94
GD-UAP (no-data)	53.62	55.27	52.18	57.18	54.04	44.89	53.62	55.80
GD-UAP (one-sample)	50.69	48.56	42.82	46.01	32.45	35.05	47.23	55.43
LAA-base	72.61	72.82	73.88	73.30	67.07	63.51	67.61	73.99
LAA-fuse	72.82	73.24	73.94	73.51	66.17	62.93	68.19	73.56
LAA-ugs	74.31	74.26	74.10	73.24	69.04	68.40	74.63	74.84
PD-UAP	72.82	60.74	59.84	62.82	65.74	49.15	60.16	73.14
SSP	72.50	71.86	73.09	72.98	66.17	59.89	71.38	73.83
STD	73.40	71.91	73.19	71.28	69.31	68.56	72.98	73.72
UAP (DeepFool)	69.26	65.69	67.02	68.67	68.19	61.01	62.29	69.89
UAPEPGD	73.46	73.19	73.40	72.82	68.40	68.14	74.10	73.78
Clean Accuracy	79.97	76.76	77.02	75.43	73.19	72.13	77.45	77.61
IAA Avg.	40.02 ↓50%	37.65 ↓51%	38.88 ↓50%	40.14 ↓50%	33.50 ↓54%	33.86 ↓53%	38.96 ↓50%	41.30 ↓47%
UAP Avg.	63.57 ↓17%	61.54 ↓20%	61.52 ↓20%	62.51 ↓17%	59.00 ↓19%	53.20 ↓26%	59.85 ↓23%	64.98 ↓16%
Adv Avg.	51.11 ↓34%	48.90 ↓36%	49.53 ↓36%	50.67 ↓33%	45.51 ↓38%	42.96 ↓40%	48.79 ↓37%	52.45 ↓32%

#### 4.8.7. Flowers

Table 23. This table presents the results of various instance and universal adversarial perturbation (UAP) attacks on the Flowers dataset, with all UAP attack names in *italics*. Different configurations of FGSM and PGD are denoted, such as  $FGSM_1$  and  $PGD_1$ . Average results for universal adversarial perturbations (UAP Avg.), instance adversarial attacks (IAA Avg.), and overall adversarial performance (Adv Avg.) are reported at the bottom, including percentage drops relative to clean accuracy.

	Barlow	BYOL	DINO	MocoV3	SimCLR	Supervised	SwAV	VICReg
$FGSM_1$	66.36	57.69	57.37	64.52	48.50	41.85	46.97	66.36
$FGSM_2$	25.96	17.49	19.44	24.96	19.00	7.68	13.33	25.96
$PGD_1$	66.03	55.99	55.60	63.31	50.45	36.97	46.65	65.81
$PGD_2$	1.51	0.37	0.17	1.10	0.15	0.00	0.06	1.65
$PGD_3$	66.19	56.37	55.95	63.50	51.00	37.31	46.72	66.44
$PGD_4$	1.21	0.38	0.13	0.90	0.13	0.00	0.02	1.29
$PGD_5$	8.03	4.90	2.81	7.17	0.92	0.72	0.89	8.05
DI2FGSM	74.42	72.08	69.73	75.75	62.56	56.94	67.56	78.12
CW	0.00	0.00	0.05	0.00	0.00	0.02	0.00	0.00
Jitter	84.93	80.12	81.87	82.53	79.85	73.62	79.24	84.33
TIFGSM	86.85	84.35	87.48	86.17	81.29	75.36	84.39	87.88
PIFGSM	53.81	43.06	39.04	51.65	29.16	27.46	28.63	53.85
EADEN	0.00	0.00	0.00	0.00	0.00	0.00	0.00	0.00
OnePixel	94.47	92.77	94.79	93.10	89.27	88.38	92.94	94.49
Pixle	35.32	38.34	31.21	45.08	32.07	20.88	24.05	35.09
SPSA	93.03	90.21	92.91	91.84	85.56	84.31	90.60	92.84
Square	6.70	4.17	4.40	5.60	4.90	0.06	3.32	6.70
TAP	94.01	92.77	94.76	93.31	89.76	75.93	93.14	94.01
ASV	81.20	81.11	88.69	86.44	77.76	68.66	80.83	81.60
FFF (mean-std)	69.41	71.24	72.18	73.24	63.71	69.07	69.08	69.32
FFF (no-data)	52.74	49.93	43.70	63.13	58.11	49.88	32.65	52.55
FFF (one-sample)	23.79	50.12	37.17	77.48	31.42	16.90	20.18	22.73
FG-UAP	7.47	9.08	9.72	10.72	22.59	5.65	5.19	7.28
GD-UAP (mean-std)	78.75	67.02	64.74	76.07	69.99	70.11	65.18	78.08
GD-UAP (no-data)	48.38	51.64	39.25	57.48	57.36	42.94	35.00	47.88
GD-UAP (one-sample)	22.13	45.88	13.95	21.55	19.79	13.95	16.12	25.00
LAA-base	56.73	69.04	82.30	76.55	47.71	40.11	31.88	56.64
LAA-fuse	57.26	68.86	82.66	76.63	48.40	38.92	31.94	56.94
LAA-ugs	89.36	86.32	91.14	90.80	81.58	63.86	77.50	89.35
PD-UAP	85.11	59.04	48.22	68.65	75.03	53.21	52.31	84.59
SSP	53.40	47.61	69.40	87.01	70.49	22.10	42.08	54.17
STD	72.29	72.70	72.37	75.94	61.46	63.29	68.90	72.30
UAP (DeepFool)	31.95	34.80	28.73	34.62	25.15	44.85	22.05	28.10
UAPEPGD	90.23	88.85	91.75	91.00	81.15	81.37	88.44	90.18
Clean Accuracy	94.92	93.36	95.23	94.07	90.57	90.59	93.84	94.92
IAA Avg.	47.71 ↓50%	43.94 ↓53%	43.76 ↓54%	47.25 ↓50%	40.25 ↓56%	34.86 ↓62%	39.92 ↓58%	47.94 ↓50%
UAP Avg.	57.51 ↓39%	59.58 ↓36%	58.50 ↓39%	66.71 ↓29%	55.73 ↓38%	46.55 ↓49%	46.21 ↓51%	57.29 ↓40%
Adv Avg.	52.32 ↓45%	51.30 ↓45%	50.70 ↓47%	56.41 ↓40%	47.54 ↓48%	40.36 ↓55%	42.88 ↓54%	52.34 ↓45%

#### 4.8.8. Food

Table 24. This table presents the results of various instance and universal adversarial perturbation (UAP) attacks on the Food dataset, with all UAP attack names in *italics*. Different configurations of FGSM and PGD are denoted, such as  $FGSM_1$  and  $PGD_1$ . Average results for universal adversarial perturbations (UAP Avg.), instance adversarial attacks (IAA Avg.), and overall adversarial performance (Adv Avg.) are reported at the bottom, including percentage drops relative to clean accuracy.

	Barlow	BYOL	DINO	MocoV3	SimCLR	Supervised	SwAV	VICReg
$FGSM_1$	26.40	19.34	14.13	28.69	12.10	13.18	12.95	23.48
$FGSM_2$	3.24	1.50	1.39	4.02	1.41	1.29	0.95	2.52
$PGD_1$	26.60	19.03	13.87	28.54	13.69	11.30	13.15	23.91
$PGD_2$	0.04	0.01	0.01	0.05	0.00	0.02	0.00	0.04
$PGD_3$	26.72	19.21	14.13	28.76	13.92	11.42	13.48	24.12
$PGD_4$	0.04	0.01	0.00	0.04	0.00	0.01	0.00	0.03
$PGD_5$	0.59	0.19	0.10	0.82	0.04	0.13	0.01	0.47
DI2FGSM	44.15	37.23	37.35	44.94	33.02	32.45	37.32	40.14
CW	0.00	0.00	0.00	0.00	0.00	0.00	0.00	0.00
Jitter	60.70	56.00	61.34	58.14	55.13	53.14	61.79	59.79
TIFGSM	57.43	51.93	53.38	56.41	48.65	45.76	54.04	56.51
PIFGSM	17.53	11.71	6.67	19.93	5.17	6.80	5.46	14.85
EADEN	0.00	0.00	0.00	0.00	0.00	0.00	0.00	0.00
OnePixel	73.54	69.95	76.00	71.41	63.59	64.63	73.65	73.22
Pixel	14.94	12.97	9.65	17.11	8.34	5.84	4.93	13.66
SPSA	68.75	64.12	69.31	66.70	57.49	56.88	67.11	68.04
Square	0.19	0.05	0.09	0.19	0.16	0.02	0.07	0.16
TAP	74.21	71.43	76.25	72.68	65.96	53.74	76.18	73.75
ASV	62.46	59.82	66.04	61.50	52.91	47.60	62.86	62.02
FFF (mean-std)	51.98	49.45	55.35	49.68	44.52	41.29	53.77	49.99
FFF (no-data)	45.78	29.52	39.07	47.63	44.67	25.60	24.66	43.53
FFF (one-sample)	20.82	34.82	29.72	36.80	4.63	20.67	10.41	19.50
FG-UAP	3.98	2.50	2.22	4.28	3.90	1.84	1.67	3.88
GD-UAP (mean-std)	59.88	49.04	52.61	51.72	47.22	44.65	51.52	58.62
GD-UAP (no-data)	42.31	38.30	30.52	46.00	37.85	22.85	32.35	40.77
GD-UAP (one-sample)	13.89	29.22	8.69	14.46	5.33	7.26	15.75	12.92
LAA-base	26.08	35.83	48.51	43.13	5.36	15.57	7.30	25.89
LAA-fuse	25.76	35.50	47.07	43.72	5.11	15.43	7.70	25.86
LAA-ugs	58.75	46.16	53.52	61.22	41.61	18.25	39.10	57.71
PD-UAP	63.56	46.55	33.67	50.59	50.14	29.66	37.59	62.90
SSP	34.22	26.85	35.80	41.64	26.52	6.07	23.58	28.30
STD	45.39	37.86	42.17	40.49	34.37	34.74	43.51	44.38
UAP (DeepFool)	16.28	18.95	16.98	17.35	19.64	15.37	7.83	10.85
UAPEPGD	69.89	65.73	71.68	68.50	57.03	59.03	68.59	69.47
Clean Accuracy	76.09	73.07	78.42	73.83	67.24	69.05	76.51	75.81
IAA Avg.	27.50 ↓64%	24.15 ↓67%	24.09 ↓69%	27.69 ↓62%	21.03 ↓69%	19.81 ↓71%	23.39 ↓69%	26.37 ↓65%
UAP Avg.	40.06 ↓47%	37.88 ↓48%	39.60 ↓50%	42.42 ↓43%	30.05 ↓55%	25.37 ↓63%	30.51 ↓60%	38.54 ↓49%
Adv Avg.	33.41 ↓56%	30.61 ↓58%	31.39 ↓60%	34.62 ↓53%	25.28 ↓62%	22.43 ↓68%	26.74 ↓65%	32.10 ↓58%

#### 4.8.9. Pets

Table 25. This table presents the results of various instance and universal adversarial perturbation (UAP) attacks on the Pets dataset, with all UAP attack names in *italics*. Different configurations of FGSM and PGD are denoted, such as  $FGSM_1$  and  $PGD_1$ . Average results for universal adversarial perturbations (UAP Avg.), instance adversarial attacks (IAA Avg.), and overall adversarial performance (Adv Avg.) are reported at the bottom, including percentage drops relative to clean accuracy.

Method	Barlow	BYOL	DINO	MocoV3	SimCLR	Supervised	SwAV	VICReg
$FGSM_1$	63.58	61.00	48.74	71.38	44.60	55.10	41.59	63.58
$FGSM_2$	25.08	21.62	11.81	34.65	17.20	14.17	8.74	25.08
$PGD_1$	64.38	60.82	48.07	71.07	46.76	52.20	43.00	64.30
$PGD_2$	0.82	0.41	0.08	2.96	0.16	0.00	0.03	0.79
$PGD_3$	64.52	61.21	48.10	71.29	47.25	52.21	43.42	64.52
$PGD_4$	0.63	0.27	0.03	2.39	0.11	0.00	0.03	0.57
$PGD_5$	6.54	5.69	0.89	14.03	0.98	1.38	0.43	6.51
DI2FGSM	73.92	71.18	63.92	78.63	61.06	68.25	59.70	74.18
CW	0.00	0.00	0.00	0.03	0.00	0.00	0.00	0.00
Jitter	80.75	79.82	75.82	84.06	74.50	78.41	75.60	80.83
TIFGSM	81.43	80.30	78.13	84.89	75.31	80.60	76.11	82.31
PIFGSM	54.24	51.35	34.23	64.67	31.70	41.02	26.11	54.24
EADEN	0.00	0.00	0.00	0.00	0.00	0.00	0.00	0.00
OnePixel	88.28	87.90	87.65	89.82	81.51	90.60	85.85	88.31
Pixle	42.04	41.46	38.47	59.12	31.61	43.01	29.16	42.31
SPSA	87.27	86.87	85.81	88.79	79.93	88.54	83.95	87.46
Square	3.28	1.71	0.49	4.79	3.88	0.05	0.46	3.30
TAP	88.97	89.04	88.41	90.66	83.01	86.83	87.09	88.97
ASV	84.04	86.07	86.52	89.11	79.46	86.89	83.59	84.07
<i>FFF (mean-std)</i>	79.82	82.97	82.04	85.08	73.86	83.03	81.53	79.69
<i>FFF (no-data)</i>	65.60	47.88	70.12	80.33	53.54	71.01	53.59	62.52
<i>FFF (one-sample)</i>	49.62	85.48	61.54	83.37	63.28	73.35	61.44	56.39
<i>FG-UAP</i>	12.32	6.27	8.53	14.09	12.36	8.46	5.18	12.34
<i>GD-UAP (mean-std)</i>	84.78	81.57	75.38	84.37	75.67	84.82	80.65	85.93
<i>GD-UAP (no-data)</i>	67.48	63.61	55.35	79.27	69.36	65.81	60.80	71.45
<i>GD-UAP (one-sample)</i>	31.59	67.83	23.04	39.50	19.63	34.28	37.79	26.46
<i>LAA-base</i>	84.68	84.02	82.28	88.44	74.45	79.91	61.65	84.55
<i>LAA-fuse</i>	84.54	83.83	81.98	88.16	73.96	79.23	61.69	83.96
<i>LAA-ugs</i>	88.28	88.31	87.47	90.22	80.84	87.68	86.17	88.39
<i>PD-UAP</i>	84.38	75.44	65.26	78.86	77.81	75.73	69.66	84.25
<i>SSP</i>	86.49	85.07	84.23	89.73	78.70	76.96	78.96	86.29
<i>STD</i>	85.41	85.83	84.30	88.53	78.35	88.91	85.46	85.54
<i>UAP (DeepFool)</i>	42.47	45.23	41.35	56.05	67.08	55.57	44.72	48.42
<i>UAPEPGD</i>	88.36	88.44	87.83	89.74	79.14	90.05	87.04	88.11
Clean Accuracy	89.13	89.08	89.15	90.77	83.23	92.06	87.47	89.13
IAA Avg.	45.87 $\downarrow 49\%$	44.48 $\downarrow 50\%$	39.48 $\downarrow 56\%$	50.74 $\downarrow 44\%$	37.75 $\downarrow 55\%$	41.79 $\downarrow 55\%$	36.73 $\downarrow 58\%$	45.95 $\downarrow 48.4\%$
UAP Avg.	69.99 $\downarrow 21\%$	72.36 $\downarrow 19\%$	67.33 $\downarrow 24\%$	76.55 $\downarrow 16\%$	66.09 $\downarrow 21\%$	71.36 $\downarrow 22\%$	64.99 $\downarrow 26\%$	70.52 $\downarrow 21\%$
Adv Avg.	57.22 $\downarrow 36\%$	57.60 $\downarrow 35\%$	52.58 $\downarrow 41\%$	62.88 $\downarrow 31\%$	51.09 $\downarrow 39\%$	55.71 $\downarrow 39\%$	50.03 $\downarrow 43\%$	57.52 $\downarrow 35\%$

## 4.9. Transfer Learning (Finetune)

Table 26. Combined results from transfer learning datasets showing Clean accuracy, UAP Avg. , IAA Avg. , and Adv Avg. with percentage drops relative to Clean accuracy.

		Barlow	BYOL	DINO	MocoV3	SimCLR	Supervised	SwAV	VICReg
Aircraft	Clean	86.71	83.14	80.38	82.74	79.35	85.08	86.17	86.95
	IAA	39.62 ↓54%	39.21 ↓53%	32.36 ↓60%	40.18 ↓51%	30.68 ↓61%	45.4 ↓47%	42.47 ↓51%	39.21 ↓55%
	UAP	36.47 ↓58%	30.12 ↓64%	30.45 ↓62%	38.95 ↓53%	33.90 ↓57%	42.25 ↓50%	26.72 ↓69%	35.36 ↓59%
	Adv	38.14 ↓56%	34.93 ↓58%	31.46 ↓61%	39.60 ↓52%	32.20 ↓59%	43.92 ↓48%	35.06 ↓59%	37.40 ↓57%
Caltech	Clean	91.44	92.03	89.77	92.92	90.39	91.81	90.37	91.32
	IAA	53.63 ↓41%	57.03 ↓38%	49.71 ↓45%	59.32 ↓36%	53.86 ↓40%	54.18 ↓41%	48.01 ↓47%	53.78 ↓41%
	UAP	62.03 ↓32%	63.09 ↓31%	55.59 ↓38%	64.37 ↓31%	67.38 ↓25%	58.60 ↓36%	37.55 ↓58%	62.47 ↓32%
	Adv	57.58 ↓37%	59.88 ↓35%	52.48 ↓42%	61.70 ↓34%	60.23 ↓33%	56.26 ↓39%	43.09 ↓52%	57.87 ↓37%
Cars	Clean	90.54	89.91	89.80	90.11	89.62	88.99	89.73	90.41
	IAA	48.69 ↓46%	54.91 ↓39%	52.72 ↓52%	55.39 ↓39%	47.63 ↓47%	55.47 ↓38%	52.04 ↓42%	48.70 ↓48%
	UAP	45.75 ↓49%	60.09 ↓33%	49.85 ↓44%	65.77 ↓27%	34.10 ↓62%	55.54 ↓38%	50.81 ↓43%	44.46 ↓51%
	Adv	47.31 ↓48%	57.35 ↓36%	52.74 ↓41%	60.28 ↓33%	42.02 ↓53%	55.50 ↓38%	52.88 ↓41%	47.90 ↓49%
CIFAR 10	Clean	97.13	96.89	96.90	96.86	97.22	96.16	96.75	97.07
	IAA	48.74 ↓50%	46.26 ↓52%	54.18 ↓44%	49.66 ↓49%	49.03 ↓50%	43.37 ↓55%	55.75 ↓43%	48.31 ↓50%
	UAP	55.07 ↓43%	31.96 ↓67%	58.16 ↓40%	44.72 ↓54%	55.76 ↓43%	36.20 ↓62%	53.76 ↓44%	50.00 ↓48%
	Adv	51.72 ↓47%	39.53 ↓59%	56.05 ↓42%	47.34 ↓51%	52.20 ↓46%	40.00 ↓58%	54.81 ↓43%	49.10 ↓49%
CIFAR 100	Clean	84.60	83.88	84.69	84.49	84.44	82.63	84.37	84.27
	IAA	35.85 ↓57%	44.11 ↓47%	39.68 ↓53%	44.95 ↓47%	35.54 ↓58%	42.33 ↓49%	40.22 ↓52%	35.59 ↓58%
	UAP	36.41 ↓57%	36.79 ↓56%	42.02 ↓50%	31.57 ↓63%	28.24 ↓67%	24.94 ↓70%	41.03 ↓51%	31.40 ↓63%
	Adv	36.12 ↓57%	40.67 ↓52%	40.78 ↓52%	38.65 ↓54%	32.10 ↓62%	34.14 ↓59%	40.60 ↓52%	33.62 ↓60%
DTD	Clean	76.12	76.28	78.09	75.43	75.90	73.30	74.47	77.29
	IAA	41.42 ↓46%	41.89 ↓45%	40.50 ↓48%	42.91 ↓43%	42.42 ↓44%	38.99 ↓47%	39.65 ↓47%	41.90 ↓46%
	UAP	62.74 ↓18%	62.74 ↓18%	61.26 ↓22%	63.58 ↓16%	57.58 ↓24%	57.78 ↓21%	62.41 ↓16%	62.54 ↓19%
	Adv	51.46 ↓32%	51.70 ↓32%	50.27 ↓36%	52.64 ↓30%	49.56 ↓35%	47.83 ↓35%	50.36 ↓32%	51.62 ↓33%
Flowers	Clean	97.41	96.74	97.18	96.70	95.18	96.73	96.68	96.86
	IAA	60.24 ↓38%	61.32 ↓37%	54.30 ↓44%	60.98 ↓37%	51.34 ↓46%	60.79 ↓37%	55.66 ↓42%	59.97 ↓38%
	UAP	60.69 ↓38%	67.75 ↓30%	54.18 ↓44%	68.26 ↓29%	60.09 ↓37%	56.33 ↓42%	54.51 ↓44%	63.09 ↓35%
	Adv	60.45 ↓38%	64.34 ↓33%	54.25 ↓44%	64.41 ↓33%	55.46 ↓42%	58.69 ↓39%	55.12 ↓43%	61.44 ↓37%
Food	Clean	83.93	85.63	87.65	85.82	82.30	84.35	87.16	83.71
	IAA	27.80 ↓67%	36.30 ↓58%	34.12 ↓61.06%	36.09 ↓58%	28.89 ↓65%	34.74 ↓59%	34.26 ↓59%	31.71 ↓62%
	UAP	35.93 ↓57%	43.98 ↓49%	46.95 ↓46%	44.88 ↓48%	32.33 ↓61%	29.07 ↓66%	39.09 ↓55%	41.18 ↓51%
	Adv	35.94 ↓57%	39.91 ↓53%	40.16 ↓54%	40.23 ↓53%	30.51 ↓63%	32.07 ↓62%	36.53 ↓58%	36.17 ↓57%
Pets	Clean	90.89	91.34	90.24	92.19	88.51	93.94	90.50	90.92
	IAA	43.21 ↓52%	44.69 ↓51%	40.01 ↓56%	48.33 ↓48%	42.03 ↓53%	46.53 ↓50%	39.53 ↓56%	43.76 ↓52%
	UAP	67.27 ↓26%	71.96 ↓21%	63.83 ↓29%	73.20 ↓21%	67.90 ↓23%	75.66 ↓19%	64.06 ↓29%	67.63 ↓26%
	Adv	54.53 ↓40%	57.52 ↓37%	51.23 ↓43%	60.03 ↓35%	54.20 ↓39%	60.24 ↓36%	51.07 ↓44%	54.99 ↓40%
All	Clean	88.75	88.43	88.30	88.58	86.99	88.11	88.47	88.76
	IAA	44.36 ↓50%	47.30 ↓47%	44.18 ↓50%	48.65 ↓45%	42.38 ↓51%	46.87 ↓47%	45.29 ↓49%	44.77 ↓50%
	UAP	51.37 ↓42%	52.05 ↓41%	51.37 ↓42%	55.03 ↓38%	48.59 ↓44%	48.49 ↓45%	47.77 ↓46%	50.90 ↓43%
	Adv	48.14 ↓46%	49.54 ↓44%	47.71 ↓46%	51.65 ↓42%	45.39 ↓48%	47.63 ↓46%	46.61 ↓47%	47.79 ↓46%



#### 4.9.1. AirCraft

Table 27. This table presents the results of various instance and universal adversarial perturbation (UAP) attacks on the AirCraft dataset, with all UAP attack names in *italics*. Different configurations of FGSM and PGD are denoted, such as  $FGSM_1$  and  $PGD_1$ . Average results for universal adversarial perturbations (UAP Avg.), instance adversarial attacks (IAA Avg.), and overall adversarial performance (Adv Avg.) are reported at the bottom, including percentage drops relative to clean accuracy.

	Barlow	BYOL	DINO	MoCoV3	SimCLR	Supervised	SwAV	VICReg
$FGSM_1$	8.92	5.94	4.84	11.41	2.7	2.58	3.64	8.86
$FGSM_2$	1.52	0.69	0.45	1.95	0.78	0.81	2.57	1.8
$PGD_1$	10.03	5.72	4.54	10.96	3.44	1.61	4	10.18
$PGD_2$	0.06	0	0	0.12	0.24	0.18	0.64	0.06
$PGD_3$	10.27	6.02	4.63	11.09	3.27	1.61	3.83	10.06
$PGD_4$	0.06	0	0	0.12	0.18	0.12	0.61	0.06
$PGD_5$	0.12	0.03	0	0.24	0.18	0.24	0.79	0.12
DIFGSM	24.56	24.16	20.83	28.01	19.39	19.43	16.74	27.41
CW	0	0	0	0	0	0	0	0
Jitter	45.87	44.28	48.39	45.42	37.43	31.98	43.75	44.73
TIFGSM	32.78	31.08	29.68	35.76	28.31	18.99	29.83	33.04
PIFGSM	3.62	2.1	1.62	4.46	0.9	0.6	1.71	3.44
EADEN	0	0	0	0	0	0	0	0
OnePixel	51.75	49.39	54.93	53.41	41.4	36.01	47.55	51.54
Pixel	3.67	1.9	2.17	6.16	2.8	1.48	2.26	3.8
SPSA	44.36	42.91	44.2	46.6	30.76	28.51	38.42	44.31
Square	0.03	0	0	0.03	0.03	0	0	0.03
TAP	55.53	53.4	58.55	57.72	42.93	32.54	52.48	55.35
ASV	53.03	55.42	49.24	59.86	51.83	64.20	62.10	52.77
<i>FFF (mean-std)</i>	48.07	41.76	42.26	39.16	43.73	66.04	48.39	54.66
<i>FFF (no-data)</i>	6.41	17.70	8.80	35.53	53.12	7.79	1.09	2.77
<i>FFF (one-sample)</i>	3.71	3.05	1.51	18.25	4.41	1.21	2.30	2.01
<i>FG-UAP</i>	1.03	1.34	1.36	1.27	1.00	1.47	1.03	1.12
<i>GD-UAP (mean-std)</i>	46.54	19.30	38.41	38.56	17.72	56.61	35.26	47.09
<i>GD-UAP (no-data)</i>	7.43	9.67	7.29	7.59	28.10	9.88	1.18	1.33
<i>GD-UAP (one-sample)</i>	2.30	2.52	1.18	2.92	3.94	1.69	1.06	1.03
<i>L4A-base</i>	63.04	52.01	58.56	56.52	42.81	69.48	10.52	56.20
<i>L4A-fuse</i>	64.09	49.22	58.50	55.87	40.42	68.70	10.54	57.69
<i>L4A-ugs</i>	74.26	64.69	60.52	73.28	55.91	73.75	67.25	74.52
<i>PD-UAP</i>	5.03	11.22	7.77	18.77	37.70	13.39	1.66	1.54
<i>SSP</i>	60.82	28.61	38.99	69.89	42.61	75.01	20.45	55.00
<i>STD</i>	63.15	54.63	48.31	65.25	49.60	75.97	76.34	66.58
<i>UAP (DeepFool)</i>	13.69	4.30	6.35	8.80	12.43	14.44	12.04	20.83
<i>UAPEPGD</i>	70.90	66.42	58.16	71.67	57.00	76.42	76.22	70.58
Clean Accuracy	86.71	83.14	80.38	82.74	79.35	85.08	86.17	86.95
IAA Avg.	39.62 ↓54%	39.21 ↓53%	32.36 ↓60%	40.18 ↓51%	30.68 ↓61%	45.4 ↓47%	42.47 ↓51%	39.21 ↓55%
UAP Avg.	36.47 ↓58%	30.12 ↓64%	30.45 ↓62%	38.95 ↓53%	33.90 ↓57%	42.25 ↓50%	26.72 ↓69%	35.36 ↓59%
Adv Avg.	38.14 ↓56%	34.93 ↓58%	31.46 ↓61%	39.60 ↓52%	32.20 ↓59%	43.92 ↓48%	35.06 ↓59%	37.40 ↓57%

#### 4.9.2. Caltech 101

Table 28. This table presents the results of various instance and universal adversarial perturbation (UAP) attacks on the AirCrafft dataset, with all UAP attack names in *italics*. Different configurations of FGSM and PGD are denoted, such as  $FGSM_1$  and  $PGD_1$ . Average results for universal adversarial perturbations (UAP Avg.), instance adversarial attacks (IAA Avg.), and overall adversarial performance (Adv Avg.) are reported at the bottom, including percentage drops relative to clean accuracy.

	Barlow	BYOL	DINO	MoCoV3	SimCLR	Supervised	SwAV	VICReg
$FGSM_1$	8.92	5.94	4.84	11.41	2.7	2.58	3.64	8.86
$FGSM_2$	1.52	0.69	0.45	1.95	0.78	0.81	2.57	1.8
$PGD_1$	10.03	5.72	4.54	10.96	3.44	1.61	4	10.18
$PGD_2$	0.06	0	0	0.12	0.24	0.18	0.64	0.06
$PGD_3$	10.27	6.02	4.63	11.09	3.27	1.61	3.83	10.06
$PGD_4$	0.06	0	0	0.12	0.18	0.12	0.61	0.06
$PGD_5$	0.12	0.03	0	0.24	0.18	0.24	0.79	0.12
DIFGSM	24.56	24.16	20.83	28.01	19.39	19.43	16.74	27.41
CW	0	0	0	0	0	0	0	0
Jitter	45.87	44.28	48.39	45.42	37.43	31.98	43.75	44.73
TIFGSM	32.78	31.08	29.68	35.76	28.31	18.99	29.83	33.04
PIFGSM	3.62	2.1	1.62	4.46	0.9	0.6	1.71	3.44
EADEN	0	0	0	0	0	0	0	0
OnePixel	51.75	49.39	54.93	53.41	41.4	36.01	47.55	51.54
Pixel	3.67	1.9	2.17	6.16	2.8	1.48	2.26	3.8
SPSA	44.36	42.91	44.2	46.6	30.76	28.51	38.42	44.31
Square	0.03	0	0	0.03	0.03	0	0	0.03
TAP	55.53	53.4	58.55	57.72	42.93	32.54	52.48	55.35
ASV	87.68	84.73	81.98	90.28	81.40	88.77	63.56	87.29
FFF (mean-std)	86.13	80.89	71.22	89.66	74.99	78.03	47.85	83.06
FFF (no-data)	77.25	74.04	42.23	48.19	86.39	41.23	64.82	70.62
FFF (one-sample)	44.59	70.90	24.11	46.35	29.45	32.53	19.60	42.75
FG-UAP	9.42	9.03	2.68	11.08	9.40	6.14	1.76	9.35
GD-UAP (mean-std)	84.10	78.40	59.99	86.99	71.77	83.20	54.39	84.00
GD-UAP (no-data)	61.24	66.08	51.16	63.14	76.93	61.03	36.66	65.29
GD-UAP (one-sample)	53.10	67.34	44.78	51.65	56.50	62.41	24.78	62.74
LAA-base	40.18	38.60	63.97	59.38	79.84	46.59	6.71	40.71
LAA-fuse	39.33	39.98	65.70	58.64	79.27	45.31	6.28	39.46
LAA-ugs	84.46	78.05	69.87	85.20	82.89	82.04	38.86	84.11
PD-UAP	89.44	71.47	62.44	65.06	76.64	58.79	56.72	88.92
SSP	38.38	48.11	64.43	50.72	81.07	39.81	5.19	43.45
STD	90.32	91.14	87.86	91.82	88.33	90.47	87.83	90.52
UAP (DeepFool)	17.40	22.13	14.11	40.02	19.29	31.40	9.62	17.39
UAPEPGD	89.50	88.60	82.84	91.80	83.98	89.76	76.12	89.86
Clean Accuracy	91.44	92.03	89.77	92.92	90.39	91.81	90.37	91.32
IAA Avg.	53.63 ↓41%	57.03 ↓38%	49.71 ↓45%	59.32 ↓36%	53.86 ↓40%	54.18 ↓41%	48.01 ↓47%	53.78 ↓41%
UAP Avg.	62.03 ↓32%	63.09 ↓31%	55.59 ↓38%	64.37 ↓31%	67.38 ↓25%	58.60 ↓36%	37.55 ↓58%	62.47 ↓32%
Adv Avg.	57.58 ↓37%	59.88 ↓35%	52.48 ↓42%	61.70 ↓34%	60.23 ↓33%	56.26 ↓39%	43.09 ↓52%	57.87 ↓37%

### 4.9.3. Cars

Table 29. This table presents the results of various instance and universal adversarial perturbation (UAP) attacks on the AirCRAFT dataset, with all UAP attack names in *italics*. Different configurations of FGSM and PGD are denoted, such as  $FGSM_1$  and  $PGD_1$ . Average results for universal adversarial perturbations (UAP Avg.), instance adversarial attacks (IAA Avg.), and overall adversarial performance (Adv Avg.) are reported at the bottom, including percentage drops relative to clean accuracy.

	Barlow	BYOL	DINO	MoCoV3	SimCLR	Supervised	SwAV	VICReg
$FGSM_1$	8.92	5.94	4.84	11.41	2.7	2.58	3.64	8.86
$FGSM_2$	1.52	0.69	0.45	1.95	0.78	0.81	2.57	1.8
$PGD_1$	10.03	5.72	4.54	10.96	3.44	1.61	4	10.18
$PGD_2$	0.06	0	0	0.12	0.24	0.18	0.64	0.06
$PGD_3$	10.27	6.02	4.63	11.09	3.27	1.61	3.83	10.06
$PGD_4$	0.06	0	0	0.12	0.18	0.12	0.61	0.06
$PGD_5$	0.12	0.03	0	0.24	0.18	0.24	0.79	0.12
DIFGSM	24.56	24.16	20.83	28.01	19.39	19.43	16.74	27.41
CW	0	0	0	0	0	0	0	0
Jitter	45.87	44.28	48.39	45.42	37.43	31.98	43.75	44.73
TIFGSM	32.78	31.08	29.68	35.76	28.31	18.99	29.83	33.04
PIFGSM	3.62	2.1	1.62	4.46	0.9	0.6	1.71	3.44
EADEN	0	0	0	0	0	0	0	0
OnePixel	51.75	49.39	54.93	53.41	41.4	36.01	47.55	51.54
Pixel	3.67	1.9	2.17	6.16	2.8	1.48	2.26	3.8
SPSA	44.36	42.91	44.2	46.6	30.76	28.51	38.42	44.31
Square	0.03	0	0	0.03	0.03	0	0	0.03
TAP	55.53	53.4	58.55	57.72	42.93	32.54	52.48	55.35
ASV	72.91	82.15	78.42	82.19	66.07	80.09	78.46	76.31
FFF (mean-std)	70.69	75.79	69.49	72.04	46.51	72.89	69.07	65.95
FFF (no-data)	31.91	37.45	46.05	60.81	35.42	20.62	49.68	47.43
FFF (one-sample)	47.34	39.57	44.55	53.91	2.18	55.48	43.60	65.58
FG-UAP	0.82	1.87	1.79	3.93	0.60	2.11	1.36	0.63
GD-UAP (mean-std)	60.14	66.63	69.87	71.37	38.22	56.11	70.99	53.70
GD-UAP (no-data)	32.32	40.18	19.64	68.37	33.95	40.78	31.25	18.19
GD-UAP (one-sample)	8.66	27.60	16.48	34.76	7.62	21.95	16.20	7.20
LAA-base	43.38	87.19	63.86	76.66	41.94	71.56	63.09	56.05
LAA-fuse	40.58	86.36	65.68	77.37	42.44	75.14	63.01	54.18
LAA-ugs	68.64	85.40	82.13	86.22	35.49	79.16	84.80	75.12
PD-UAP	55.27	64.43	36.02	77.24	57.46	46.35	57.79	31.04
SSP	28.33	56.45	52.54	68.45	13.66	60.51	39.88	26.18
STD	75.91	79.33	82.30	80.89	68.19	76.01	80.03	78.03
UAP (DeepFool)	11.27	42.93	28.39	49.53	5.38	43.58	24.75	13.23
UAPEPGD	83.88	88.09	87.02	88.56	76.12	86.32	87.23	83.14
Clean Accuracy	90.54	89.91	89.80	90.11	89.62	88.99	89.73	90.41
IAA Avg.	48.69 ↓46%	54.91 ↓39%	52.72 ↓52%	55.39 ↓39%	47.63 ↓47%	55.47 ↓38%	52.04 ↓42%	48.70 ↓48%
UAP Avg.	45.75 ↓49%	60.09 ↓33%	49.85 ↓44%	65.77 ↓27%	34.10 ↓62%	55.54 ↓38%	50.81 ↓43%	44.46 ↓51%
Adv Avg.	47.31 ↓48%	57.35 ↓36%	52.74 ↓41%	60.28 ↓33%	42.02 ↓53%	55.50 ↓38%	52.88 ↓41%	47.90 ↓47%

#### 4.9.4. CIFAR 10

Table 30. This table presents the results of various instance and universal adversarial perturbation (UAP) attacks on the AirCRAFT dataset, with all UAP attack names in *italics*. Different configurations of FGSM and PGD are denoted, such as  $FGSM_1$  and  $PGD_1$ . Average results for universal adversarial perturbations (UAP Avg.), instance adversarial attacks (IAA Avg.), and overall adversarial performance (Adv Avg.) are reported at the bottom, including percentage drops relative to clean accuracy.

	Barlow	BYOL	DINO	MoCoV3	SimCLR	Supervised	SwAV	VICReg
$FGSM_1$	8.92	5.94	4.84	11.41	2.7	2.58	3.64	8.86
$FGSM_2$	1.52	0.69	0.45	1.95	0.78	0.81	2.57	1.8
$PGD_1$	10.03	5.72	4.54	10.96	3.44	1.61	4	10.18
$PGD_2$	0.06	0	0	0.12	0.24	0.18	0.64	0.06
$PGD_3$	10.27	6.02	4.63	11.09	3.27	1.61	3.83	10.06
$PGD_4$	0.06	0	0	0.12	0.18	0.12	0.61	0.06
$PGD_5$	0.12	0.03	0	0.24	0.18	0.24	0.79	0.12
DIFGSM	24.56	24.16	20.83	28.01	19.39	19.43	16.74	27.41
CW	0	0	0	0	0	0	0	0
Jitter	45.87	44.28	48.39	45.42	37.43	31.98	43.75	44.73
TIFGSM	32.78	31.08	29.68	35.76	28.31	18.99	29.83	33.04
PIFGSM	3.62	2.1	1.62	4.46	0.9	0.6	1.71	3.44
EADEN	0	0	0	0	0	0	0	0
OnePixel	51.75	49.39	54.93	53.41	41.4	36.01	47.55	51.54
Pixel	3.67	1.9	2.17	6.16	2.8	1.48	2.26	3.8
SPSA	44.36	42.91	44.2	46.6	30.76	28.51	38.42	44.31
Square	0.03	0	0	0.03	0.03	0	0	0.03
TAP	55.53	53.4	58.55	57.72	42.93	32.54	52.48	55.35
ASV	93.41	71.89	94.31	86.68	88.88	76.26	93.55	91.31
FFF (mean-std)	85.96	63.01	44.25	72.36	86.67	55.1	29.72	77.9
FFF (no-data)	68.68	12.87	52.85	52.54	71.1	25.55	35.1	36.08
FFF (one-sample)	16.72	13.51	47.16	12.91	12.22	10.25	23.85	14.84
FG-UAP	10.03	10.27	11.52	11.15	11.46	10.76	14.94	10.63
GD-UAP (mean-std)	71.66	20.62	34.9	61.37	85.5	33.53	24.17	72.08
GD-UAP (no-data)	71.78	10.31	39.89	33.17	15.38	17.34	38.98	54.72
GD-UAP (one-sample)	12.43	10.12	26.46	10.35	10.26	10.05	22.34	12.13
LAA-base	33.41	14.15	71.00	25.06	58.13	14.48	73.48	29.14
LAA-fuse	32.70	13.32	71.38	27.32	57.63	14.83	74.09	29.74
LAA-ugs	80.68	52.12	91.30	78.32	88.76	61.03	79.24	68.42
PD-UAP	86.15	18.99	87.32	27.60	92.59	27.82	82.89	81.42
SSP	17.16	10.66	43.62	23.58	16.46	21.83	61.30	20.30
STD	88.90	86.48	92.52	81.73	89.29	88.23	88.49	90.13
UAP (DeepFool)	15.98	12.61	26.41	17.99	14.46	20.88	22.31	17.42
UAPEPGD	95.39	90.42	95.70	93.44	93.36	91.23	95.63	93.73
Clean Accuracy	97.13	96.89	96.90	96.86	97.22	96.16	96.75	97.07
IAA Avg.	48.74 ↓50%	46.26 ↓52%	54.18 ↓44%	49.66 ↓49%	49.03 ↓50%	43.37 ↓55%	55.75 ↓43%	48.31 ↓50%
UAP Avg.	55.07 ↓43%	31.96 ↓67%	58.16 ↓40%	44.72 ↓54%	55.76 ↓43%	36.20 ↓62%	53.76 ↓44%	50.00 ↓48%
Adv Avg.	51.72 ↓47%	39.53 ↓59%	56.05 ↓42%	47.34 ↓51%	52.20 ↓46%	40.00 ↓58%	54.81 ↓43%	49.10 ↓49%

#### 4.9.5. CIFAR 100

Table 31. This table presents the results of various instance and universal adversarial perturbation (UAP) attacks on the AirCRAFT dataset, with all UAP attack names in *italics*. Different configurations of FGSM and PGD are denoted, such as  $FGSM_1$  and  $PGD_1$ . Average results for universal adversarial perturbations (UAP Avg.), instance adversarial attacks (IAA Avg.), and overall adversarial performance (Adv Avg.) are reported at the bottom, including percentage drops relative to clean accuracy.

	Barlow	BYOL	DINO	MoCoV3	SimCLR	Supervised	SwAV	VICReg
$FGSM_1$	8.92	5.94	4.84	11.41	2.7	2.58	3.64	8.86
$FGSM_2$	1.52	0.69	0.45	1.95	0.78	0.81	2.57	1.8
$PGD_1$	10.03	5.72	4.54	10.96	3.44	1.61	4	10.18
$PGD_2$	0.06	0	0	0.12	0.24	0.18	0.64	0.06
$PGD_3$	10.27	6.02	4.63	11.09	3.27	1.61	3.83	10.06
$PGD_4$	0.06	0	0	0.12	0.18	0.12	0.61	0.06
$PGD_5$	0.12	0.03	0	0.24	0.18	0.24	0.79	0.12
DIFGSM	24.56	24.16	20.83	28.01	19.39	19.43	16.74	27.41
CW	0	0	0	0	0	0	0	0
Jitter	45.87	44.28	48.39	45.42	37.43	31.98	43.75	44.73
TIFGSM	32.78	31.08	29.68	35.76	28.31	18.99	29.83	33.04
PIFGSM	3.62	2.1	1.62	4.46	0.9	0.6	1.71	3.44
EADEN	0	0	0	0	0	0	0	0
OnePixel	51.75	49.39	54.93	53.41	41.4	36.01	47.55	51.54
Pixel	3.67	1.9	2.17	6.16	2.8	1.48	2.26	3.8
SPSA	44.36	42.91	44.2	46.6	30.76	28.51	38.42	44.31
Square	0.03	0	0	0.03	0.03	0	0	0.03
TAP	55.53	53.4	58.55	57.72	42.93	32.54	52.48	55.35
ASV	76.76	64.38	74.69	54.69	49.74	61.44	72.13	75.5
FFF (mean-std)	61.98	35.03	38.93	19.71	18.57	5.46	48.25	36.28
FFF (no-data)	27.47	34.56	37.48	21.76	34.83	12.85	28.24	21.22
FFF (one-sampl)	1.83	14.42	27.3	15.76	1.53	5.2	22.05	5.92
FG-UAP	1.65	3.13	6.22	2.38	1.49	3.99	4.3	1.02
GD-UAP (mean-std)	48.83	22.66	17.57	14.95	43.36	7.59	51.07	36.65
GD-UAP (no-sample)	52.7	31.68	48.65	36.84	4.43	18.53	42.65	25.12
GD-UAP (one-sample)	4.45	11.91	9.57	11.5	4.57	7.88	18.26	2.17
LAA-base	8.49	24.86	41.34	16.66	17.31	19.07	27.93	8.92
LAA-fuse	8.92	24.55	40.87	17.12	18.88	20.3	26.87	9.18
LAA-ugs	57.08	61.96	73.13	46.77	49.34	45.16	70.88	59.27
PD-UAP	66.13	64.98	65.27	60.42	53.51	17.84	53.14	66.23
SSP	24.29	32.31	29.39	31.57	7.48	13.24	36.67	8.23
STD	57.19	66.71	64.13	57.24	65.29	68.65	55.1	61.38
UAP (DeepFool)	5.2	14.25	16.71	16.07	7.15	11.73	18.48	6.07
UAPEPGD	79.63	81.17	81.13	81.71	74.3	80.04	80.4	79.19
Clean Accuracy	84.60	83.88	84.69	84.49	84.44	82.63	84.37	84.27
IAA Avg.	35.85 ↓57%	44.11 ↓47%	39.68 ↓53%	44.95 ↓47%	35.54 ↓58%	42.33 ↓49%	40.22 ↓52%	35.59 ↓58%
UAP Avg.	36.41 ↓57%	36.79 ↓56%	42.02 ↓50%	31.57 ↓63%	28.24 ↓67%	24.94 ↓70%	41.03 ↓51%	31.40 ↓63%
Adv Avg.	36.12 ↓57%	40.67 ↓52%	40.78 ↓52%	38.65 ↓54%	32.10 ↓62%	34.14 ↓59%	40.60 ↓52%	33.62 ↓60%

#### 4.9.6. DTD

Table 32. This table presents the results of various instance and universal adversarial perturbation (UAP) attacks on the AirCRAFT dataset, with all UAP attack names in *italics*. Different configurations of FGSM and PGD are denoted, such as  $FGSM_1$  and  $PGD_1$ . Average results for universal adversarial perturbations (UAP Avg.), instance adversarial attacks (IAA Avg.), and overall adversarial performance (Adv Avg.) are reported at the bottom, including percentage drops relative to clean accuracy.

	Barlow	BYOL	DINO	MoCoV3	SimCLR	Supervised	SwAV	VICReg
$FGSM_1$	8.92	5.94	4.84	11.41	2.7	2.58	3.64	8.86
$FGSM_2$	1.52	0.69	0.45	1.95	0.78	0.81	2.57	1.8
$PGD_1$	10.03	5.72	4.54	10.96	3.44	1.61	4	10.18
$PGD_2$	0.06	0	0	0.12	0.24	0.18	0.64	0.06
$PGD_3$	10.27	6.02	4.63	11.09	3.27	1.61	3.83	10.06
$PGD_4$	0.06	0	0	0.12	0.18	0.12	0.61	0.06
$PGD_5$	0.12	0.03	0	0.24	0.18	0.24	0.79	0.12
DIFGSM	24.56	24.16	20.83	28.01	19.39	19.43	16.74	27.41
CW	0	0	0	0	0	0	0	0
Jitter	45.87	44.28	48.39	45.42	37.43	31.98	43.75	44.73
TIFGSM	32.78	31.08	29.68	35.76	28.31	18.99	29.83	33.04
PIFGSM	3.62	2.1	1.62	4.46	0.9	0.6	1.71	3.44
EADEN	0	0	0	0	0	0	0	0
OnePixel	51.75	49.39	54.93	53.41	41.4	36.01	47.55	51.54
Pixel	3.67	1.9	2.17	6.16	2.8	1.48	2.26	3.8
SPSA	44.36	42.91	44.2	46.6	30.76	28.51	38.42	44.31
Square	0.03	0	0	0.03	0.03	0	0	0.03
TAP	55.53	53.4	58.55	57.72	42.93	32.54	52.48	55.35
ASV	68.51	67.77	69.20	65.11	61.76	65.74	69.15	68.56
FFF (mean-std)	67.87	64.95	69.52	66.54	56.97	52.34	67.50	68.72
FFF (no-data)	57.18	57.13	46.91	59.52	57.39	46.22	58.56	51.97
FFF (one-sample)	40.16	54.63	51.86	57.29	49.95	47.29	60.16	38.56
FG-UAP	19.10	21.54	13.30	21.28	24.84	18.94	13.46	17.23
GD-UAP (mean-std)	64.47	61.91	69.68	65.27	52.82	57.18	63.67	66.33
GD-UAP (no-data)	57.13	59.47	46.54	58.62	57.23	50.48	56.86	56.22
GD-UAP (one-sample)	57.66	52.29	42.55	48.94	45.64	47.02	47.71	55.64
LAA-base	72.61	73.35	72.13	73.51	64.26	68.14	71.01	72.66
LAA-fuse	72.55	72.71	72.29	73.40	64.20	68.30	71.38	72.93
LAA-ugs	71.60	70.69	72.39	73.30	66.65	71.12	72.93	72.87
PD-UAP	72.13	69.79	65.74	70.90	60.11	60.64	63.35	73.24
SSP	72.45	70.21	73.03	71.70	59.73	66.17	69.63	72.18
STD	71.44	71.49	73.30	72.39	69.73	71.54	72.93	72.18
UAP (DeepFool)	68.03	66.49	69.47	67.71	63.09	62.77	67.93	68.56
UAPEPGD	70.96	69.41	72.23	71.76	66.91	70.59	72.39	72.77
Clean Accuracy	76.12	76.28	78.09	75.43	75.90	73.30	74.47	77.29
IAA Avg.	41.42 ↓46%	41.89 ↓45%	40.50 ↓48%	42.91 ↓43%	42.42 ↓44%	38.99 ↓47%	39.65 ↓47%	41.90 ↓46%
UAP Avg.	62.74 ↓18%	62.74 ↓18%	61.26 ↓22%	63.58 ↓16%	57.58 ↓24%	57.78 ↓21%	62.41 ↓16%	62.54 ↓19%
Adv Avg.	51.46 ↓32%	51.70 ↓32%	50.27 ↓36%	52.64 ↓30%	49.56 ↓35%	47.83 ↓35%	50.36 ↓32%	51.62 ↓33%



#### 4.9.7. Flowers

Table 33. This table presents the results of various instance and universal adversarial perturbation (UAP) attacks on the AirCraFt dataset, with all UAP attack names in *italics*. Different configurations of FGSM and PGD are denoted, such as  $FGSM_1$  and  $PGD_1$ . Average results for universal adversarial perturbations (UAP Avg.), instance adversarial attacks (IAA Avg.), and overall adversarial performance (Adv Avg.) are reported at the bottom, including percentage drops relative to clean accuracy.

	Barlow	BYOL	DINO	MoCoV3	SimCLR	Supervised	SwAV	VICReg
$FGSM_1$	8.92	5.94	4.84	11.41	2.7	2.58	3.64	8.86
$FGSM_2$	1.52	0.69	0.45	1.95	0.78	0.81	2.57	1.8
$PGD_1$	10.03	5.72	4.54	10.96	3.44	1.61	4	10.18
$PGD_2$	0.06	0	0	0.12	0.24	0.18	0.64	0.06
$PGD_3$	10.27	6.02	4.63	11.09	3.27	1.61	3.83	10.06
$PGD_4$	0.06	0	0	0.12	0.18	0.12	0.61	0.06
$PGD_5$	0.12	0.03	0	0.24	0.18	0.24	0.79	0.12
DIFGSM	24.56	24.16	20.83	28.01	19.39	19.43	16.74	27.41
CW	0	0	0	0	0	0	0	0
Jitter	45.87	44.28	48.39	45.42	37.43	31.98	43.75	44.73
TIFGSM	32.78	31.08	29.68	35.76	28.31	18.99	29.83	33.04
PIFGSM	3.62	2.1	1.62	4.46	0.9	0.6	1.71	3.44
EADEN	0	0	0	0	0	0	0	0
OnePixel	51.75	49.39	54.93	53.41	41.4	36.01	47.55	51.54
Pixel	3.67	1.9	2.17	6.16	2.8	1.48	2.26	3.8
SPSA	44.36	42.91	44.2	46.6	30.76	28.51	38.42	44.31
Square	0.03	0	0	0.03	0.03	0	0	0.03
TAP	55.53	53.4	58.55	57.72	42.93	32.54	52.48	55.35
ASV	69.45	77.27	69.56	82.40	75.33	77.53	63.57	73.27
FFF (mean-std)	67.79	90.99	54.47	71.41	61.67	77.85	56.39	57.47
FFF (no-data)	57.49	74.01	53.72	61.22	58.68	39.71	52.00	72.22
FFF (one-sample)	57.62	68.44	36.91	62.99	62.40	25.02	66.46	51.71
FG-UAP	14.02	17.87	2.56	13.45	6.25	10.20	4.10	11.32
GD-UAP (mean-std)	63.39	70.67	58.55	75.25	61.16	70.12	56.21	63.13
GD-UAP (no-data)	66.62	95.02	46.14	62.45	60.30	47.44	55.74	74.80
GD-UAP (one-sample)	30.40	14.74	26.38	41.49	59.61	11.85	22.44	40.30
LAA-base	67.70	81.02	81.03	75.93	56.36	70.48	64.16	72.19
LAA-fuse	68.34	83.02	81.59	76.85	56.86	71.46	67.54	72.42
LAA-ugs	84.09	84.89	63.96	88.48	75.71	85.65	81.73	84.32
PD-UAP	81.61	87.36	47.50	77.88	70.19	71.09	52.30	78.08
SSP	55.77	43.54	62.99	77.63	63.71	43.64	64.75	65.42
STD	69.43	74.60	66.85	71.59	67.20	69.42	67.86	67.67
UAP (DeepFool)	30.68	30.28	31.87	61.57	40.14	38.88	13.47	37.46
UAPEPGD	86.74	90.21	82.86	91.61	85.85	90.96	83.43	87.68
Clean Accuracy	97.41	96.74	97.18	96.70	95.18	96.73	96.68	96.86
IAA Avg.	60.24 ↓38%	61.32 ↓37%	54.30 ↓44%	60.98 ↓37%	51.34 ↓46%	60.79 ↓37%	55.66 ↓42%	59.97 ↓38%
UAP Avg.	60.69 ↓38%	67.75 ↓30%	54.18 ↓44%	68.26 ↓29%	60.09 ↓37%	56.33 ↓42%	54.51 ↓44%	63.09 ↓35%
Adv Avg.	60.45 ↓38%	64.34 ↓33%	54.25 ↓44%	64.41 ↓33%	55.46 ↓42%	58.69 ↓39%	55.12 ↓43%	61.44 ↓37%

#### 4.9.8. Food

Table 34. This table presents the results of various instance and universal adversarial perturbation (UAP) attacks on the AirCrafft dataset, with all UAP attack names in *italics*. Different configurations of FGSM and PGD are denoted, such as  $FGSM_1$  and  $PGD_1$ . Average results for universal adversarial perturbations (UAP Avg.), instance adversarial attacks (IAA Avg.), and overall adversarial performance (Adv Avg.) are reported at the bottom, including percentage drops relative to clean accuracy.

	Barlow	BYOL	DINO	MoCoV3	SimCLR	Supervised	SwAV	VICReg
$FGSM_1$	8.92	5.94	4.84	11.41	2.7	2.58	3.64	8.86
$FGSM_2$	1.52	0.69	0.45	1.95	0.78	0.81	2.57	1.8
$PGD_1$	10.03	5.72	4.54	10.96	3.44	1.61	4	10.18
$PGD_2$	0.06	0	0	0.12	0.24	0.18	0.64	0.06
$PGD_3$	10.27	6.02	4.63	11.09	3.27	1.61	3.83	10.06
$PGD_4$	0.06	0	0	0.12	0.18	0.12	0.61	0.06
$PGD_5$	0.12	0.03	0	0.24	0.18	0.24	0.79	0.12
DIFGSM	24.56	24.16	20.83	28.01	19.39	19.43	16.74	27.41
CW	0	0	0	0	0	0	0	0
Jitter	45.87	44.28	48.39	45.42	37.43	31.98	43.75	44.73
TIFGSM	32.78	31.08	29.68	35.76	28.31	18.99	29.83	33.04
PIFGSM	3.62	2.1	1.62	4.46	0.9	0.6	1.71	3.44
EADEN	0	0	0	0	0	0	0	0
OnePixel	51.75	49.39	54.93	53.41	41.4	36.01	47.55	51.54
Pixel	3.67	1.9	2.17	6.16	2.8	1.48	2.26	3.8
SPSA	44.36	42.91	44.2	46.6	30.76	28.51	38.42	44.31
Square	0.03	0	0	0.03	0.03	0	0	0.03
TAP	55.53	53.4	58.55	57.72	42.93	32.54	52.48	55.35
ASV	66.85	72.56	76.44	67.11	63.10	68.71	73.28	68.88
<i>FFF (mean-std)</i>	56.35	64.24	72.43	62.39	46.44	21.16	70.21	63.32
<i>FFF (no-data)</i>	27.32	42.11	34.44	43.99	30.61	24.10	35.49	36.72
<i>FFF (one-sample)</i>	16.11	20.92	49.03	22.00	11.71	6.63	23.65	18.35
<i>FG-UAP</i>	3.60	3.51	5.25	3.18	2.35	5.27	5.69	3.48
<i>GD-UAP (mean-std)</i>	51.73	47.56	64.19	69.35	51.11	34.44	68.26	66.41
<i>GD-UAP (no-data)</i>	20.73	49.44	30.21	45.98	25.59	15.42	25.43	39.66
<i>GD-UAP (one-sample)</i>	14.78	18.09	24.88	41.16	22.17	7.45	7.39	31.94
<i>LAA-base</i>	34.63	40.48	42.81	32.70	26.26	34.83	18.31	31.63
<i>LAA-fuse</i>	33.93	40.76	42.48	33.41	24.73	34.40	17.74	24.70
<i>LAA-ugs</i>	59.73	67.54	72.25	60.77	10.41	35.42	58.80	34.90
<i>PD-UAP</i>	28.06	67.88	57.45	62.27	65.10	34.61	36.81	75.30
<i>SSP</i>	18.81	25.50	25.47	32.13	8.99	6.28	32.83	21.57
<i>STD</i>	57.58	55.80	60.02	50.13	42.12	52.72	61.46	55.82
<i>UAP (DeepFool)</i>	7.20	7.26	12.26	10.01	13.10	5.28	8.71	8.13
<i>UAPEPGD</i>	77.46	80.01	81.65	81.49	73.45	78.37	81.32	78.15
Clean Accuracy	83.93	85.63	87.65	85.82	82.30	84.35	87.16	83.71
IAA Avg.	27.80 ↓67%	36.30 ↓58%	34.12 ↓61.06%	36.09 ↓58%	28.89 ↓65%	34.74 ↓59%	34.26 ↓59%	31.71 ↓62%
UAP Avg.	35.93 ↓57%	43.98 ↓49%	46.95 ↓46%	44.88 ↓48%	32.33 ↓61%	29.07 ↓66%	39.09 ↓55%	41.18 ↓51%
Adv Avg.	35.94 ↓57%	39.91 ↓53%	40.16 ↓54%	40.23 ↓53%	30.51 ↓63%	32.07 ↓62%	36.53 ↓58%	36.17 ↓57%

#### 4.9.9. Pets

Table 35. This table presents the results of various instance and universal adversarial perturbation (UAP) attacks on the AirCrafft dataset, with all UAP attack names in *italics*. Different configurations of FGSM and PGD are denoted, such as  $FGSM_1$  and  $PGD_1$ . Average results for universal adversarial perturbations (UAP Avg.), instance adversarial attacks (IAA Avg.), and overall adversarial performance (Adv Avg.) are reported at the bottom, including percentage drops relative to clean accuracy.

	Barlow	BYOL	DINO	MoCoV3	SimCLR	Supervised	SwAV	VICReg
$FGSM_1$	8.92	5.94	4.84	11.41	2.7	2.58	3.64	8.86
$FGSM_2$	1.52	0.69	0.45	1.95	0.78	0.81	2.57	1.8
$PGD_1$	10.03	5.72	4.54	10.96	3.44	1.61	4	10.18
$PGD_2$	0.06	0	0	0.12	0.24	0.18	0.64	0.06
$PGD_3$	10.27	6.02	4.63	11.09	3.27	1.61	3.83	10.06
$PGD_4$	0.06	0	0	0.12	0.18	0.12	0.61	0.06
$PGD_5$	0.12	0.03	0	0.24	0.18	0.24	0.79	0.12
DIFGSM	24.56	24.16	20.83	28.01	19.39	19.43	16.74	27.41
CW	0	0	0	0	0	0	0	0
Jitter	45.87	44.28	48.39	45.42	37.43	31.98	43.75	44.73
TIFGSM	32.78	31.08	29.68	35.76	28.31	18.99	29.83	33.04
PIFGSM	3.62	2.1	1.62	4.46	0.9	0.6	1.71	3.44
EADEN	0	0	0	0	0	0	0	0
OnePixel	51.75	49.39	54.93	53.41	41.4	36.01	47.55	51.54
Pixel	3.67	1.9	2.17	6.16	2.8	1.48	2.26	3.8
SPSA	44.36	42.91	44.2	46.6	30.76	28.51	38.42	44.31
Square	0.03	0	0	0.03	0.03	0	0	0.03
TAP	55.53	53.4	58.55	57.72	42.93	32.54	52.48	55.35
ASV	86.65	87.60	86.78	85.55	78.08	87.31	86.05	86.12
FFF (mean-std)	84.69	84.25	79.83	85.91	73.65	85.76	68.35	83.45
FFF (no-data)	48.95	75.83	47.83	74.82	66.53	70.05	73.33	64.11
FFF (one-sample)	26.50	79.70	45.52	68.01	50.15	74.97	54.46	29.36
FG-UAP	8.10	6.85	7.12	13.08	25.21	6.23	5.79	5.42
GD-UAP (mean-std)	82.46	85.03	76.63	85.23	66.49	83.99	81.65	84.72
GD-UAP (no-data)	65.76	68.77	53.73	66.01	72.91	75.24	76.37	62.12
GD-UAP (one-sample)	34.98	28.91	16.56	50.63	52.54	55.38	25.65	31.27
LAA-base	83.76	81.41	83.84	82.30	72.93	88.88	58.86	83.19
LAA-fuse	83.03	81.08	83.04	82.39	72.59	88.36	57.81	82.03
LAA-ugs	88.82	88.76	86.91	90.43	77.88	90.76	87.71	88.77
PD-UAP	86.63	81.05	63.30	79.72	74.99	76.75	74.91	86.63
SSP	79.54	81.60	83.18	82.57	72.05	84.12	70.15	76.15
STD	86.94	86.94	81.23	89.15	79.74	90.81	84.33	86.63
UAP (DeepFool)	40.81	44.95	38.77	44.69	69.07	60.11	31.96	43.56
UAPEPGD	88.68	88.69	87.07	90.78	81.50	91.88	87.52	88.64
Clean Accuracy	90.89	91.34	90.24	92.19	88.51	93.94	90.50	90.92
IAA Avg.	43.21 ↓52%	44.69 ↓51%	40.01 ↓56%	48.33 ↓48%	42.03 ↓53%	46.53 ↓50%	39.53 ↓56%	43.76 ↓52%
UAP Avg.	67.27 ↓26%	71.96 ↓21%	63.83 ↓29%	73.20 ↓21%	67.90 ↓23%	75.66 ↓19%	64.06 ↓29%	67.63 ↓26%
Adv Avg.	54.53 ↓40%	57.52 ↓37%	51.23 ↓43%	60.03 ↓35%	54.20 ↓39%	60.24 ↓36%	51.07 ↓44%	54.99 ↓40%